Summer 1995

Identification and Characterization of Mitochondrial DNA Variants in Alzheimer's Disease

Natasha Singh Hamblet
Old Dominion University

IDENTIFICATION AND CHARACTERIZATION OF MITOCHONDRIAL DNA VARIANTS IN ALZHEIMER'S DISEASE

by

Natasha Singh Hamblet
B.S. August 1987
State University of New York at Stony Brook

A Dissertation submitted to the Faculty of
Eastern Virginia Medical School
and
Old Dominion University
in Partial Fulfillment of the Requirement for the Degree of

DOCTOR OF PHILOSOPHY
BIOMEDICAL SCIENCES

EASTERN VIRGINIA MEDICAL SCHOOL
and
OLD DOMINION UNIVERSITY
August, 1995

Approved By:

Frank J. Castora, PhD Director

Laura K. Moen, PhD

Bruce W. Tedeschi, PhD

Frank K. Lattanzio, PhD

William J. Wasilenko, PhD

ABSTRACT

Identification and Characterization of Mitochondrial DNA Variants in Alzheimer's Disease

Natasha Singh Hamblet

Eastern Virginia Medical School
and
Old Dominion University
1995

Director: Frank J. Castora

Alzheimer's Disease (AD) is a complex neurodegenerative disorder that affects a significant portion of the human population regardless of ethnicity or gender. A mitochondrial hypothesis of AD has been proposed based on a number of studies which establish altered oxidative phosphorylation (OXPHOS) and ATP synthesis in AD tissue. ATP demand is most prevalent in the brain; damage to OXPHOS could severely impair brain metabolism, thereby leading to a decline in cognitive function. Four out of five complexes in the OXPHOS pathway are partly encoded by mitochondrial DNA (mtDNA); thus, this may be a crucial site of lesions that alter brain activity. Within the last decade a number of neuromuscular disorders have been found to be associated with mutations in mtDNA. AD patients share a number of similarities with the mitochondrial encephalomyopathies such as reduced oxidative metabolism, delayed onset of neurological symptoms, and pathological changes that damage tissues with high ATP demand. For these reasons we have been studying AD brain tissue for known, as well

as any uncharacterized, mtDNA mutations.

We examined brain autopsy tissue for deleted mtDNA by PCR-based methods and Southern analysis. AD brain tissue was obtained from autopsy-confirmed cases. Using a rat brain model system to examine postmortem effects, we found no mtDNA degradation after 30 hours at RT by Southern analysis. We then assessed brain tissue for the 5 kb deletion ($mtDNA^{\Delta 4977}$) by PCR-based methods. While optimizing quantitative techniques we found that serial dilution PCR and kinetic PCR yielded different deletion levels although both methods indicated a greater ratio of $mtDNA^{\Delta 4977}$ in the caudate than in the parietal cortex of a cognitively intact control. By serial dilution PCR we determined that AD temporal cortex had a 12 fold greater frequency of $mtDNA^{\Delta 4977}$ than controls (0.0628% vs 0.0053%).

Using diagnostic restriction enzyme analysis, we detected the previously described point mutation, $tRNA^{gln4336}$, in one Caucasian AD patient and in none of the controls. Biochemical studies indicated that there is a significant decrease in cytochrome *c* oxidase (COX) activity in platelets and brain tissue of AD patients as well as perturbed COX I, II and III mRNA levels. We examined the mitochondrially encoded COX subunits by single strand conformation polymorphism (SSCP) and DNA sequencing and identified thirty two variants. SSCP efficiency was estimated at 80%. Sixteen of the mutations are new mtDNA variants including a moderately conserved phe->leu missense change in COX III at np 9861 which was observed in 4.2% (1/24) of the AD patients and in 0% (0/16) of the controls. Further studies will define if this mutation plays any pathogenic role in AD or in COX activity suppression.

DEDICATION

This work is dedicated to my wonderful husband and naval officer extraordinaire, Lt. James C. Hamblet who always gave much needed love and support despite his own arduous career -
From you I gained strength,

And to my dear mother, Jean C. Reis to whom I owe all of my successes and happiness -
From you I gained faith.

ACKNOWLEDGEMENTS

First and foremost I am deeply indebted to Dr. Frank J. Castora, director of this project, for his steadfast belief in my abilities and for allowing me to pursue science in an independent yet guided arena. I thank Catherine E. Burgess, who greatly assisted me throughout a number of stages of this work, for her infectious enthusiasm towards research and Jia-Hwei Lin who provided words of wisdom during my many dark days of research. I would like to extend my appreciation to Charles Goldman for his photographic skills, and to Surafel Mulageta for help with polylysine techniques. I also wish to thank Liz Allen and Erni Foye for administrative assistance and Dr. Karl A. Schellenberg, Chairman of the Biochemistry Department at EVMS, for his support of graduate student research.

Finally, I would like to express my sincere gratitude to all of my thesis committee members, to Dr. Bill Wasilenko and to Dr. Frank Lattanzio for their recommendations during the various phases of this study, and to Dr. Bruce Tedeschi for his expertise in the growth and maintenance of the PC-12 cell line. However, I am most grateful to Dr. Laura Moen, my guidance committee chairman, whose guidance and encouragement were instrumental during my early graduate studies.

TABLE OF CONTENTS

LIST OF TABLES

LIST OF FIGURES

CHAPTER I INTRODUCTION

A. BACKGROUND AND SIGNIFICANCE

Alzheimer's Diseases (AD), the most common dementing illness in humans, is a neurodegenerative disorder that currently affects 4 million Americans. These numbers are expected to triple within the next fifty years. The cost of caring for AD patients is estimated at $40 billion per year (1). Clinically, AD affects memory, language, visuospatial pathways, the motor system and induces neuropsychiatric problems. Information processing as well as recall is impaired. Initially, only short term memory is affected; but as the disease progresses, long term memory is affected as well (2). Language problems include difficulty in word list generation, confrontation naming and an inability to link phrases together (aphasia) (3). Most family members notice personality changes - the patient is either more passive, self centered and agitated and in some instances is less reasonable and affectionate (3). Motor system abnormalities rarely occur until the later stages of the disease but mild rigidity can occur as well as loss of facial expression and grasping (4). Myoclonus and seizures occur in 10-50% of all cases (5,6). A number of neurotransmitter systems are affected by AD but the cholinergic system and associated pathways such as the nucleus basalis of Meynert projection are most altered (7). Substantial cell loss occurs in the pyramidal cells of the hippocampus and other limbic areas such as the amygdala. The cerebral cortex shows

severe neuronal dysplasia with the temporal, frontal and parietal cortex usually being more affected than the occipital cortex (8).

The major pathological change in AD brain is the presence of neurofibrillary tangles (NFTs) and amyloid plaques. NFTs are intracellular deposits composed of the microtubule associated tau protein whereas the plaques are extracellular deposits of β-amyloid fibrils (9). Mutations in the amyloid precursor protein (APP) gene as well as in the β-amyloid peptide have been linked to familial early onset AD (10,11) and to hereditary cerebral hemorrhage with amyloidosis-Dutch type (12). However, familial Alzheimer's Disease (FAD) accounts for only 5% of all cases whereas approximately 95% are considered late onset and sporadic in nature. Specific cases of late onset AD have been shown to be positively correlated with the apolipoprotein type ϵ 4 allele (either heterozygous or homozygous carriers) (13). The frequency of the ϵ4 allele in normal cognitive intact controls was found to be 7% in one study (14) but 20 to 30% in another study (15). In the study which found a normal frequency of 7%, 57% of the AD individuals carried one or more copies of the ϵ 4 allele while 43 % of the AD cases were not carriers (14). Thus, despite these advances there are still a significant number of AD cases that are neither familial early onset nor sporadic ϵ4 carriers. Where then does the current information on Alzheimer's lead? One needs to rexamine the genetic, biochemical and morphological evidence available.

The clinical genetics of AD have been widely studied in an effort to identify potential risk factors for the disease. Twin studies have shown that dizygotic twins are usually discordant for the disease whereas monozygotic twins are usually concordant for

the disease (16,17). Monozygotic twins tend to have a higher frequency of affected relatives. This points to some cases of AD being heritable while others are not. In fact, whereas heritable cases linked to APP mutations on chromosome 21 have an age of onset between 40 to 50 years (18), 68% - 78% of AD patients have a later age of onset between 60 to 84 years of age (19). Clearly advanced age is a major risk factor. Indeed it tops the list of risk factors before head trauma, genetic inheritance or advanced paternal and/or maternal age (parental age as a risk factor remains controversial) (20,21). However no clear mode of inheritance has been defined in the late onset group. Studies are further complicated by individuals of advanced age dying of other diseases such as cancer or stroke before potentially manifesting symptoms of AD. Thus, it is believed that AD is an etiologically heterogeneous disease which in a small number of cases has a single genetic basis. In a majority of cases, however, AD may be due to a multiplicity of factors similar to cancer, in which one, or more genetic defects present are influenced by environmental factors.

While the genetic studies have proven perplexing, biochemical analyses have generated a number of informative findings. Most studies have examined cerebral oxygen and glucose metabolism in AD patients using Positron Emission Tomography (PET) which monitors metabolism. Three main conclusions emerged - the first was that global and regional glucose and oxygen metabolism were reduced compared to age-matched controls (22). Secondly, the extent of the reduction was regionally variable in the four lobes of the cerebral cortex and lastly, the extent of the reduction was correlated with the degree of dementia (22). These three conclusions have, for the large part,

remained intact. However, in later studies there often seemed to be discrepancies as to whether a reduction or increase in metabolism was occurring. This is due to the use of the phrases "glucose production" , "glucose oxidation" and "oxidative metabolism". If the production of $^{14}CO_2$ from (U^{14}-C) glucose is *increased* (also referred to as a greater rate of oxidation of glucose) then this demonstrates a *lower* oxidative metabolism. In other words, glucose consumption is increased in order to compensate for deficient ATP production. One of the earliest *in vivo* brain studies found that the rate of oxidative metabolism was decreased (23). Brown et al. using *in vivo* phosphorous NMR spectroscopy found a lower phosphocreatine (PC) to inorganic phosphorous (P_i) ratio in AD individuals compared to those with multi-infarct dementia, a vascular disease that can mimic symptoms of AD. The PC/P_i ratio which measures the energy state of a tissue indicates a compromised bioenergetic system in AD (24). Sims et al. in a study in brain *ex vivo* (biopsies) found a 39% greater rate of oxidation of glucose in AD brain (25). Later, using whole homogenates of brain samples obtained from the biopsy material, they measured the rate of oxygen uptake for controls vs an AD group. They found O_2 uptake similar for AD and controls, but the respiratory control index (RCI) was lower in AD brain. This result indicates that O_2 consumption was normal whereas the abnormal RCI implicated that uncoupling of the mitochondria was occurring (25). In autopsy tissue direct enzymatic studies have found decreases in the activities in the thiamine pyrophosphate dependent multisubunit enzymes, pyruvate dehydrogenase and alpha ketoglutarate dehydrogenase (26). The activity of other TCA cycle enzymes such as fumarase and citrate synthetase was normal, indicating that the decreased activity was not

due simply to a loss of mitochondria (27).

Further studies have been carried out in non-neuronal tissue. Sims et al. studied glucose metabolism in cultured skin fibroblasts and found that the production of $^{14}CO_2$ from (U^{14}-C) glucose was elevated indicating deficient oxidative metabolism while lactate production was higher than in control brains (28). On the other hand, they found that the production of $^{14}CO_2$ from (U^{14}-C) glutamine was reduced, indicating a high glutamine oxidation state. Glutamine is converted to α-ketoglutarate, a TCA cycle intermediate which in the process of oxidative decarboxylation produces NADH. NADH then enters the electron transport chain. It is generally accepted that oxidation of glucose in cultured fibroblasts can be sensitive to experimental conditions. Based on this observation, the glucose metabolism findings are difficult to interpret. However, lactic acid production was increased, implying problems in oxygen metabolism (pyruvate is shunted to lactate production under anaerobic conditions). A benefit of serially passaging fibroblast lines however is that materials present in the original sample are eventually diluted out. Thus the effects seen are most likely due to a primary change rather than some aspect of the original culture such as medication, hormonal levels, etc (29). The alteration in glutamine oxidation then can most likely be attributed to a primary defect. In muscle Maraini et al. found a higher mitochondrial metabolism rather than the reduction seen in fibroblasts (30). This discrepancy was postulated to be due to the different metabolic requirements of muscle cells versus fibroblasts with respect to their primary substrate for oxygen metabolism; the primary substrate for cultured fibroblasts is probably glutamine and not glucose (31). Other groups however have found decreased

glucose and glutamine oxidation in cultured skin fibroblasts from AD patients (32). Additional studies have been done in other tissue types such as white blood cells and T-cells all of which parallel the alterations in glucose and oxidative metabolism seen in brain (33).

Interestingly in a study using normal fibroblasts, an uncoupler of OXPHOS, carbonyl cyanide m-chlorophenylhydrazone (CCCP) stimulated the production of the Alzheimer specific antigen Alz-50 150 fold over control cells demonstrating that oxidative abnormalities can induce some of the pathological changes seen in AD. AD fibroblasts cultured even in the absence of CCCP reacted with the Alz-50 monoclonal antibody in a greater percentage than in control lines consistent with the measurement of an abnormal respiratory control index in AD patients (34).

All of these studies establish altered oxidative metabolism in AD brain and in AD non-neuronal tissue. Oxidative metabolism pathways such as oxidative phosphorylation (OXPHOS) and electron transport all take place within the organelle considered to be the "powerhouse" of the cell, the mitochondria. Morphological studies support the presence of abnormal mitochondria in AD brain. Paracrystalline inclusions, granular dense bodies, have been observed in AD tissue similar to abnormal mitochondria seen in patients suffering from mitochondrial myopathies, neuromuscular diseases caused by mutations affecting mitochondrial function (35). Other ultrastructure studies have found mitochondria which are granular and dense with large, swollen cristae (36). Thus, the initial biochemical and morphological evidence all strongly argue for an inherent problem in the mitochondria of Alzheimer's patients. Furthermore, as biochemical studies have

continued, a direct link to one complex of the oxidative phosphorylation pathway has emerged.

An interesting aspect of the mitochondria of all aerobic organisms is that they contain their own DNA, a point that as will be described in the following section, could explain some of the complex genetics observed in AD.

Human mitochondria contain a compact, intronless, 16,569 kb closed circular double stranded DNA molecule that codes for 2 rRNAs, 22 tRNAs, and 13 polypeptides (cytochrome c oxidase subunits I,II, III, cytochrome b, ATPase subunits 6 and 8, and 7 subunits of the NADH dehydrogenase). All of these endogenously synthesized proteins are components of the electron transport chain and therefore are involved in OXPHOS. The respiratory chain is composed of 5 complexes, four of which have subunits encoded by mitochondrial DNA (mtDNA) whereas the remaining subunits are coded by nuclear DNA (see Table 1) (37). Two to ten molecules of mtDNA are present in each mitochondrion, thus, each mitochondrion can have a mixture of normal and abnormal (mutant) mtDNA (38). This mixed state is termed heteroplasmy. Mitochondria are subject to two processes that could lead to changes in the output frequency of mutant and normal molecules, random drift and random partitioning (39). Random partitioning refers to the process whereby individual organelles will segregate at random during cell division. Cells will be created that are dissimilar due to the particular combination of mitochondria. However it has been found that a more effective way of producing "allelic" changes occurs during the random segregation of *individual* mtDNA molecules. A mutant mtDNA molecule has two pathways during random drift, either the mutation

Table 1

OXPHOS SUBUNITS THAT ARE ENCODED BY MITOCHONDRIAL DNA

COMPLEX	NAME	mtDNA SUBUNITS	NUCLEAR SUBUNITS
I	NADH CoQ reductase	7	>18
II	Succinate CoQ reductase	0	4
III	Ubiquinol cytochrome c reductase	1	8
IV	cytochrome c oxidase	3	10
V	ATP synthase	2	10

will be lost or the mutation could be fixed leading eventually to a homoplasmic mutant state.

During the acrosome reaction that takes place prior to fertilization no paternal mitochondria are transmitted to the zygote, thus, one manner of inheriting mutant mtDNA is through the maternal lineage. Homoplasmic mutations usually result in immediate, overt problems in oxidative capacity. On the other hand heteroplasmic mutations cause a much slower progression of symptoms. This would fit in with the progressive disease course observed in AD. The threshold level at which disease occurs is dependent on three factors: percentage of mutant mtDNA, tissue type affected and age of the individual (40). An abnormal phenotype is expressed when a combination of these factors causes levels to decline beyond normal cellular functioning. "Cellular functioning" is defined by the oxidative demands of individual cells or organs; toxicological studies done by Wallace place cerebral cortex as the primary areas dependent on mitochondrial energy followed by type I skeletal muscle, auditory pathway, cerebellum, brain stem and heart (41). The brain, which has the highest content of mtDNA per gram of mitochondria (42), is at the top of this pyramid. Thus, one can see how a mutation that affects mitochondrial function can have severe consequences on brain functioning. This is especially true for neuronal transmission and the synthesis of neurotransmitters, two processes that are highly dependent on ATP production (43,44) and both of which are perturbed in Alzheimer's.

Early opinion believed that since normal mtDNA was abundant, there was no threat of disease due to mutant mtDNA. Within the last decade however a subset of

mitochondrial myopathies and mitochondrial encephalomyopathies have been found to be associated with point mutations in the mitochondrial genome. These include Leber's Hereditary Optic Neuropathy (LHON) (45), Neurogenic Muscle Weakness, Ataxia,and Retinitis Pigmentosa (NARP) (46), Leigh's Syndrome (47), Myoclonic Epilepsy and Ragged Red Fiber (MERRF) (48) and Mitochondrial Encephalomyopathy with Lactic Acidosis and Stroke Like Episodes (MELAS) (49). These diseases were initially linked to a mtDNA defect due to respiratory chain deficiencies and evidence of maternal inheritance. That a mtDNA point mutation was indeed the culprit in these diseases was still controversial. The coup de grace was the development of an elegant system for the study of mtDNA mutations. Cell lines were developed that contained no mtDNA. These cells were termed rho zero, ρ^0, after yeast mutants that had lost their mtDNA but not their mitochondria (39). Mitochondria from patients harboring either the MERRF $tRNA^{lys}$ mutation at position 8344 or, the MELAS $tRNA^{leu}$ transition at position 3243 were fused with ρ^0 cells. The mtDNA mutations associated with MERRF and MELAS transferred respiratory chain abnormalities to the ρ^0 cells analogous to deficiencies seen in the respective patients (50,51,52). Interestingly, AD patients share some clinical characteristics of mitochondrial encephalomyopathy patients; myoclonus and epilepsy have been reported in some of the later stages of AD (5,6) and a study using single photon emission computed tomography (SPECT) found reduced blood flow in a MELAS patient similar to the pattern seen in AD (53).

Advanced age has been found to be one factor that predisposes an individual to a second type of mtDNA alteration - deletions. As mentioned age is the number one risk

factor for AD. Deletions that span over 40% of the mitochondrial genome have been found in normal aged liver, heart, skeletal muscle and brain (54,55,56,57,58,59). They have also been implicated in late onset type II Diabetes Mellitus (60) as well as in acquired deafness (61). The mitochondrial myopathy Kearns-Sayre Syndrome (KSS) is due to a 5 kb deletion in mtDNA (62,63) and is referred to as the "common deletion" since it is found in many normal aged tissues. The KSS deletion which deletes 5 tRNAs and 5 protein genes increases with age in normal individuals but is elevated almost 1000-fold in KSS. KSS is a systemic disorder that is usually fatal and is marked by opthalmoplegia, onset before age 20, ataxia and ragged red fibers (due to overly proliferative mitochondria). Most deletions are believed to be generated at tandem repeat sequences between the two origins of replication (termed the "hotspot" area) by a slippage mispair mechanism (Fig 1) (64). During replication part of the mitochondrial genome is single stranded. At a small region of complementarity, single stranded sequences hybridize forming a loop structure that is later excised. Few deletions have been detected in the non-hotspot or minor region. The production of a deletion represents another way, besides maternal inheritance, that a mtDNA mutation is generated - a sporadic alteration in a single individual.

MtDNA is extremely susceptible to the generation and accumulation of sporadic point mutations. Mitochondria do not contain efficient excision/repair systems similar to the nucleus although the presence of DNA ligases (65), endonucleases (66) and glycosylases (67) do hint at a limited excision repair system (68). Uracil glycosylases do correct cytosine deamination but do not have excision repair systems to correct 5-

Figure 1

MITOCHONDRIAL GENOME MORBID DELETION MAP

Map depicting deletions that have been detected in mtDNA. The * indicates the KSS or common deletion as it is known. Note that all of these deletions occur between the origin of heavy strand replication (O_H) and the origin of light strand replication (O_L). This is considered to be the "hotspot" or area that deletions predominate.

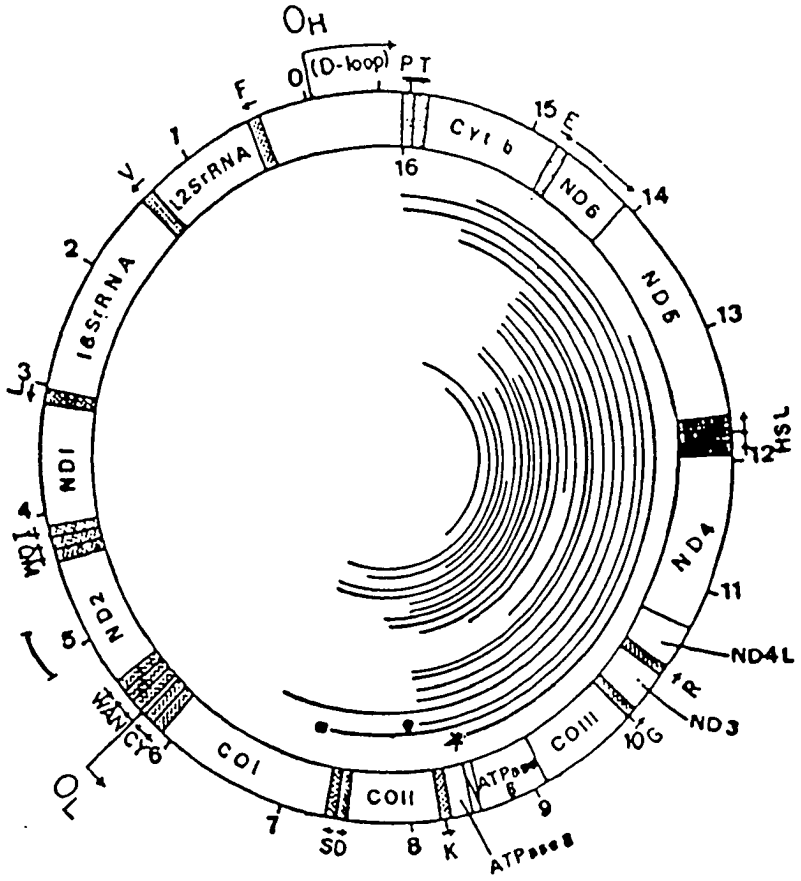

methyl cytosine deamination (69). The gamma polymerase which is responsible for mtDNA replication incorporates an incorrect nucleotide 1 every 8000 bp as compared to 1 per 30,000 bp for the alpha polymerase (70). A lack of protective histones around the mitochondrial genome further increases susceptibility to DNA damaging agents. All of these factors are believed to cause mtDNA to have a mutation rate that is 10 to 17 times that of the nuclear genome (71). Any of these somatic mutations can occur at different intervals of human development from embryogenesis throughout adult life. Thus, the development of point mutations in the mitochondrial genome could explain the sporadic nature of some cases of late onset AD that are believed to have a polygenic mode of inheritance.

Primary genetic alterations such as point mutations and deletions are not the only type of changes that occur in mtDNA with advanced age. Epigenetic changes such as hydroxylation, peroxidation, deamination and depurination may damage the mitochondrial genome. Oxidative damage of the mtDNA by reactive oxygen species is believed to be one major aspect of cellular injury and therefore aging (72,73). Approximately 1% of the oxygen used in the mitochondria is converted to the highly reactive superoxide radical O_2^- (74). Lipid peroxidation likewise induces mtDNA damage (75). Oxidative damage is observed by measuring the oxidized nucleoside, 8-hydroxydeoxyguanosine (8-OHdG). The presence of 8-OHdG is a result of oxidative damage since the adduct is due to base oxidation by the free radical, OH^-. It was found to be .02% in persons under age 55 whereas in subjects over 65 the level increased at a rate of 0.25% per decade (76). Additionally, in Alzheimer's brain, the level of 8-hydroxydeoxyguanosine was increased

significantly three-fold over age matched controls (77). The hypothesis that mtDNA is susceptible to free radical attack was first suggested by Harman (78) who believed that oxidative damage occurred in all cell types. However Miquel proposed that mtDNA damage and subsequent cell aging only occurred in differentiated (somatic) tissues and not in fast replicating cells. As Miquel stated:

> "Under normal physiological conditions replicating cells in the stem cell compartment and elsewhere do not suffer oxidation stress and resulting organellar injury, because of the relatively low rates of oxygen utilization in their mitochondria. By contrast, differentiated cells (especially fixed-postmitotic cells, such as neurons) sustain mtDNA mutation, inactivation or loss owing to the high mitochondrial respiration (with concomitant oxygen radical release) needed to support their specialized physiological work (74)."

While mtDNA replication can take place without cytokinesis or karyokinesis (79) the turnover of mtDNA is greater in highly proliferative tissue. Thus, mtDNA in neurons is in an ideal environment for the generation and accumulation of mutations. Ageing therefore would only compound the oxidative problems that are already taking place by a decreased ability to remove reactive oxygen species (67). Oxidative damage to mtDNA then may play an etiological role in age related neurodegenerative diseases such as Alzheimer's Disease.

Alzheimer's Disease therefore fits a number of criteria for establishing a defect in the mitochondrial genome:

1. MtDNA is susceptible to the generation of sporadic mutations. The majority of AD cases are sporadic showing no linkage despite many attempts at pedigree analysis.

2. Late onset AD is an age -related brain disorder. A number of age-associated mtDNA alterations have been observed in tissues with high oxidative demand such as brain. These mutations have been shown to increase as we age, thus, the accumulation of mutations fits the slow progressive disease course observed in late onset AD.

3. The population of normal and mutated mtDNA can drift towards entirely mutant or normal mtDNA or it can exist as a mixture of varying proportions of mutant and normal mtDNA. The threshold level at which symptoms are manifested are in part dependent on the mosaic pattern of expression determined by the mtDNA heteroplasmy; mitochondrial genetics could explain the delayed and altered gradients of cognitive deficits observed in different patients.

This hypothesis is further supported by biochemical studies which have found a deficiency in Complex IV (cytochrome c oxidase) of the respiratory chain in AD. Reduced activity of Complex IV was originally observed in platelets of AD patients (80,81) but a 17 to 26% reduction was later demonstrated in temporal and frontal cortex (82). This finding by Kish et al. was substantiated by another group that found cytochrome c oxidase (COX) activity to be severely defective in AD brain although Complexes I, II and III also showed some depressed activity (83). Three of the thirteen COX subunits COX I, COX II and COX III are encoded by mtDNA (Table 1). Since cytochrome c oxidase consists of subunits that are encoded by both nuclear DNA as well

as mtDNA it is entirely possible that the metabolic deficiencies are linked to a nuclear DNA defect, however, an investigation of mRNA levels for COX I, COX II and COX III found a reduction in the COX I and COX III message levels in the temporal cortex of brain autopsy tissue from Alzheimer's patients (84). This suggests a possible alteration directly in these mtDNA encoded subunits.

In fact, recently a mutation in mtDNA encoding $tRNA^{gln}$ has been reported to be associated with AD in as many as 3.2% of the cases examined (85). Additionally a 12s rRNA 9 bp insertion, a 16s $rRNA^{3196}$ variant, and an NADH dehydrogenase subunit 1^{3397} base change were detected in various AD patients (85) although these mutations have to be further characterized to determine what their relevance, if any, is in the pathogenesis of the disease. The possibility that other mtDNA mutations are associated with AD requires further investigation, especially those that may be age related such as deletions as well as a search for mutations in the cytochrome c oxidase complex.

B. STATEMENT OF PROBLEM

Alzheimer's Disease is a complex neurodegenerative disorder that affects a significant portion of the human population regardless of ethnicity or gender. Despite advances in understanding the early onset form of the disease the etiological agent in the majority of the sporadic late onset cases remains less well understood. A mitochondrial hypothesis of AD has been proposed based on a number of studies which establish altered oxidative metabolism in AD tissue. Mitochondria are cellular organelles that consume 90% of all oxygen incorporated and convert O_2 into cellular energy in the form of ATP. Of all the organs that require ATP for vital functioning, demand is most prevalent in the brain. Oxidative phosphorylation (OXPHOS) is a process that drives ATP synthesis across the inner mitochondrial membrane. Damage to OXPHOS proteins could severely impair brain metabolism thereby leading to a decline in certain cognitive functions. Four out of five complexes in the OXPHOS pathway are partly encoded by mtDNA thus this may be a crucial site of lesions that alter brain activity. Within the last decade a number of neuromuscular disorders, such as certain mitochondrial myopathies, have been found to be associated with mutations in mtDNA. These include MERRF, MELAS, LHON, LEIGH'S SYNDROME, NARP and KSS. AD patients share a number of similarities with the mitochondrial encephalomyopathies such as reduced oxidative metabolism, delayed onset of neurological symptoms often into late adulthood, slow progression and pathological changes that damage specific tissues with high ATP demand.

The overall aim of this study is to determine the role that mtDNA plays in Alzheimer's disease which could yield valuable information on etiology, the success of treatments that target OXPHOS deficiencies and potential diagnostic markers.

The investigation of mtDNA in AD uses tissue obtained from autopsy confirmed cases. The samples are frozen in liquid nitrogen immediately after autopsy yet variability exists in postmortem time. The initial phase of this study will determine by Southern analysis whether any gross mtDNA alterations are induced by postmortem tissue decay using a rat brain model. Southern analysis is effective at detecting deletions in patients with mitochondrial myopathies because a large percentage of the patients mtDNA is affected. However, Southern analysis does not provide the level of sensitivity necessary for measurement of deleted mtDNA in normal aged tissue. Sensitivity can be increased by using PCR-based methods. Thus current methods such as serial dilution PCR and kinetic PCR will be compared for consistency. Subsequently, AD patient mtDNA will be analyzed for the presence of the KSS deletion as well as for any novel deletions in the minor region of the mitochondrial genome.

The second phase of this study deals with the screening of mtDNA for point mutations in different regions of the genome but primarily in the COX I,II and III subunits. Restriction fragment length polymorphism (RFLP) analysis will be used to detect known mtDNA mutations whereas new variants will be identified by single strand conformation polymorphism (SSCP). Conditions for SSCP will first be optimized. The appropriate genes will be PCR amplified, restriction digested then electrophoresed on SSCP gels and polymorphisms will be confirmed by dideoxy sequencing.

The final stage of this research aims to develop an *in vitro* neuronal system for the study of mtDNA mutations. ρ^0 cells have previously been produced for this purpose. Originally the ρ^0 line was derived in cancer cells such as HeLa. A rat neuronal cell line that undergoes differentiation upon addition of nerve growth factor will be used in an effort to generate a novel ρ^0 system that can be used in the study of mtDNA mutations in neurological disorders. Progress on developing the rat ρ^0 will be described.

All of these studies will enable researchers to better define the significance, if any, of mtDNA abnormalities in Alzheimer's Disease.

CHAPTER II MATERIALS AND METHODS

A. EQUIPMENT

Tissue culture was done in a Purifier Class II Safety Cabinet (Labconco and SteriGard), CO_2 tanks were obtained from Norfolk Welders. Cell incubator was a Nuaire IR Autoflow, water baths were Precision Model 182 and Lab Line, the microscope was an Olympus CK2, the table top centrifuge was an IEC Centra MP4R, the spectrophotometer for quantitating DNA was an LKB Ultraspec II and the laser densitometer was a Pharmacia LKB Ultroscan XL. The thermal cycler used for PCR was a Barnstead Thermolyne Temp Tronic, the DNA synthesizer was a Cyclone Plus (Biosearch Inc.), power supplies used for sequencing were a BioRad Power Pac 3000 and an IBI MBP 3000D and the sequencing apparatti was from IBI. The dry bath incubator was from Fisher Scientific, the gel dryer was a BioRad Model 483, the speed-vac concentrator and refrigerant were from Savant and the crosslinker used for Southern analysis was a Stratagene UV Stratalinker 1800. All microfuges were from Beckman, balances were from Mettler, the land camera for all photographic work was a Polaroid MP4 and the UV transilluminator was from UVP.

B. MATERIALS

Taq polymerase used was from Perkin Elmer Cetus and Promega. The T_4 polynucleotide kinase, Proteinase K and the *fmol* kit were from Promega. All radioisotopes were from NEN. Various restriction enzymes were from Promega, Boehringer Mannheim and New England BioLabs. DNA molecular weight markers were from Promega. Primer synthesis kits and purification columns were from Milligen/Millipore, reagents for buffers were mainly from Fisher Scientific, and for mutation detection the MDE-Hydrolink gel was from J.T. Baker/A.P.Biochem. Silver Stain and Silver Stain Plus were from BioRad. For PCR purification Magic PCR Purification kits from Promega and Prep-a-Gene purification kits from Bio-Rad werre used. The Genius Chemiluminescent Detection kit was from Boehringer Mannheim. For Southern transfer MagnaGraph nylon membrane from Schleicher and Schuell was used. Tissue culture reagents such as RPMI 1640 powder, trypsin, antibiotics were from Gibco-BRL while the fetal bovine serum was from Hyclone and the donor horse serum was from JRH Biosciences. Disposables were from Fisher, Sarstedt and Costar) and polylysine, 6-thioguanine, Fungizone, pyruvate and uridine were from Sigma. Polaroid type 55 +/- film was from Qualex, Fuji RX autoradiography film Agarose High EEO, polyacrylamide and bis-acrylamide powder were from Fisher. SigmaCote from Sigma was used to siliconize plates.

C. RAT mtDNA AUTOLYSIS

Sprague Dawley rat brains were obtained from Dr. Dieter Bartschat of the Department of Physiology at Eastern Virginia Medical School. Veterinary care was provided by the Division of Animal Resources, Medical College of Hampton Roads. One to two month old rats were sacrificed by decapitation and brains were immediately placed in mitochondrial isolation buffer B (see Fig 2.) and frozen at -70°C. Since three rats were sacrificed at a time rat brains were collected over a period of 2 weeks and frozen at -70°C until 12 intact brains (minus the hippocampus which was being used for another experiment) were obtained for 6 time points. The experiment was repeated with another complete set of rat brains. Samples were then thawed on ice, weighed and placed in sterile weighing boats at RT for 0, 6, 12, 24 and 30 hours. At individual time points samples were placed in 2 mls Buffer B until DNA isolation. The average brain mass was 1.124g +/-0.013 and the amount of DNA recovered as determined by spectrophotometry ranged from 70 to 90 μgs.

1. Rat brain mtDNA isolation - Total DNA enriched for mtDNA was isolated from frozen rat brains using the techniques of Swierczynski (86) and Drouin (87) with modifications for the analysis of small amounts of tissue. The techniques were modified by omitting the cesium chloride differential centrifugation step. After proteinase K digestion, samples were phenol/chloroform extracted, ethanol precipitated, resuspended in 10 mM Tris/1 mM EDTA (TE) then dialyzed in TE overnight. (see Fig. 2 for

Figure 2

MtDNA ISOLATION FROM SMALL AMOUNTS OF BRAIN TISSUE

Mitochondrial DNA isolation procedure used for milligram amounts of brain tissue.

1. Weigh samples. Homogenize in Buffer B, 1 ml/100 mg of tissue (.25 M sucrose/5mM EDTA/10mM Tris-HCL pH 7.4) at 7 RPM using a teflon pestle.

2. Centrifuge homogenate at 1000 x g for 10 minutes. Discard nuclear pellet.

3. Centrifuge supernatant 16,000 x g for 10 minutes.

4. Resuspend mitochondrial fraction in 2mls Buffer C (.25 M sucrose/10mM Tris-HCL, pH 7.4).

5. Centrifuge 500 x g for 10 minutes. Discard pellet.

6. Sediment supernatant 7000 x g for 10 minutes.

7. Resuspend pellet in 1 ml Buffer D (25mM Tris pH 7.5/50mM EDTA/75mM NaCl).

8. Lyse with 10mg/ml Proteinase K (1mg/ml final), 20% SDS (1% SDS final) for 5 hours at 50°C or at 37°C overnight.

9. Phenol/Chloroform extract (1:1 volume, aqueous:organic) to remove protein.

10. Ethanol precipitate at -20°C overnight using 3M NaOAc (1/10 Volume) and 95% Ethanol (2x Volume).

11. Sediment precipitated DNA at 12,000 RPM for 30 minutes.

12. Wash pellet with 70% Ethanol, dry and resuspend in 10 mM Tris (pH 7.5), 1mM EDTA and store at 4°C.

complete description).

2. Southern transfer of Rat mtDNA

Approximately 2 μg of total rat DNA enriched for mtDNA was restriction digested with either Bam H1 (which cuts at np 9361 and np 14433) or Xho I (which cleaves at np 11178) and loaded onto a 0.8% TAE agarose gel and electrophoresed at 100 V until the xylene cyanol was three fourths of the way into the gel (~7 hours). Bands were visualized with ethidium bromide then prepared for transfer. The gel was depurinated in 0.25 N HCL for exactly 10 minutes, denatured twice (30 minutes each in 1.5 M NaCL, .5 M NaOH) then neutralized twice, (30 minutes each in 1 M Tris-HCL pH 8.0, 1.5M NaCl). The gel was transfered overnight using Southern transfer (88) in 10X SSC onto a nylon membrane (S & S Magna Graph) that was pretreated for 1 hour in 10 X SSC. The next day the DNA was crosslinked (Stratagene Stratalinker) at 120,000 μjoules/cm^2.

3. Chemiluminescent Detection

Cesium chloride purified placental mtDNA (see Fig. 3) to be used as probe was prepared according to the Genius™ System protocols (Boehringer Mannheim) with the following note: placental mtDNA was random primer labeled for 11 hours at 37°C but was not ethanol precipitated after labeling. The mass of the labeled probe determined as described by the manufacturer was estimated to be 400 ngs. Three membranes were prehybridized (.5x SSC, 1% blocking reagent, 0.1% N-lauroyl sarcosine, 0.02% SDS)

Figure 3

PLACENTAL MtDNA ISOLATION

DNA isolation procedure used to purify mitochondrial DNA from human placenta.

HUMAN PLACENTA SHOULD BE PREPARED WITHIN 30 MINS OF DELIVERY

1. Drain blood from placenta; remove membranes with sterile scalpel and weigh tissue.
2. Rinse tissue 3x's in Buffer A (0.9% NaCL/5 mM EDTA/10 mM Tris-HCL pH 7.4). [~600 ml/placenta]
3. Rinse tissue 2x's in Buffer B (0.25 M sucrose/5 mM EDTA/10 mM Tris pH 7.4). [400 ml/placenta]
4. Grind tissue in meat grinder.
5. Suspend in isolation media (Buffer B). [~100 g tissue in 200 ml]
6. Homogenize in glass blender.
7. Filter homogenate through three layers surgical gauze.
8. Centrifuge 1000 x g or 10 min. Discard pellet.
9. Sediment supernatant 10,000 x g for 10 min. [crude mitochondria]
10. Resuspend pellet in 70 ml Buffer C (0.25 M sucrose/10 mM Tris pH 7.4).
11. Centrifuge 500 x g for 5 min. Discard pellet.
12. Sediment supernatant 10,000 x g for 10 min.
13. Wash pellet once with 20 ml Buffer C.
14. Sediment 10,000 x g for 10 min. [~50 mg mtprotein/100g tissue]
15. Resuspend in 10 ml 25 mM Tris pH 7.5/50 mM EDTA/75 mM NaCl.
16. Lyse with 1.7 ml 10% SDS at 37°C for 5 min.
17. Add 3 ml 7 M CsCl and cool lysate on ice for 10 min.
18. Remove cesium dodecyl sulphate precipitate by centrifugation - 20, 000 x g for 10 min.
19. Add ethidium bromide to 500 ug/ml.
20. Adjust refractive index to 1.39 with solid CsCl.
21. Centrifuge in Vti65.1 for 16 hours at 55 k at 20°^C.
22. Collect lower band and recentrifuge at same conditions for 4 hours at 55k.
23. Collect lower band and extract with CsCl-saturated isopropanol.
24. Transfer to 30 ml corex tube and add 1x volume water and 2x final volume ethanol. Precipitate on ice for 30 min or overnight at 20°C.
25. Centrifuge at 10,000 RPM for 30 minutes at 4°C in JA-20 rotor.
26. Pour of supernatant and save.
27. Dissolve mtDNA pellet in 10 mM Tris (pH 7.9)/1 mM EDTA and store at 4°C.

at 65°C for 3 hours in a seal-a-meal bag in a rocking shaker. Afterwards, the same prehybridization solution was emptied into a 50 ml conical tube and the denatured probe was added directly for a final concentration of 10 ng/ml. Each membrane was hybridized overnight at 65°C in a separate bag. After hybridization, the membranes were washed twice (5 min each at RT) in 2X SSC, 0.1% SDS, once 15 min at RT in .5x SSC, 0.1% SDS, and a final wash for 15 min at 65°C in 0.5X SSC, 0.01% SDS. Detection was carried out essentially as described, however, we found that instead of discarding the blocking reagent after the blocking step the antibody can be added directly (first pour out blocking reagent, add antibody, mix, then cover membranes). Once Lumi-Phos™ was added the membranes were exposed to X-Ray film (Fuji) for 5 to 50 minutes. Films were scanned on a laser densitometer (Pharmacia LKB Ultroscan XL).

D. KSS ANALYSIS

1. Tissue Acquisition and Isolation of Brain mtDNA

Dr. W. W. Tourtelotte of the National Neurological Research Specimen Bank (NNRSB) kindly supplied brain samples. Tissue/fluid specimens obtained from the NNRSB, VAMC (VA Wadsworth Medical Center), Los Angeles, CA 90073, are sponsored by the National Institutes of Neurological Diseases and Stroke, National Institutes of Mental Health, National Multiple Sclerosis Society, Hereditary Disease Foundation, Comprehensive Epilepsy Program, Tourette Syndrome Association, Dystonia Medical Research Foundation, and Veterans Health Services and Research

Figure 4

TOTAL DNA ISOLATION FORM PARAFFIN-EMBEDDED TISSUE

Outline of total DNA isolation procedure used for paraffin embedded brain tissue.

Cut off excess paraffin while sample is on block and collect 8 micron slices using a microtome

↓

Place slices in . 5 ml microfuge tube

↓

Add 400 μl 100% ethanol, place at RT for 5 minutes

↓

Centrifuge 5 minutes, decant ethanol

↓

Air dry pellet at RT or in heat block at 50°C

↓

Add 150 μl sterile water and resuspend tissue

↓

Incubate tissue at 95°C for 10 minutes

↓

Centrifuge 5 minutes, collect pellet

↓

Digest tissue using 200 μg/ml proteinase K in 200 μl digestion buffer (50 mM Tris, 1 mM EDTA, .5% Tween 20)

↓

Incubate at 55°C for 3 hours

↓

Heat inactivate proteinase K at 90°C for 10 minutes

↓

Spin 5 minutes, collect supernatant for PCR

Administration, and Department of Veterans Affairs (Appendix A). Dr. Peter Davies of the Department of Pathology at Albert Einstein College of Medicine also provided frozen brain samples (Appendix B). Total DNA enriched for mtDNA was isolated from frozen autopsy brain samples as described for rat brains. Paraffin embedded brain tissue was obtained from Dr. William Rosenblum of the Department of Pathology at the Medical College of Virginia. Details of the paraffin DNA isolation are described in Fig. 4. Briefly, 8 micron paraffin slices were dissolved using xylene, digested with proteinase K then ethanol precipitated.

2. PCR Conditions and Primer Synthesis

Oligonucleotides, synthesized (Biosearch Cyclone Plus DNA Synthesizer) using phosphoramidite precursors, were column purified (Milligen Oligopak). Primer sequences were derived from the Cambridge human mitochondrial genome sequence (89) and were selected using Primer Designer Version 1.01. To amplify normal and deleted mtDNA PCR was performed (Barnstead Thermolyne Temp-Tronic Cycler) using a multiplex buffer (90). The 50 μl cocktail contained 1.5 mM each dNTP, 16.6 mM $(NH_4)_2$ SO_4, 67 mM Tris-HCL, 6.7 mM $MgCl_2$, 10 mM β mercaptoethanol, 170 μg/ml BSA, 6.8 μM EDTA, 20 pm each primer, 2.0 U *Taq* polymerase (Perkin Elmer Cetus) and 5 μl DMSO. Cycle parameters were 30 s @ 94°C, 30 s @ 53°C, and a 1 min extension @ 65°C. Primer sequences were as follows:

D_1 Left:	CCATCTTTGCAGGCACACTCATC	(np 4504-4526)
E_2 Right:	ATCCACCTCAACTGCCTGCTATG	(np 4955-4977)
J_1 Left:	AGCAAACCACAGTTTCATGCCCA	(np 8188-8210)
K_m Right:	TAATGTTAGTAAGGGTGGGGAAG	(np 13644-13666)
Li_1 Left:	TTCTCATAATCGCCCACGGG	(np 11700-11719)
L_2 Right:	GTCGTAAGCCTCTGTTGTCAGAT	(np 12172-12194)

3. Serial Dilution PCR

The serial dilution PCR method of Corral-Debrinski et al. (91) was used for quantifying deleted mtDNA. Total DNA was diluted in two ranges; one for deleted mtDNA amplification and one for wild type mtDNA amplification. Primers were synthesized (J_1-K_m) that span the deleted junction. Amplification across the deletion breakpoints yields a 500 bp fragment representative of the 4977 bp deletion whereas wild type DNA yields a 5478 bp fragment. If a short polymerization step is used; only the deleted 500 bp fragment will be amplified. However, instead of comparing wild type (5478 bp) to deleted mtDNA (500 bp), the ratio is determined using amplification of a product having a size similar to the deleted fragment. Thus, primer set D1-E2 which yields a 473 bp fragment was selected to amplify total mtDNA since this region near the light strand origin of replication is not as susceptible to deletions. Samples were linearized with Bam H1 (which does not cleave within the deleted area) prior to amplification. This was done in order to eliminate catenates of the mitochondrial genome which could alter access by primers. PCR products were electrophoresed on an 8%

polyacrylamide gel and visualized by ethidium bromide staining and UV illumination. Photographs were taken using Polaroid type 55 film and negatives were scanned using a laser densitometer (Pharmacia Ultroscan XL).

4. Kinetic PCR

Kinetic PCR was performed as described by Ozawa et al. (92). For kinetic PCR the same principle applies as for serial dilution PCR; the intensity of deleted mtDNA amplification products is compared to undeleted mtDNA PCR products. For kinetic PCR however, a ratio is generated based on normal mtDNA only (not total mtDNA). Primer set Li_1-L_2 amplifies a 494 bp fragment that is internal to the KSS deletion area, thus this amplification reflects only normal mtDNA. Each reaction contained the same starting amount of mitochondrial enriched DNA (25 ng). Reaction tubes were removed from 10 to 20 cycles for undeleted mtDNA (Li1-L2) and stopped from 22 to 32 cycles for deleted mtDNA (J1-KM). [α-^{32}P] dATP (7 Kbq; 800 Ci/mM) was added to each PCR tube. Products were separated by gel electrophoresis, the gel was dried and radioactivity was determined by phosphorimaging (Molecular Dynamics PhosphorImager SF).

E. MINOR REGION ANALYSIS

1. PCR Conditions

Primer set B_1-F_2 (1257-5720) was used to amplify the minor region of brain mtDNA using the following cycling parameters: 30 s @ 94°C, 30 s @ 58°C and either 1 min

(short program) or 5 min (long program) @ 65°C. A standard PCR buffer (90) (50 mM Tris-HCl, pH 8.4, 50 mM KCl, 1.5 mM $MgCl_2$. .01% gelatin) containing 200 μM each dNTP, and 0.5 μM each primer (final conc.) was used in a 100 μl reaction volume. Primer sequences were as follows:

B_2: 5'GCCAGTTGATTAGGGTGCTT 3' (np 1257-1276)

F_2: 5'TATACCGCCATCTTCAGCAA 3' (np 5700-5720)

2. Restriction Digestion and Dideoxy Sequencing

All digests for restriction mapping were carrried out at 37°C. Sanger dideoxy cycle sequencing (93) was performed using the *fmol* kit (Promega). Primers were synthesized to give a sequence read length of 250 to 350 bp using 1.5 hr and 3.0 electrophoretic hr runs @ 65 W. Specific primers were end-labeled with T_4PNK and [γ-^{32}P] ATP (3000 Ci/mM). To obtain sequence data further from the primer, some electrophoretic separations were for 4 to 5 hours. Template was PCR amplified then purified with either Magic PCR Preps (Promega) or Prep-a-Gene DNA Purification kits (BioRad). The final *fmol* reaction volume was 6 λ to which an equal amount of dye (95% formamide, 0.25% BPB, 0.25% XC) was added. The samples were denatured at 95°C for 3 minutes and 3 λ was loaded on either 6 % or 8 % Instagels (8 M Urea), electrophoresed, transferred to 3M Whatman and exposed overnight without an intensifying screen.

F. DIAGNOSTIC RESTRICTION ENZYME DIGESTION

1. Mutation Detection in Brain

Analysis for the MERRF^{8344}, MELAS^{3243}, ND1^{3397} and tRNA$^{gln\ 4336}$ mutations were primarily done in the same manner; the region of interest was PCR amplified followed by restriction enyme digestion in which case the presence of the mutation created a restriction site. Since these mutations are heteroplasmic containing both mutant and normal mtDNA, [α-^{32}P] dATP was incorporated into the PCR products during amplification to increase detection of low amounts of heteroplasmy. Sequences for the MERRF mismatch primers were obtained from Siebel et al. (94). The remaining primer sequences were designed by Primer Design Version 1.01 and are based on the human mitochondrial sequence except for T_1 which is derived from bovine mitochondrial DNA.

MER_1: 5'CCCCTCTAGAGCCCACTGTAAAGC (np 8282-8305)

MER_2: 5'GGGGCATTTCACTGTAAAGAGGTGCCGG (np 8345-8372)

T_1: 5'TACGACCTCGATGTTGGATCAGGAC (np 2980-3004)

B_2: 5'CGATTAGAATGGGTACAATGAGG (np 3330-3352)

C_1: 5'GCAATGGCATTCCTAATGCTTAC (np 3352-3375)

D_2: 5'ACTTGATGGCAGCTTCTGTGGAA (np 4496-4506)

2. Mutation Detection in Lymphoblasts

Fifteen lymphoblast cultures from AD patients, unaffected spouses and age matched controls were supplied by Dr. P. Michael Conneally of the Department of

Medical and Molecular Genetics at Indiana University, Alzheimer's Disease Cell Bank (Appendix C). Cell lines were received in frozen ampules and were thawed one at a time in a 37°C water bath. Cells were grown in 5% CO_2, 15% FBS/RPMI 1640 media containing antibiotics and glutamine. Cultures were split every 2 to 3 days. DNA enriched for mtDNA was isolated as for small scale brain isolation (Fig 1.) from approximately 2 - 4 x 10^6 cells.

G. SINGLE STRAND CONFORMATION POLYMORPHISM ANALYSIS

1. SSCP-PCR Conditions

The COI, COII and COIII subunits were screened using the mutation detection technique, single strand conformation polymorphism (SSCP) (95,96). Left and right primer sequences are listed below; primers with subscript 1 notation represent the light strand sequence and subscript 2 denotes the heavy strand.

COI_1:	(np 5900-5919)	5' ACTGATGTTCGCCGACCGTT
H_2:	(np 6451-6473)	5' GATTAGGACGGATCAGACGAAGA
I_1:	(np 6471-6492)	5' ATCACAGCAGTCCTACTTCTCC
COI_2:	(np 7581-7600)	5' CGCTGCATGTGCCATTAAGA
$COII_1$:	(np 7600-7620)	5' GCAAGTAGGTCTACAAGACGC
I_2:	(np 8167-8189)	5' CTCCACAGATTTCAGAGCATTGA
J_1:	(np 8188-8210)	5' AGCAAACCACAGTTTCATGCCCA

$COII_i$:	(np 8421-8438)	5' GGGTGATGAGGAATAGTGT
$COIII_1$:	(np 9186-9205)	5' CTACCTGCACGACAACACAT
$COIII_2$:	(np 10126-10145)	5' GCCGTTGAGTTGTGGTAGTC

Complex IV genes were PCR amplified in separate tubes (Barnstead Thermolyne TempTronic Cycler) from brain mtDNA using a multiplex PCR buffer (1.5 mM each dNTP, 16.6 mM $(NH_4)_2$ SO_4, 67 mM Tris-HCl, 6.7 mM $MgCl_2$, 10 mM β-mercaptoethanol, 170 μg/ml BSA, 6.8 μM EDTA, 20 pm each primer, 2.0 U *Taq* polymerase (Perkin Elmer Cetus) and 5 μl DMSO). Cycle parameters were: 30 sec @ 94°C, 30s @ 53°C and a 2 min extension at 65°C.

The COI gene (5904-7444) was amplified using two primer sets: COI_1 -H_2 and I_1 -COI_2, the COII gene (7586-8262) using primer sets: $COII_1$ - I_2 and J_1 -$COII_{2i}$ and COIII (9207-9990) using $COIII_1$ - $COIII_2$. The PCR-amplified regions were labeled by incorporating [α-^{32} P] dATP during amplification and restriction digested @ 37°C for 2 hours to yield fragments of optimal size for SSCP (Table 2). The digestion products were heat denatured in 95% formamide, 20 mM EDTA and electrophoresed in a 0.5X MDE, 10% glycerol-hydrolink gel (J.T.Baker) for 16 hours at 8 W then autoradiographed usually for 3 days with an intensifying screen. Sanger dideoxy cycle sequencing was performed as described above. Optimization of SSCP was done using the LHON cell line which was a generous gift of Douglas C. Wallace, Department of Genetics and Molecular Medicine, Emory University School of Medicine.

Table 2

RESTRICTION DIGESTS USED TO OPTIMIZE SSCP MUTATION DETECTION

Amplified Region	Restriction Enzyme Digest	Size of Fragments[a]
COI:		
COI_1-H_2	Hae III	233,213,127
I_1-COI_2	HpaII, XbaI	354,236,162,160,117,100
I_1-COI_2	HpaII, PstI, BglI	386,246,162,117,100,60,48
COII:		
$COII_1$-I_2	Hae III	303,286
J_1-$COII_{2i}$		250
COIII:		
$COIII_1$-$COIII_2$	SfaN1, HhaI, HincII	236,194,185,157,131,56
$COIII_1$-$COIII_2$	AluI, HhaI, HincII	370,264,194,131

[a] Restriction enzyme generated DNA fragments are arranged in order of decreasing size not in order of position along the original PCR amplified region.

2. Silver Staining

Silver staining was done according to the method of Anolles and Gresshoff (97). Acrylamide gels were fixed (1.5 mm thick, 15x18 cm) in 50 mls of 7.5% acetic acid for approximately 15 minutes. Gels were then washed in ultrapure water 3 times for about 4 - 6 minutes each. Silver impregnation was then accomplished by soaking gel in 50 mls of 1.5g/L $AgNO_3$, 0.056% formaldehyde for about 45 minutes. After a brief rinse in sterile water, the gel was developed in 30g/L Na_2CO_3, 0.056% formaldehyde, 400ug/L sodium thiosulfate. This solution should be between 8-10°C and image development took between 5 to 20 minutes. Image development was then stopped with cold (4°C) 7.5% acetic acid.

H. PC-12 ANALYSIS

1. Generation of rho zero (ρ^0) cells

One flask of PC-12 (HGPRT$^-$) cells were obtained from Llyod A. Greene, Department of Pathology, Columbia University, New York, New York. Cells were transferred into 75 cm^2 flasks that were pretreated with polylysine to aid cell adhesion. This was done according to the method of Yavin et al. (98). 100x polylysine stock solution was diluted to 1x in 10mM Na_2CO_3. Phenol red was added, the pH was adjusted to 9.0 to 9.3 (solution turns a deep purple) then filter sterilized. Polylysine was added to flasks

for 30 min then removed, flasks remained at RT for another 30 min then were washed (2x with sterile water). Flasks were placed at 4°C until needed. Cells were routinely grown in 7% CO_2, 5% fetal bovine serum/10% horse serum/RPMI 1640 media that contained antibiotics (25 units/ml penicillin, 25 μg/ml streptomyocin), glucose (4500 mg/L) and Fungizone (.5μg/ml). To more accurately determine cell density prior to an experimental measurement, cell clumping was prevented by treatment with EGTA (99). PC-12 cells were removed from the flask surface by positive pressure, centrifuged to collect cells, then resuspended in 1 mM EGTA media. Cells were returned to flasks and remained in EGTA/RPMI media for six hours. After this treatment cells were collected in 50 ml conical tubes and washed in medium diluted 1:1 with sterile water (twice, 2800 RPM, 5 min spins). After the last wash cells were forcefully resuspended in complete media and counted. The generation of ρ^0 cells was designed according to the method of King and Attardi (100) with modifications. Cells were cultured in EtBr at two different concentrations for 7 days (100 ng/ml and 200 ng/ml) at a density of 2 x 10^5 cells/ml in 12 well plates, 1 ml/well. The EtBr concentrations were based on methods described by (101, 102,103,104). The EtBr concentration was then increased to 500 ng/ml and 1000 ng/ml for an additional 11 days. One group of cells were supplemented with pyruvate (1mM/ml) and uridine (.05mg/ml) as follows:

EtBr	Py	Ur
0 ng/ml	(-)	(-)
100	(-)	(-)
200	(-)	(-)
0	(+)	(+)
100	(+)	(+)
200	(+)	(+)

At 3 day intervals cells were assessed for viability and cell growth using trypan blue exclusion in triplicate. After counting, cells were centrifuged and cell pellets were frozen at -70°C until DNA isolation. At day 18 two sets of wells/experiment were counted and the third set of cells were expanded into 10 cm petri dishes. These cells are presently being maintained in 0, 100, and 200 ng/ml EtBr supplemented with pyruvate and uridine.

2. Southern Transfer and Chemiluminescent Detection

To assess mtDNA content of drug treated PC-12 cells, Southern hybridization was performed using chemiluminescent detection as described in part C, section 3.

I. BIOHAZARDOUS PRECAUTIONS AND USE OF HUMAN SUBJECTS

Lymphoblast cell lines obtained from the Alzheimer's Disease Cell Bank are EBV transformed. Tissue culture was done in a Labconco Purifier Class II Safety Cabinet. All personnel involved in this project have been certified to handle radioisotopes. Vertebrate animal (rat) decapitation was carried out in the Department of Physiology by Troy Rhodes however, Dr. Frank Castora has animal welfare assurance #A3012-01. Pathological specimens are exempt from IRB review according to exemption #4 (exemption for autopsy samples).

CHAPTER III. RESULTS

This study began when it was reported that deleted mtDNA had been linked not only to mitochondrial myopathies such as KSS, but also with the general aging process and with Parkinson's Disease (PD). Previous studies have pointed out the similarities between AD and PD and have identified common features suggesting that AD and PD may be on a clinical spectrum. Therefore, we undertook a study of deleted mtDNA of AD patients in order to assess the involvement of mutant mtDNA in this degenerative disease. We obtained brain tissue and lymphoblast cultures from AD and neuropathologically normal individuals and began an investigation. As we progressed we realized that specific issues had to be resolved; this included the use of frozen postmortem tissue in the analysis as well as appropriate methods for studying deletions. Thus, the first section of this project addresses these issues. Afterward we assessed deleted mtDNA involvement. In phase II we looked at point mutations in the genome using RFLP analysis. Later, we turned towards recently developed mutation detection systems such as heteroduplex and SSCP to unmask point mutations that do not lie in restriction sites. After optimizing SSCP we applied this technique to mutation analysis in AD and aged patients. The final phase, the ρ^0 study, reflects a rather recent avenue that we embarked upon. Currently, it does not directly involve the study of AD mtDNA but it was designed with the intent of eventually using it for AD complementation studies

and represents the first attempts at developing this unique neurological system.

A. STUDY OF MITOCHONDRIAL DELETIONS IN BRAIN

1. Integrity of Brain Mitochondrial DNA during Postmortem Delay

The investigation of mtDNA isolated from brain autopsy tissue of human subjects has the potential for complications caused by tissue decay (autolysis). Samples are frozen at -70°C immediately after autopsy yet variability existed between the time of death and subsequent time of freezing (postmortem delay). To address the question of whether any significant mtDNA degradation is induced during postmortem delay, a kinetic study was designed using rat brain tissue. Using a small scale isolation, total DNA enriched for mtDNA was purified without the need for extensive overnight CsCl gradient ultracentrifugations. Time points were taken for intact rat brains that remained at room temperature for 0, 6, 12, 24 and 30 hours. MtDNA was restriction digested with Bam H1 or XhoI, then electrophoresed on an 8% agarose gel. To enhance detection of abnormal mtDNA, chemiluminescent Southern analysis was performed. Fig. 5, lanes 1 - 5 shows a Bam H1 digest of the isolated rat mtDNA which generates an 11226 bp and a 5072 bp fragment. From this initial blot one can see that the mtDNA appears to be intact even after 30 hours. However, there seems to be a large amount of undigested

Figure 5

SOUTHERN ANALYSIS OF POSTMORTEM RAT BRAIN MtDNA

Southern blot of rat mtDNA digested with Bam H1. Bam H1 generates two bands of 11226 bp and 5072 bp. DNA was isolated from brain tissue that remained at room temperature for 0, 6, 12, 24 and 30 hours. In the origin of lanes 2 and 3 one can see undigested mtDNA. The DNA was probed with CsCl purified placental mtDNA.

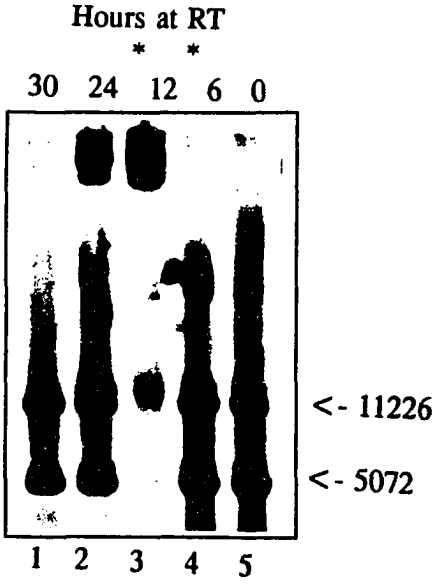

mtDNA near the origin for the 12 hr and 24 hr time points as seen in Fig. 5 lanes 2 and 3. This was probably due to a large amount of salt carry over during the ethanol precipitation step. This may have been due to an extended precipitation overnight at -20°C . Thus, samples were redigested in a larger volume of sterile water in order to decrease the salt concentration. Fig. 6 more clearly demonstrates that there was no gross deletions or insertions generated as a result of the brains remaining at RT for 30 hours in either the Bam H1 (lane 1) or the Xho I digest (lane 5). (Time point 6 for the Bam H1 digest was accidentally lost after digestion). Additionally digestion appeared complete as evidenced by the lack of slow molecular weight products near the origin. However, upon extended film exposure of the blot shown in 6, numerous bands appeared in the Bam H1 digest, Fig. 7, lanes 1 - 4 but not in the Xho I digest lanes 5 - 9. We believe that the appearance of bands in the Bam H1 digest does not reflect degradation of mtDNA due to postmortem delay; instead it is most likely due to star activity of the enzyme. Star activity refers to the loss of specificity of restriction enzymes under conditions of high enzyme concentration, variation in pH or changes in salt concentration. Of these three factors the last seems the most probable and very likely. (Salt crystals were visible after precipitation). The loss of specificity for the Bam H1 recognition site, **GGATCC** could result in four other sites which would produce numerous cuts in rat mtDNA. These four potential sites are as follows:

GGAT: 157 sites, **GATCC:** 15 sites, **GGATC:** 15 sites and **ATCC:** 157 sites. On the other hand the Xho I recognition site, **CTCGAC** does not lend itself to any 5 or 4 bp restriction sites in rat mtDNA. This explanation is supported by the extended exposures

Figure 6

SOUTHERN ANALYSIS OF RAT MtDNA WITH BAM HI AND XHO I

Southern blot of rat digests with Bam H1 (lanes 1-4) and XhoI (lanes 5-10). XhoI linearizes rat mtDNA into a 16298 bp band. Bam H1 generates an 11226 bp and 5072 bp band. Hours at RT are indicated above the lanes.

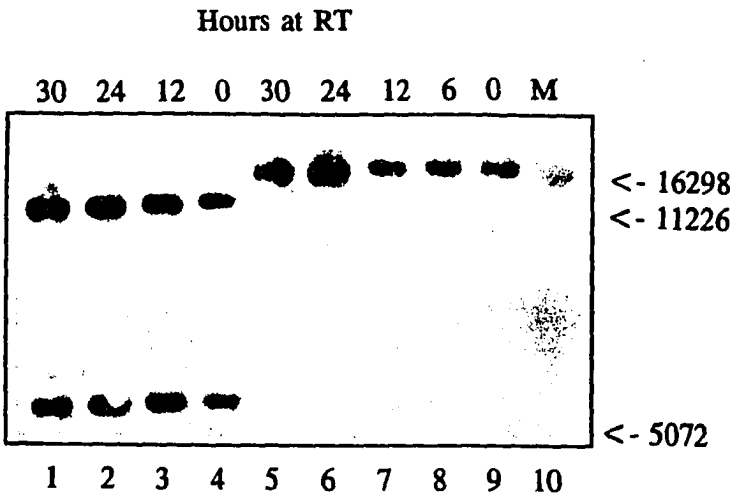

Figure 7

EXTENDED CHEMILUMINESCENT EXPOSURE OF RAT MtDNA SOUTHERN BLOT

Extended exposure of the Southern blot shown in Fig. 6. Discrete minor bands appear in the Bam H1 digests but not in the XhoI digests.

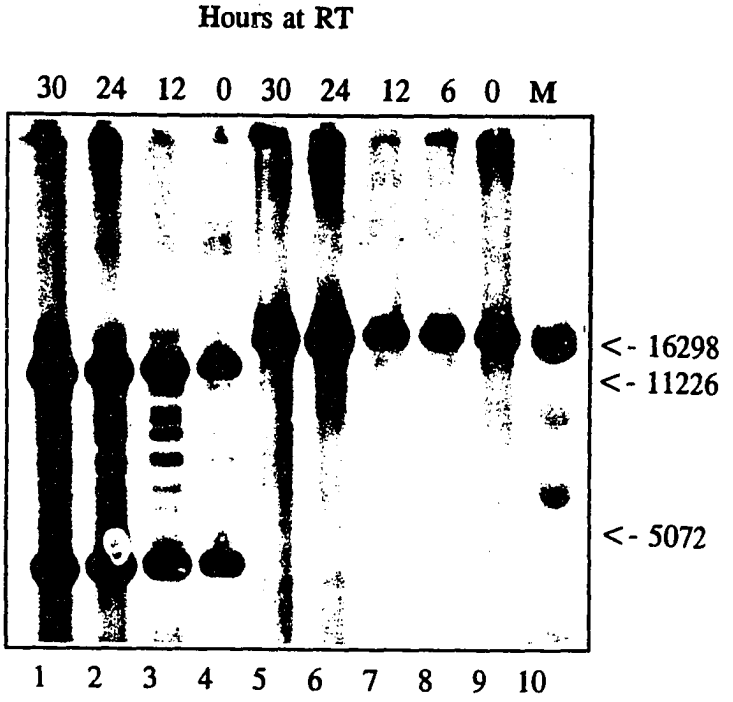

and densitometric scans of the chemiluminescent Southern blots for the Bam H1 and Xho I digests. If the mtDNA was indeed actually being degraded, then the extended Xho I exposure would have revealed other species of mtDNA similar to the extended exposure of the Bam H1 digest. If, on the other hand, the enzymes were beginning to exhibit star activity, then the Bam H1 digest should show an increased number of bands while the Xho 1 digest (which does not lend itself to star activity) would still only show one band (linearized mtDNA) upon extended exposure. This is the case as seen in Fig. 7 (lanes 5-9) where only 1 band was detected after the 30 min exposure.

Densitometric scanning was also done on the chemiluminescent Southern blots to determine whether there were other species of degraded mtDNA that was not evident upon visual examination. Fig. 8 shows the area scan peaks for the 12 hour timepoint. The 10 min exposure indicates that for both the Bam H1 (A) and the Xho I digest (B) no intermediate size DNAs were produced. (The 1 % peak for the Bam H1 digest is due to a spot on the film in this lane). The 30 min exposure similar to the actual blot indicates that for the Bam H1 digest minor species of mtDNA are evident (C) whereas the Xho I digest (D) still shows only one peak representative of linearized mtDNA.

Figure 8

DENSITOMETRIC SCANS OF RAT MtDNA SOUTHERN BLOTS

Densitometric scans of the Southern chemiluminescent blots of rat mtDNA isolated for studying effects of postmortem delay. (A) and (B) represent traces of the 12 hour timepoint lane seen in Fig. 6. (C) and (D) represent traces of the same lane for the extended exposure blot shown in Fig. 7.

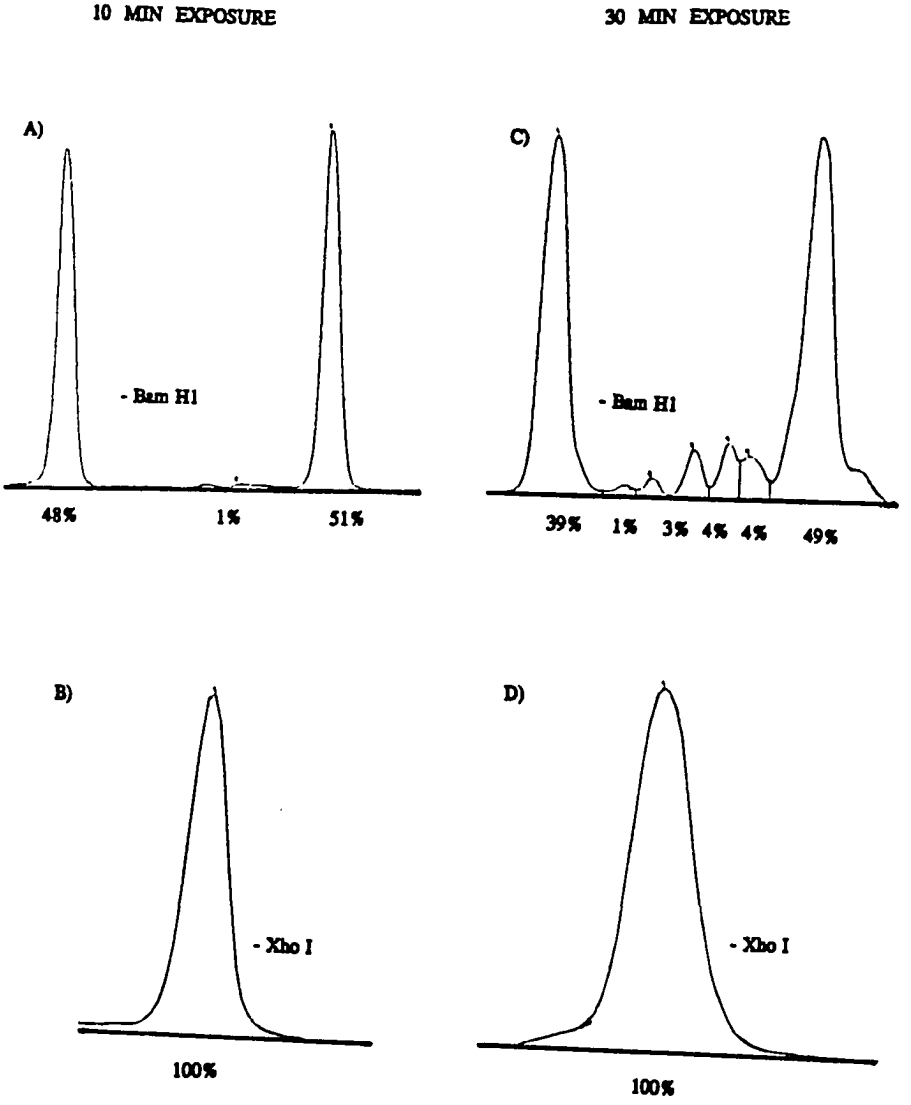

2. *Comparison of Quantitative Methods Used in Deletion Studies*

Since our rat study on autolysis indicated, that even after having sat at room temperature for 30 hours no appreciable mtDNA degradation occurred, we proceeded to investigate the well characterized $mtDNA^{\Delta 4977}$ (bp 8470- bp 13477) in AD brain. PCR primers that flank the deletion region were used to discern deleted from undeleted mtDNA. Although primers have been published that scan the deletion area, we used a left primer, J_1 (8188) that was previously synthesized in the lab and prepared a new right primer KM_2 (13666). The right primer was selected based on primer pair criteria described in the **Methods.** If the $mtDNA^{\Delta 4977}$ is not present, a 5.5 kb PCR product is generated whereas the deleted PCR product is only 500 bp (Fig. 9). A long extension time of 5 min was used to allow amplification of both deleted and undeleted mtDNA. As can be seen in Fig. 10 the samples seem to fall into three categories: one is composed almost entirely of deleted mtDNA; another has about a 50:50 distribution of deleted and normal mtDNA; and the third has a small amount of deleted DNA but a predominance of normal mtDNA (105). Since a large proportion of the $mtDNA^{\Delta 4977}$ seemed to be present in some of the AD samples, we reasoned that the deleted mtDNA should easily be visible by Southern hybridization. For this analysis mtDNA from 9 AD samples was linearized with Bam H1; normal undeleted mtDNA is 16 kb long whereas the $mtDNA^{\Delta 4977}$ yields an 11 kb band. Southern analysis of these 9 AD samples did not reveal any 11 kb bands indicating that the high proportion of deleted mtDNA in Fig. 10 was, perhaps, the result of preferential amplification of the smaller undeleted band during

Figure 9

DIAGRAM DEPICTING PCR AMPLIFICATION ACROSS THE KSS DELETION JUNCTION

Map depicting location of the Kearns-Sayre Syndrome (KSS) deletion and PCR primers used to amplify across the junction breakpoints.

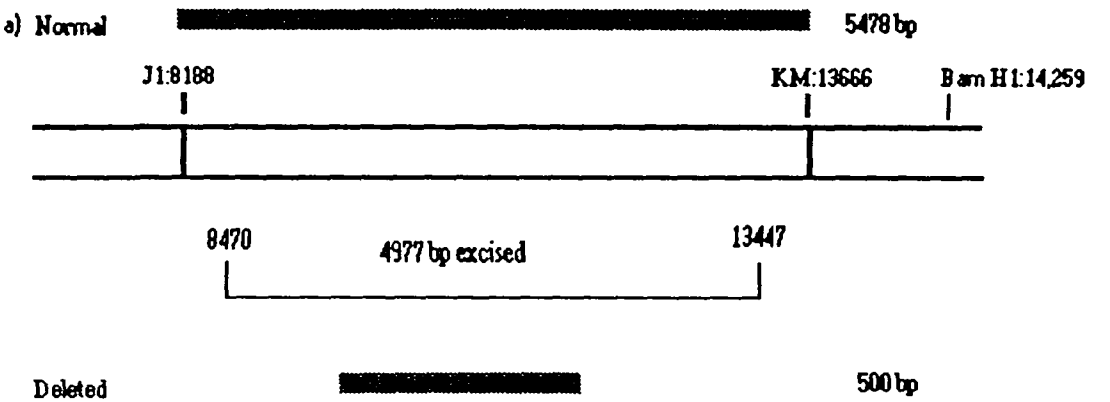

b) Sequences flanking breakpoints

CCACACCT ACCTCCCTCACCA / AAGCC.....CTTCA ACCTCCCTCACCA / TTGGCA

Figure 10

DETECTION OF THE KSS DELETION IN AD AND AGED BRAIN

Agarose gel of PCR amplification of mtDNA from Ad patients using primers flanking the 5 kb deletion associated with KSS and aging. Lane a, marker, lane b - o, frozen Ad brain samples (note that many samples have the 500 bp fragment indicative of deleted mtDNA. Note also that a number of samples have a mixture of deleted and undeleted mtDNA); lane p, PCR amplification of human placental mtDNA; lane q, PCR amplification of HL60 mtDNA.

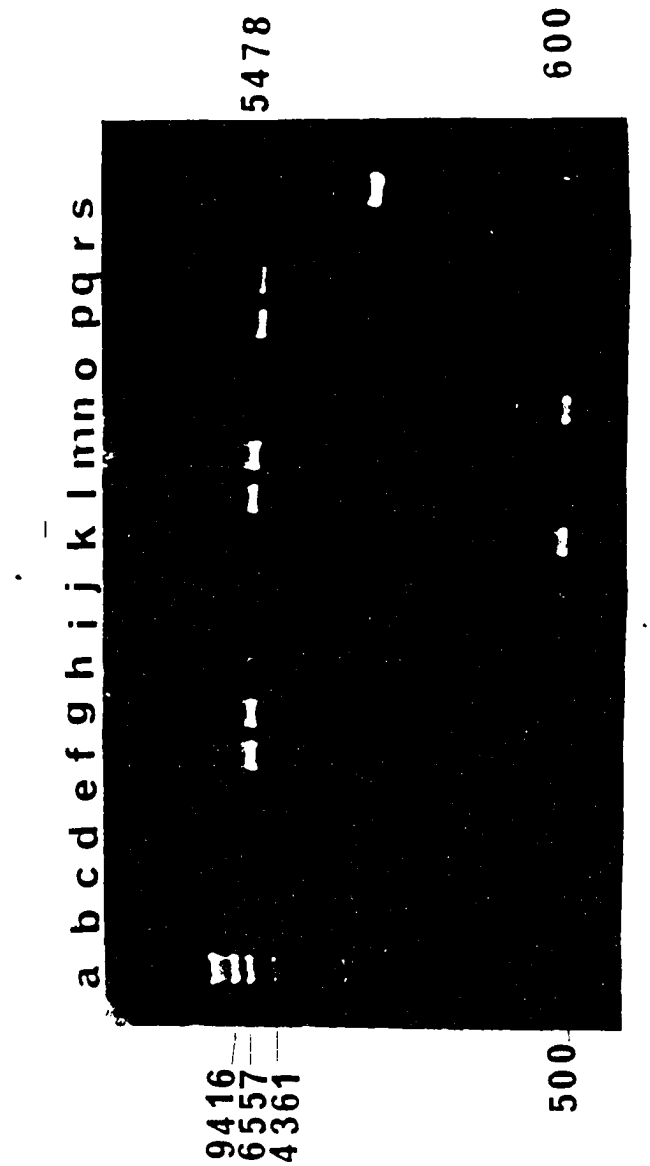

long extension PCR. Thus, in order to better measure the KSS deletion we turned to two PCR-based methods for measuring deleted mtDNA, serial dilution PCR and kinetic PCR. As we began to work with both of these techniques we observed that these two methods were yielding disparate results. This was an important observation in light of the fact that in articles aimed at reviewing the role of mtDNA deletions in aging and neurodegenerative disease the percent of deleted mtDNA in different tissue types is compared from studies using different quantitative approaches (106,107). Thus we sought to determine how comparable the PCR-based methods are in their estimation of deleted mtDNA given the propensity for PCR amplification to vary due to cycle efficiency, structure of the template, the presence of tissue inhibitors, and primer requirements. We have compared the two most widely used techniques by determining the amount of the $mtDNA^{\Delta 4977}$ in two regions of the brain from autopsy tissue of an individual with lung cancer (108).

Quantitation of deleted mtDNA by serial dilution PCR - We used a serial dilution PCR procedure to quantify the amount of deleted mtDNA in two regions of the brain from a patient with lung cancer (CA). The parietal cortex and the caudate were selected because these regions often show neuronal degeneration in neurodegenerative diseases such as Alzheimer's Disease and Parkinson's Disease. The primers D1-E2 would be expected to amplify a 473 bp DNA fragment from total mtDNA (both wild type and deleted) in the sample while the primers J1-Km would give a 500 bp PCR product amplified only from deleted mtDNA. Fig. 11 shows such PCR products generated using

Figure 11

SERIAL DILUTION PCR GEL OF THE KSS DELETION IN A LUNG CANCER PATIENT

Serial dilution PCR of the common deletion 5 kb deletion in parietal cortex from a lung cancer patient. Polyacrylamide gel of PCR products representing amplification of deleted mtDNA (500 bp) and total mtDNA from serial dilutions. MtDNA was diluted in two ranges, one for deleted mtDNA (.25 μg - 976 pg) and another for undeleted mtDNA (.5 ng - 1.95 pg) amplification. Starting concentrations were determined by spectrophotometry at 260 nm.

DNA samples from the parietal cortex. The left half of Fig. 11 shows a serial dilution of the 500 bp product decreasing as the amount of substrate DNA is reduced from 250 ng to 976 pg. It can be seen that a significant amount of deleted mtDNA is detectable at all levels of input DNA examined. Similarly, as seen in the right half of Fig. 11, there is the expected decrease in the 473 bp PCR product amplified from total mtDNA as the amount of input DNA is reduced from 500 to 1.95 pg.

The ratio of deleted to wild type mtDNA was determined by densitometric measurement of the intensity of each DNA band and subsequent plotting of the optical density versus the log of weight of DNA in the reaction mix. The optical density was adjusted so that the area of each DNA band was normalized by the size of the DNA fragment. A typical result of this quantitation is shown in Fig. 12. In order to calculate the ratio of deleted mtDNA, the plots of deleted and wild type PCR products generated by J1-Km and D1-E2, respectively, were examined to determine the logarithmic values on the x axis at which the optical densities of the deleted and undeleted PCR products were equivalent. To maintain accuracy using the serial dilution method it is important that an O.D. value is selected that is within the linear range of the density curve and has low standard deviation. For Fig. 12 an O.D. of 1.4 was used to determine the amount of deleted mtDNA (17.78 pg) and total mtDNA (12,590 pg). Thus, by serial dilution PCR methodology, in this patient's parietal cortex there is a ratio of deleted mtDNA:total mtDNA of 0.0014 or a percentage of deleted mtDNA of 0.14%.

Table 3 shows the results of this analysis for the parietal cortex as well as the caudate region of this CA brain sample. Interestingly, the identical analysis of the

Figure 12

OPTICAL DENSITY GRAPH OF SERIAL DILUTION PCR FOR QUANTITATION

After visualization with ethidium bromide, negatives were scanned by laser densitometry to determine the area of each band. A plot of normalized optical density versus the log of the weight of DNA was generated for both primer sets. A ratio of deleted to undeleted mtDNA was determined by locating a unit of equal optical density for both plots, then comparing the DNA weights needed to yield such an O.D.

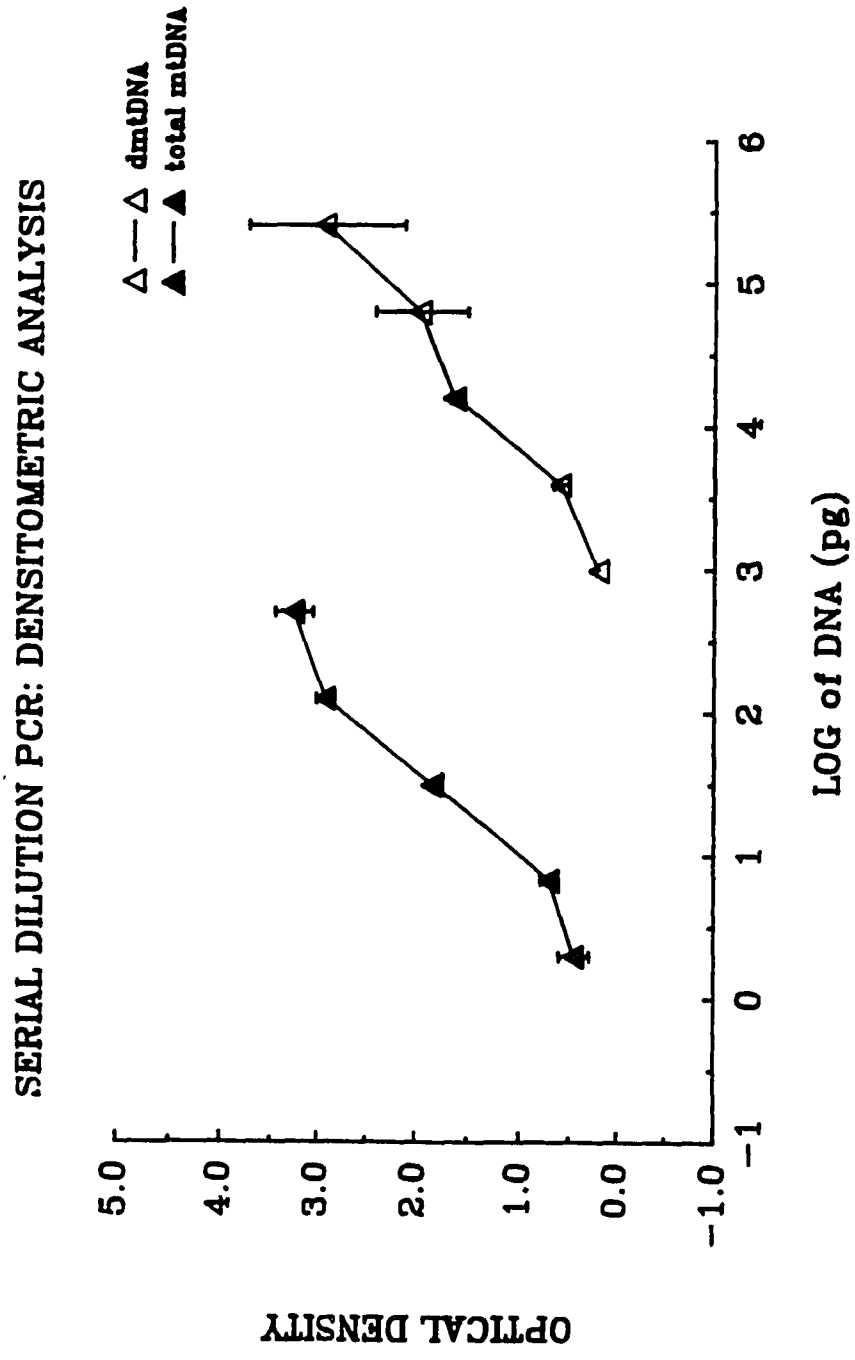

Table 3

PERCENTAGE COMPARISON OF THE KSS DELETION AS DETERMINED BY KINETIC PCR AND SERIAL DILUTION PCR

Region	Percentage of the 5 kb common deletion by:	
	Serial Dilution PCR[a]	Kinetic PCR[b]
Parietal Cortex	0.14[c]	3.16
Caudate	1.41	12.58

a. by optical density
b. by phosphorimaging
c. tissue analyzed in triplicate

caudate region showed that there was a 10-fold higher percentage of deleted mtDNA in the caudate of the CA brain than in the parietal cortex (1.41 vs 0.14%).

Quantitation of deleted mtDNA by kinetic PCR - The same CA brain sample was assessed for the amount of deleted mtDNA by another often used procedure - the kinetic PCR method. In this approach, PCR products were examined after variable cycles of reaction, usually ranging from 10 to 40 cycles depending on whether total or deleted DNA were to be detected. Fig. 13 shows that the 500 bp band of deleted mtDNA produced from primer J1-Km is visible after 24 cycles and it increases in intensity up to 32 cycles. Similarly, to assess the amount of normal mtDNA, primers Li1-L2 were used to generate a 494 bp fragment, which is detectable at low cycle numbers due to the greater amount of normal mtDNA in these samples.

During the amplification reaction, radioactive dATP was included so the quantitation of these samples was obtained by phosphorimaging. A plot of log of pixel density versus cycle number was used to determine the ratio of deleted mtDNA to normal mtDNA (Fig. 14). Pixel density was normalized by the number of A's present in each fragment. Extrapolation to zero cycles allows estimation of the ratio of wild type to deleted mtDNA in the starting material. For the parietal cortex sample seen in Fig. 14, this ratio is 0.001/0.0316227 indicating that the percentage of deleted mtDNA is 3.16%. A similar kinetic PCR analysis of the caudate yielded a value of 12.58% for deleted mtDNA. Thus, there is about a 4-fold higher amount of deleted mtDNA in the caudate than in the parietal cortex, as determined by kinetic PCR (Table 3).

Figure 13

KINETIC PCR GEL OF THE KSS DELETION IN A LUNG CANCER PATIENT

Kinetic PCR quantitation of the common deletion in parietal cortex from lung cancer patient. Polyacrylamide gel electrophoresis of PCR products generated by Li1-L2 (494 bp fragment internal to KSS deletion, reflecting normal mtDNA) and J1-KM (500 bp fragment from deleted mtDNA).

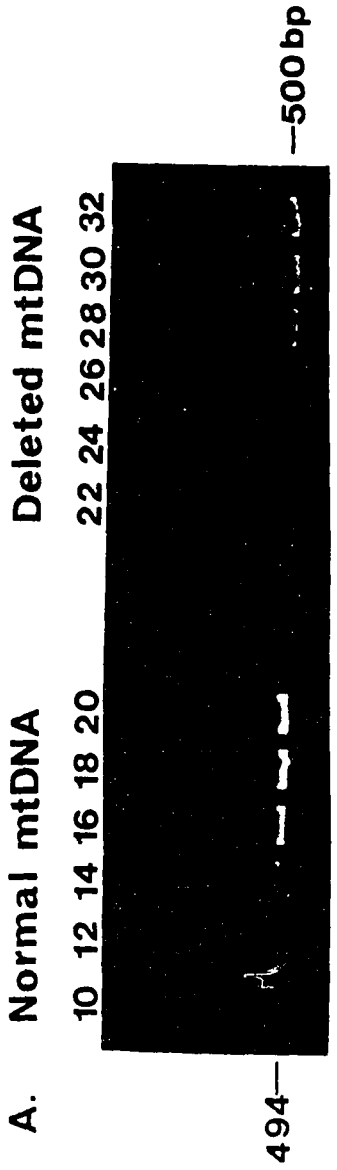

Figure 14

RADIOACTIVITY GRAPH OF KINETIC PCR FOR QUANTITATION

The gel was dried at 60°C for 1 hr and radioactivity was quantified by phosphorimaging. A plot of normalized radioactivity versus the number of PCR cycles is used to calculate a regression line from normal and deleted mtDNA. Extrapolation to 0 cycles is used to determine the starting ratios of deleted to wild type mtDNA.

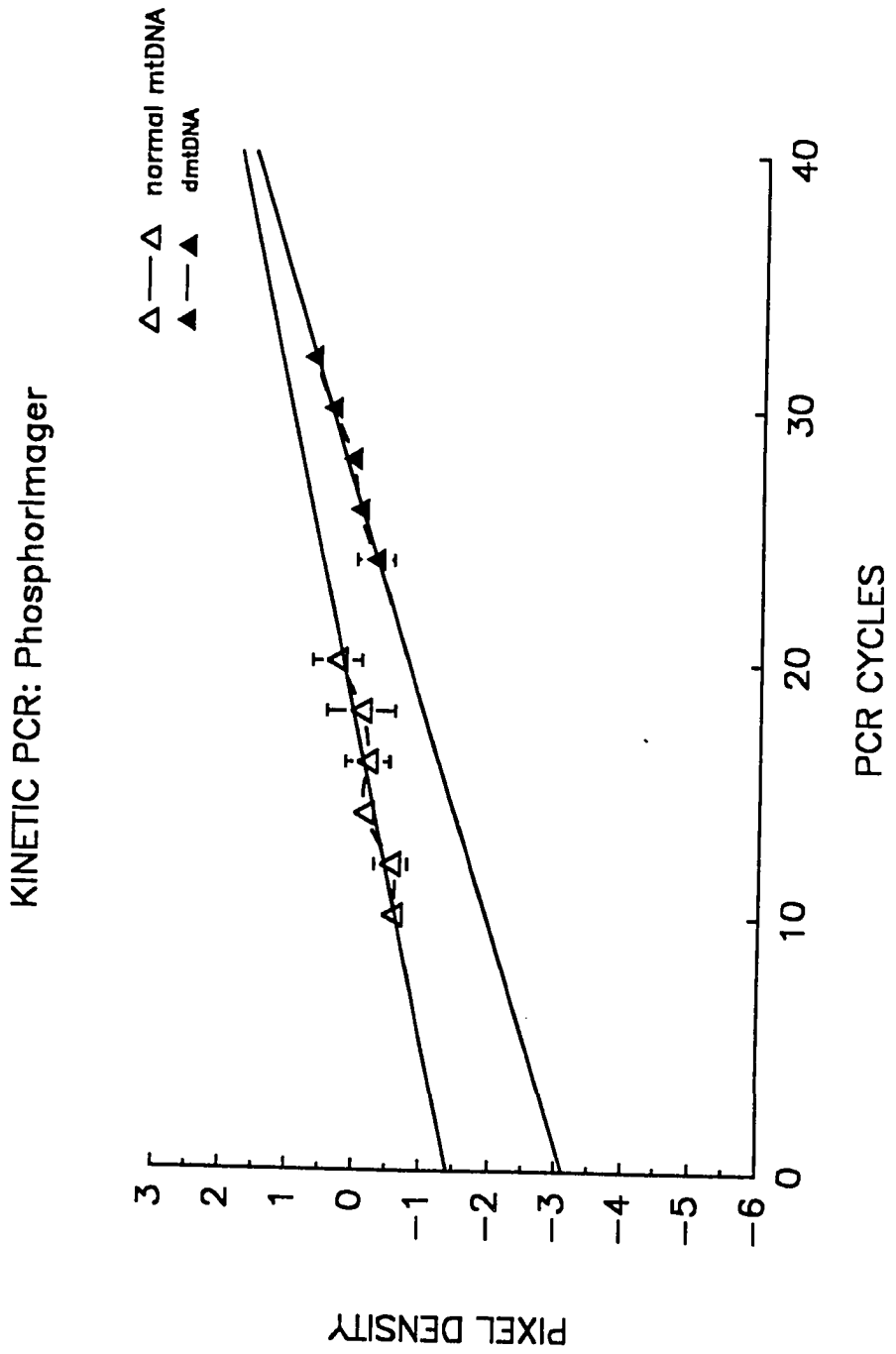

For accurate kinetic PCR it is necessary to perform preliminary amplification to determine the linear range in which to work. For example, if the number of cycles selected is too high, the later PCR cycle products will be in a plateau region, and thus, the PCR products will be amplified to the same intensity. As seen in Fig. 15, from 32 to 40 cycles there is no increase in amount of PCR product being amplified. Therefore, inclusion of data in this cycle range would skew the regression line leading to an overestimation of the percentage of deleted mtDNA. If, however, time points are taken from 22 to 32 cycles, a linear range of amplification can be achieved. In Fig. 16, PCR products were run on a polyacrylamide gel and bands scanned using laser densitometry to determine optical density. As can be seen, cycles 12 -18 for wild type and cycles 24 - 30 for deleted mtDNA yield points in a linear phase of amplification.

Figure 15

AGAROSE GEL OF PLATEAU EFFECT - KINETIC PCR

Plateau effect when cycle points for kinetic PCR are taken during the non-linear range of amplification. For kinetic PCR it is essential to empirically determine the linear range of amplification for deleted mtDNA. For time points 32 to 40, amplification using J1-KM resulted in bands of equal intensity when stained by ethidium bromide.

Figure 16

OPTICAL DENSITY PLOT DURING NON-LINEAR PHASE OF AMPLIFICATION

As determined by scanning the negatives taken of the EtBr stained gel a plot of O.D. versus the number of cycles for the same sample indicates that a range of 22 to 32 cycles results in amplification in the linear range.

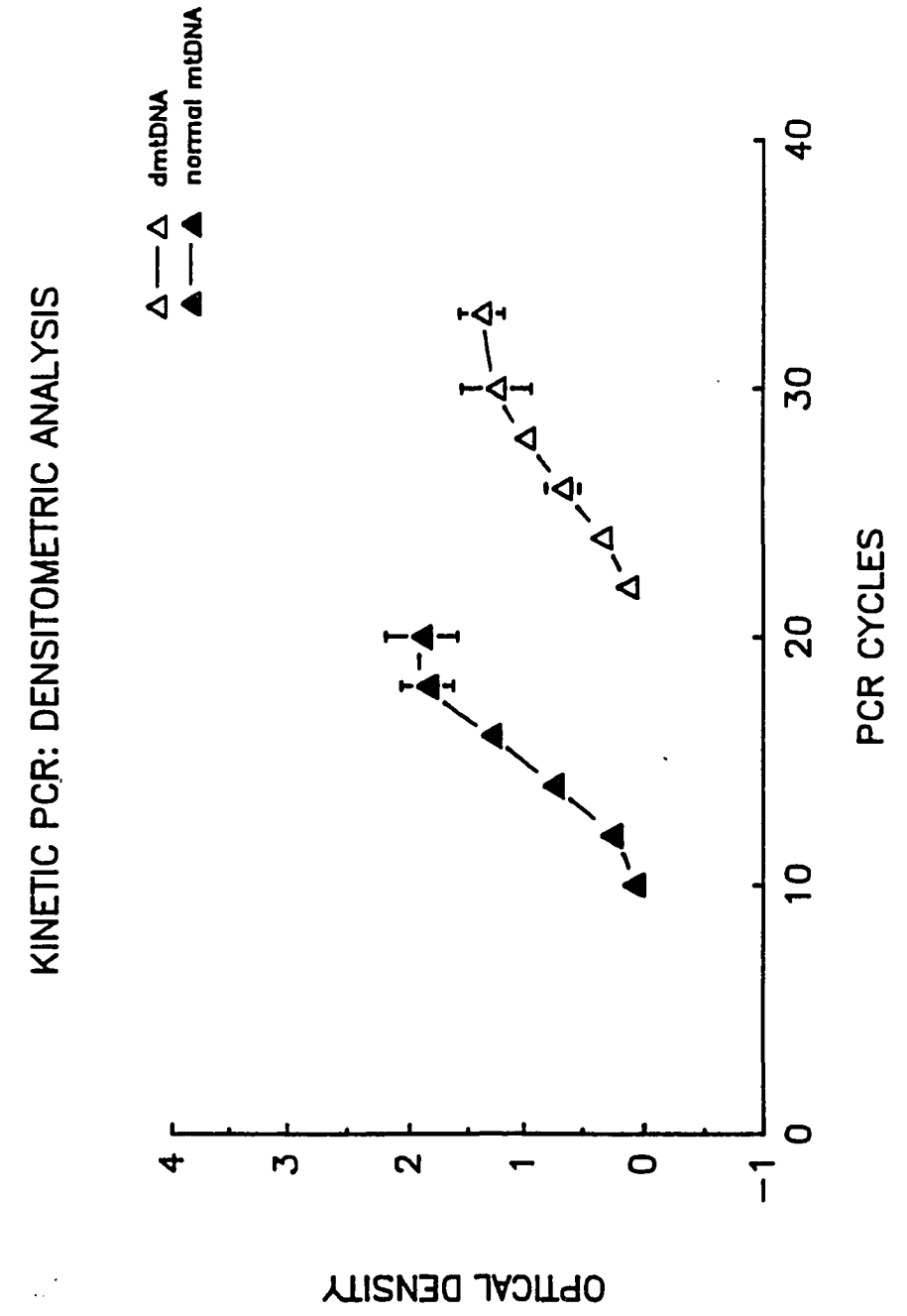

3. *Evaluation of mtDNA$^{\Delta 4977}$ in Alzheimers's Brain versus Aged Individuals*

Since serial dilution PCR seemed to be a more accurate method for measuring deleted mtDNA we proceeded to use this technique in our study of the KSS deletion in AD brain. Initially we used mtDNA that had been isolated from paraffin embedded tissue. While we could amplify mtDNA from these samples the amplification was often sporadic. Later, we received frozen brain tissue which yielded consistent positive PCR, thus, we continued our investigation with the frozen autopsy samples rather than the paraffin embedded tissue. We wanted to assess the difference in mtDNA$^{\Delta 4977}$ in the hippocampus, an area predominantly affected in AD with plaques and tangles. However, tissue in this area was almost impossible to obtain from any of the brain banks. We were able to obtain tissue from the parietal cortex, caudate and temporal cortex; of these three regions the temporal cortex is most affected by plaques and tangles. Thus, mtDNA was prepared from the temporal cortex of 5 AD subjects with a median age of 69 yrs and from 5 control subjects with a median age of 68 yrs. All of the control brain samples were histologically normal whereas the AD brain tissue were all autopsy confirmed. The percentage of mtDNA$^{\Delta 4977}$ was calculated as described in the previous serial dilution section. As can be seen in Table 4 the mean % mtDNA$^{\Delta 4977}$ for the control group was .0053% while the AD group had a level of .0628%. This represents a 12 fold difference for the Alzheimer's group. To determine statistical significance the mean % mtDNA$^{\Delta 4977}$ was compared using the student's t test. Since the variance for the two groups was different, .008 (AD) vs .00003 (control) a separate t-test instead of a pooled t-test was

Table 4

QUANTITATION OF THE KSS DELETION IN TEMPORAL CORTEX OF AD AND AGED BRAINS

GROUP 1 ALZHEIMER'S				GROUP 2 CONTROL		
CASE #	AGE	% DELETED		CASE #	AGE	% DELETED
1537	64	.0070		1569	61	.0079
1802	65	.2230		1413	67	.0014
694	68	.0141		1539	68	.0013
576	72	.0560		1903	70	.0141
1807	75	.0138		1846	73	.0016
Mean Age: 69 yrs Mean % $mtDNA^{4977}$: .0628% +/-.041 s^2 = .008				Mean Age: 68 yrs Mean % $mtDNA^{4977}$: .0053% +/- .003 s^2 = .00003		

performed. A t-value of 1.4 was obtained with a p = 0.116 for a one-tailed test and p = .223 for a two tailed test. For one AD case # 1802 the % $mtDNA^{4977}$ is almost 10 fold higher than the other samples in this group. If we treat this point as an outlier then the mean level of the KSS deletion in the AD group is .0027% which represents a four fold difference over the control group level of .0053%. The four fold difference is not statistically significant at the .05 to .10 level. The t values and variances were calculated using formulas described by Munro, Visintainer and Page (109) and QuattroPro Version 5.0. Each sample was analyzed in duplicate. No conclusions could be made for the parietal cortex and caudate since the AD samples for these regions are at minimum 10 years older than the control group.

4. Minor Region Analysis

Whereas most deletions such as the KSS deletion occur between the H_s and the L_s origins of replication in the "hotspot" region of the genome minor region deletions can occur. Wei et al. detected a 3 kb deletion ($mtDNA^{\Delta 3610}$) in aged skeletal muscle in the minor region at a CCCC junction (110). The authors noted that this deletion had not been detected in other tissues examined. This is an unusual observation because most mtDNA deletions associated with mitochondrial myopathies accumulate as we age in a number of tissues with the exception of hematopoietic tissue due to its high turnover rate. Thus we wanted to determine first whether this deletion occurred in aged brain and second whether there any unique minor region deletions associated with AD. To detect

Figure 17

DIAGRAM OF PCR AMPLIFICATION OF MtDNA^{3610} MINOR REGION DELETION

Map depicting location of the skeletal muscle deletion in the minor region of the genome.

The PCR primer pair used to detect this mutation is shown as well.

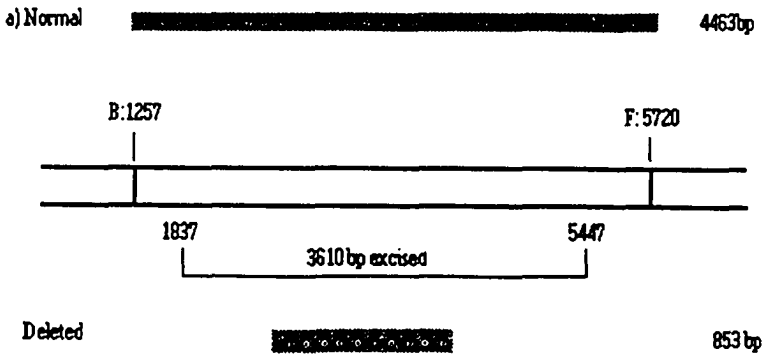

the mtDNA$^{\Delta 3610}$ PCR amplification across the deletion junction (bp 1837-bp 5447) similar to the KSS amplification was performed using primer pair B_1 (bp 1257)- F_2 (bp 5720). The presence of the mtDNA$^{\Delta 3610}$ should generate an 853 bp band as depicted in Fig. 17. However no bands migrating at 853 bp was detected in either the AD brain tissue or in any normal aged brain using a short (1 min) extension time for the PCR. Rather another smaller molecular weight band was observed that was migrating at approximately 600 bp (Fig 18A. lanes A, B) while a long extension time of 5 minutes amplified the expected undeleted product of 4463 bp (lanes C and D). We proceeded to restriction map the 600 bp band using the restriction enzymes HincII, Kpn I, Pvu II, Xba I, Hha I and Hae III. The 600 bp band was electroeluted and reamplified for restriction analysis. This was a necessary step due to the small amount of this deleted product visible on the acrylamide gel.

The cleavage sites and the respective cleavage products expected for the B_1-F_2 4463 bp band are summarized in Table 5. Restriction digestion of the 600 bp deleted band (Fig. 18B) with Kpn I; lane B, Pvu II: lane C, and Xba I; lane C, resulted in a single undigested band indicating that the 2573, 2650, 2953 recognition sites are missing (Table 5). The Hinc II digest at first glance appears to generate only an uncut band but upon closer examination of the negative there is faint small molecular weight band of approximately 30 bp (Fig. 18C, lane A). This band was not readily detected in the polaroid print since as a small band it does not bind a large amount of ethidium bromide. Thus, the Hinc II data indicates that the 2421, 3597 recognition sites are missing but not the 5691 site (Table 5). Taken together this information indicates that np 2421 -> 3592

Table 5

EXPECTED RESTRICTION ENZYME DIGESTS - MINOR REGION RFLP

Enzyme	Cleavage Position	Fragments Expected (bp)
Hinc II	2421, 3592,5691	2099,1171,1164,29
Kpn I	2573	1316,3047
Pvu II	2650	1393, 3050
Xba I	2953	1696,2797
Hha I	1301,1472,1768,2941, 3161,3698,4530	1190,1173,832,537,296, 220,171,44
Hae III	1463,2173,2567,3146, 3315,3412,3427,3607, 3849,3958,4428,4481, 4563,4848,5226,5261	710,579,470,459,394, 378,285,242,206,180, 169,109,97,82,53,35,15

Figure 18

PAGE GEL OF RFLP ANALYSIS TO IDENTIFY A UNIQUE DELETION IN THE MINOR REGION

Deletion analysis in the minor region of human brain mtDNA. Using primer pair B_1-F_2 (1257-5720) we detected a unique band of approximately 670 bp. (A) Lanes A and B, PCR using a 1 min extension on an AD and MS caudate sample; lanes B and C, the same samples using a long 5 min extension. The undeleted 4 kb band is visible as well as the 670 bp band, lane E, marker. (B) the 670 bp band was restriction mapped with Hinc II lane A; Kpn I, lane B; Pvu II, lane C; Xba I, lane D; Hha I, lane E; Hae III, lane F. Lane G, markers.

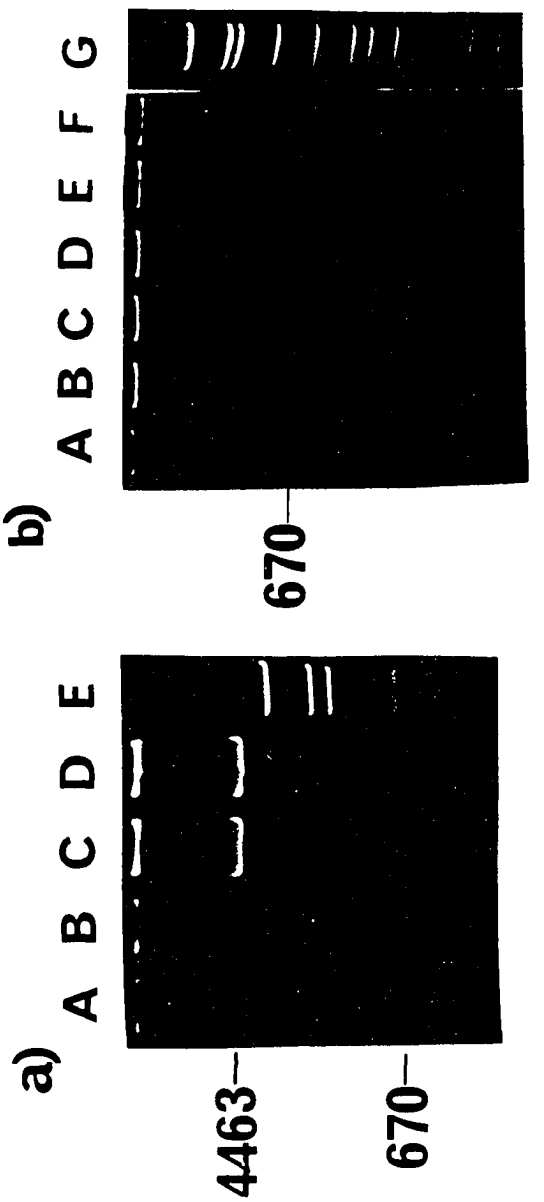

are missing, however np 5691 -> np 5720 is present. Hha I digestion yields three bands, one at ~ 450 bp, another at 170 bp and a third at ~ 44 bp. Again here, the 44 bp band was only visible in the negative (Fig. 18C, lane E). The Hha I digestion reveals that at least the np 1257-> 1301 and 1301->1472 are present since the expected bands from these sites are generated (Table 5). All other expected fragments are missing. There is also a 450 bp band present which is not expected given the Hha I cleavage sites. This could be due to partial digestion or it may be that a particular site is mutated. A point mutation at site 1768 could explain the presence of the 450 bp band in the following manner: if site 1768 is mutated and we include the 3.8 kb deletion, then a 443 bp band would be generated as diagrammed below:

1472----------1768------1893----------5698----5720

↓ ↓ ↓ ↓

296 bp 125 bp deleted ~3800 bp 22 bp

296 + 125 + 22 = 443 bp

This would not necessarily be unexpected since the Hha I site, **GCGC**, is known to be a highly polymorphic site. The Hae III digestion is expected to generate numerous bands however only two bands of ~ 460 bp and 250 bp are evident (lane F). The 460 bp band is most likely due to cleavage at np 5261 and 5720 which yields a 459 bp band. However, analysis of the 250 bp band is unclear since there are 6 possible cleavage sites that produce fragments around this size: 1257-1463 (207), 3607-3849 (242) and 4563-4848 (285). A summary of all of the restriction data reveals that np 2421-3592 is missing while np 1257-1472 and np 5691-5720 is not deleted.

Before proceeding to sequencing of the deletion breakpoints we tested the specificity of the B_1-F_2 primer set since it was possible that the 600 bp product was actually the result of mispriming rather than a true deletion. Thus, we amplified the primer set under different conditions of magnesium concentration, an ion which is known to increase stringency of the reaction. The addition of $MgCl_2$ to a final concentration of 1 mM greatly enhanced amplification (Fig. 19A laneA) whereas 3 - 9 mM inhibited amplification (lanes B,C and D). When AD and aged brain tissue was amplified with 1 mM $MgCl_2$ to increase primer specificity the 600 bp fragment was still evident (Fig. 19B lanes A-F). Additionally, it seemed that even with the short extension time of 1 min the undeleted 4463 bp band was also amplified in some of the samples (lanes A and C). Since the 600 bp band seemed to indicate a true deletion product we proceeded to sequence the deletion breakpoints. As restriction mapping data indicated that np 1257-1472 was intact we synthesized left primers at 1488_1, 1702_1, and 1941_1. The 1488_1 and 1702_1 primers gave readable sequence data whereas the 1941_1 lanes were blank as if the primer had no complementary site to which to anneal. According to the read data the deletion spans 1893-5698 or 1899-5703 ($mtDNA^{\Delta 3800}$). A "**GCTAAG**" motif was found to bracket the deletion breakpoints. Unfortunately closer investigation of the "**GCTAAG**" indicated that the F_2 left primer was indeed misannealing. As seen in Fig. 20 the F_2 primer does have the potential for forming 11 Watson-Crick bonds around np 1900. After a few rounds of PCR this primer sequence generates a new template in this region such that sequencing comparison to the Cambridge mitochondrial sequence would appear as if a jump to np 5700 had taken place.

Figure 19

MgCL SENSITIVITY OF B_1-F_2 PRIMER SET

Effect of $MgCl_2$ concentration on primer pair B_1-F_2 PCR reaction. (A) Amplification with placental mtDNA, lane A; 1 mM, lane B; 3 mM lane C; 9 mM, lane D; marker. (B) Amplification on control and AD brain tissue, lanes A through F using 1 mM $MgCl_2$.

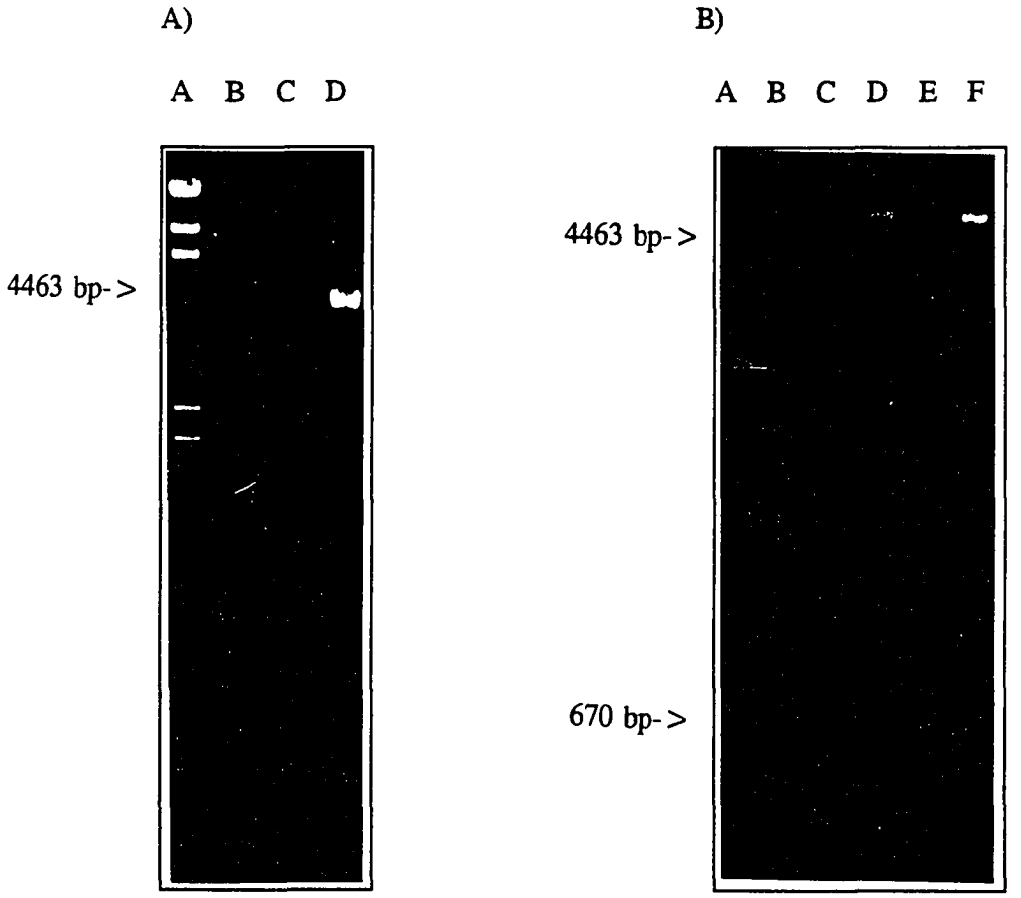

Figure 20

SCHEMATIC OF MISPRIMING BY F_2 RIGHT PRIMER

Region of mitochondrial genome that depicts mispriming by right primer F_2. F_2 can hybridize to its exact complementary sequence at 5720 as well as base pairing incorrectly around nucleotide position (np) 1900.

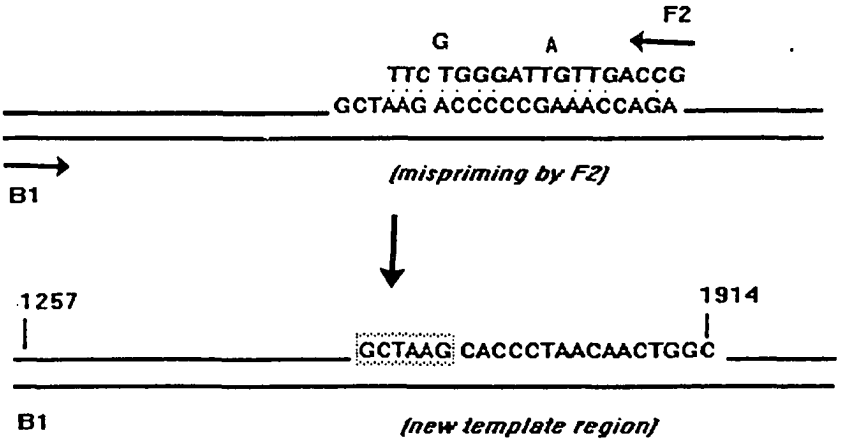

Our investigation of the presence of deletions in the hotspot region of mtDNA suggested a difference in the accumulation of a specific deletion that is elevated in the temporal cortex of AD brain. However, we decided to pursue another avenue of research that we believed would better lead to understanding mitochondrial abnormalities in AD. This is not to say that the deletion studies should not be continued. However, numerous other groups had started to look at the level of the KSS deletion in AD brain (111,112,113). Additionally, we reasoned that while the accumulation of specific deletion would have implications on energy metabolism in the brain of AD patients, the deletion measurements have been in general a very small percentage of the normal mtDNA, usually less than 1%. When the disease termed KSS is actually diagnosed, over 50% of the mtDNA has to be deleted in order for dysfunction to be manifested. Corral-Debrinski et al. have documented the greatest amount of the KSS deletion in AD brain approximately 10% (111). However, such a large percentage should be be easily visible on a Southern blot - thus, how accurate this measurement is may be difficult to assess until the Southern analysis supports these elevated percentages. Additionally, the KSS deletion deletes a number of subunits and complexes (part of ATPase 8, all of ATPase 6, COIII, ND3, ND4L, ND4 and part of ND5); thus, one should expect to see a generalized systemic defect in all of the OXPHOS complexes not necessarily only Complex IV. Therefore, for these reasons, we proceeded to analyze AD brain tissue for specific point mutations that could explain some of the specific respiratory chain deficiencies and physical symptoms in AD. We wished to determine whether the muscular deficits such as myoclonus, rigidity and seizures seen in Alzheimer's

patients were linked to mtDNA mutations that are known to cause muscle wasting such as that seen in the mitochondrial myopathies MERRF and MELAS. Additionally, we screened for two mtDNA mutations that occur in an elevated frequency in AD and Parkinson's Disease (PD) individuals.

C. KNOWN MUTATION ANALYSIS - MERRF, MELAS AND AD-ASSOCIATED

MERRF is the result of an A -> G transition in $tRNA^{lys}$ at np 8344. This mutation is detected using mismatch PCR which creates a Nae I restriction site in positive individuals. A 90 bp fragment was amplified using MER_1 - MER_2 (8282-8372) which is cleaved into a 64 and 26 bp fragment if the mutation is present. (Fig. 21A). [α-^{32}P] dATP was incorporated during amplification. Since the MERRF mutation is heteroplasmic, staining of acrylamide gels with ethidium bromide would not be sensitive enough to detect a small percentage of mutant mtDNA. Thus, gels were dried then exposed to autoradiography film. With this increased sensitivity however, there was still no evidence of the MERRF mutation in these samples. (Table 6).

The primary mtDNA mutation associated with MELAS is an A->G transition at np 3243 in $tRNA^{leu}$. This mutation can be detected by either the creation of a Hae III or an Apa I site (Fig. 21B). A 372 bp fragment using primer set T_1-B_2 (2980-3352) was PCR amplified. With Apa I the 372 bp fragment is cleaved into 263bp and a 109 bp fragments if the A -> G transition is present whereas Hae III digestion cleaves a 169 bp

Figure 21

DIAGNOSTIC RESTRICTION ENZYMES USED TO IDENTIFY THE MERRF, MELAS, $tRNA^{gln}$ AND ND1 MUTATIONS

Diagnostic restriction enzyme digestion used to detect the MERRF, MELAS, AD-ND1 and AD-$tRNA^{gln}$ mutations. (A) The MERRF A->G substitution at np 8344 is detected by mismatch PCR, if the mutation is present a Nae I site is created. (B) The MELAS A->G substitution at np 3243 creates an Apa I site. (C) The AD-ND1 A->G transition at np 3397 creates and Rsa I site whereas the AD associated $tRNA^{gln}$ change at np 4336 (D) generates a new Ava II site.

A) MERRF

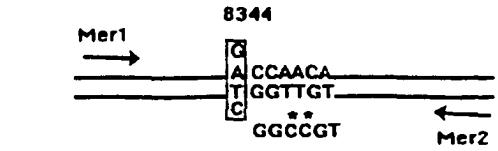

90 bp ACCGGC / TGGCCG Normal — GCCGGC / CGGCCG Nae I — 64 bp 26 bp

B) MELAS

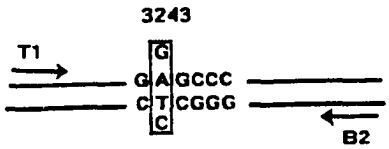

372bp GAGCCC / CTCGGG Normal — GGGCCC / CCCGGG Ape I — 263bp 109bp

C) AD-ND1

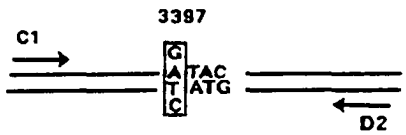

1113 bp ATAC / 179 bp TATG Normal — GTAC / CATG Rse I — 1068 bp 179 bp 45 bp

D) AD-tRNA^{gln}

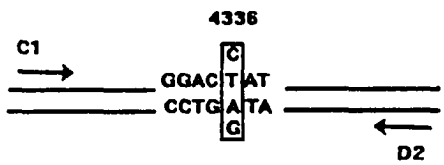

1292bp GGACT / CCTGA Normal — GGACC / CCTGG Ave II — 984bp 308bp

Table 6

SUMMARY - MERRF, MELAS AND AD ASSOCIATED MUTATIONS

PATIENT	MERRF^{8344}	MELAS^{3243}	ND1^{3397}	tRNA^{Gln4336}
AD	0/24	0/9	0/24	1/24
Control	0/16	0/2	0/16	0/16

fragment into a 72 and 97 bp fragments. As with the MERRF analysis, extended exposure of the polyacrylamide gels did not reveal any samples that carried this mutation. (Table 6). For MELAS we did not continue our analysis on more than 9 AD patients since at this time reports of four other AD associated mtDNA mutations surfaced; one in the $tRNA^{gln}$ at bp 4336, in the NADH Dehydrogenase subunit I gene ($ND1^{3397}$), in NADH Dehydrogenase subunit 2 gene ($ND4^{5460}$) and one in the 16S rRNA at bp 3196. We did not screen for ND^{5460} (114) since one report was subsequently published stating that this variant was not detected in 15 AD patients examined (115) nor did we screen for 16S $rRNA^{3196}$ since this variant was found to be heteroplasmic in an AD patient but homoplasmic in a control.

Instead we investigated AD brain mtDNA for the $tRNA^{gln}$ (np 4329 - 4400) mutation that has been reported in as many as 3.2% of the cases examined (5% in patients exhibiting both pathology of AD and PD), and for the ND1 gene (np 3307 - 4262) mutation. The $ND1^{3397}$ mutation was detected using diagnostic restriction enzyme analysis where an Rsa I site is created if the A -> G substitution is present. A 1292 bp fragment was amplified with primers C_1-D_2 (3352-4644). Rsa I digestion yields a 1113 bp and 179 bp fragment unless the mutation is present in which case the 1113 bp fragment is cleaved into a 1068 and 45 bp fragment (Fig. 21C). For the $tRNA^{gln4336}$ mutation the same primer set C_1 - D_2 was used. In this case if the A->G mutation is present an Ava II site is created resulting in a 984 and a 308 bp fragment (Fig. 21D). As can be seen in Fig. 22A one of our AD patients carried this variant which is near the TψC stem of this tRNA (Fig. 22B). We additionally screened lymphoblast DNA from

Figure 22

AVA II DIGEST DEMONSTRATING THE $tRNA^{gln\ 4336}$ VARIANT IN AN AD PATIENT

Detection of the $tRNA^{gln\ 4336}$ mutation in the temporal cortex of AD patient #1802. (A) Agarose gel indicating creation of Ava II site by mutation. Region was amplified with C_1-D_2 which yields a 1292 bp band. If the T- > C mutation is present a 984 and a 308 bp band is generated. (B) tRNA region affected by mutation (Shoffner et al. 1994).

5 AD patients for the $tRNA^{gln4336}$ mutation and did not find this alteration. We did not include this information in Table 6, however, because only one of these patients was actually biopsy confirmed. Results of the $ND1^{3397}$ and the $tRNA^{gln4336}$ mutations are summarized in Table 6.

The ND1 and $tRNA^{gln}$ variants were detected by Shoffner et al. using RFLP analysis. The entire mitochondrial genome was screened by RFLP yet out of the four mutations identified by this group, three of them were focused in one specific region of the genome (np 3100 -> np 4400). We wanted to determine whether other mutations were present in this area that were missed by RFLP analysis. We used PCR-SSCP to screen this region for additional changes. AD and control samples were amplified with C_1-D_2 digested with Ecor RI and Alu I which generate then run on a 10% glycerol SSCP gel. Polymorphisms were detected in 9 samples, 8 AD and 1 control. Sequencing analysis revealed this was due to 4 different mutations; one a G->A change at np 3421 which by itself does not alter the val residue, however, a second G->T mutation in this same AD patient at np 3423 alters the val to ile. The change at 3423 has been detected by other groups (116,117,118) while 3421 is a new variant. The third A->G substitution at np 3480 is a silent change in lys while the A->G mutation at np 3843 maintains a trp residue. These variants have been identified by Howell (116) and Masucci (119) respectively. Sequence variants for this region are summarized in Table 7.

Table 7

MtDNA POLYMORPHISMS IN THE ND1 GENE

Case	Diagnosis	SSCP	Mutation	Position	Amino Acid
1702	AD	(+)	G->A	3421	val -> ile
1702	AD	(+)	G->T	3423	
1539	CA	ND	G->T	3423	val*
1816	AD	(+)	G->T	3423	val*
1539	CA	ND	A->G	3480	lys
1630	AD	(+)	A->G	3480	lys
1739	AD	(+)	A->G	3480	lys
1816	AD	(+)	A->G	3480	lys
1974	AD	(+)	A->G	3480	lys
4073	AD	(+)	A->G	3480	lys
1816	AD	(+)	A->G	3843	trp*
1807	AD	(+)	A->G	3843	trp

C. CYTOCHROME C OXIDASE (COMPLEX IV) ANALYSIS

After analyzing AD brain tissue for previously characterized mtDNA mutations, we focused our investigation on Complex IV (Cytochrome C Oxidase) of the electron transport chain. This was due to the number of studies that indicated there was a cytochrome c oxidase deficiency in AD platelets and in AD brain tissue. Furthermore, a reduction in message levels for mitochondrially encoded subunits I and III of the thirteen subunit Complex IV protein was found. We decided to first determine whether there were any deletions or insertions in the COX I, COX II or COX III genes using PCR amplification across the respective areas. Later we turned to an investigation of point mutations that may exist and for this analysis we used the mutation detection technique SSCP.

1. Deletion analysis of cytochrome c oxidase subunits I,II and III

To determine whether deletions or insertions were present in CO I, II and III of Alzheimer's patients, PCR amplification was performed on four brain regions (three regions normally affected by AD, hippocampus, parietal cortex, temporal cortex and one non-affected area, caudate). For a number of samples tissue was available from the parietal cortex, temporal cortex and caudate but unavailable from the hippocampus. DNA enriched for mtDNA (250 ng) was PCR amplified using overlapping primer sets to each of the three mtDNA-encoded subunits of cytochrome c oxidase (Fig. 23). If a

Figure 23

PRIMER PAIRS USED TO SCREEN COX SUBUNITS I, II AND III FOR INSERTIONS AND/OR DELETIONS

Depiction of primers used to screen cytochrome c oxidase genes I, II and II for mitochondrial DNA deletions and insertions.

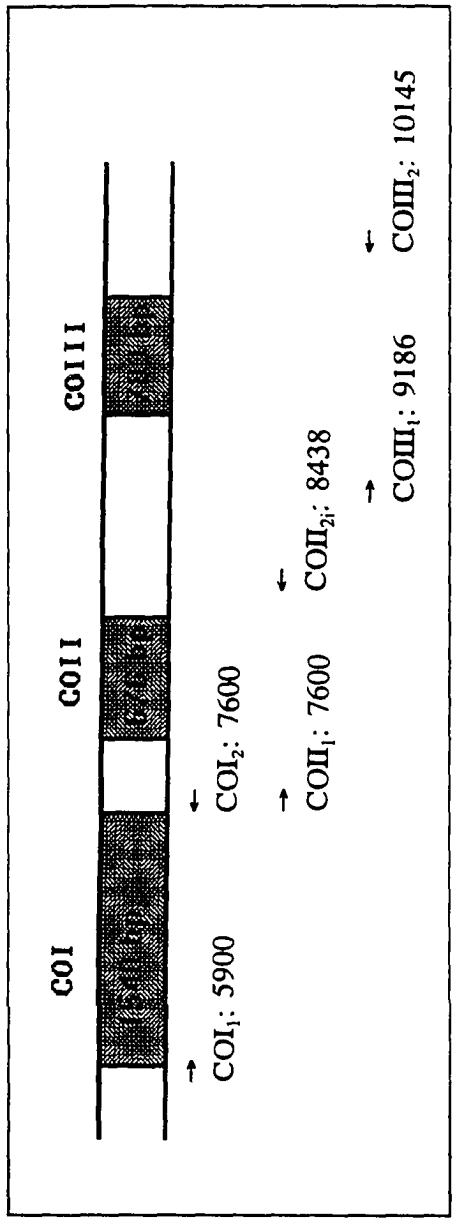

Figure 24

AGARSOE GEL OF PCR AMPLIFICATION ACROSS COX I, II AND III

Agarose gel of PCR deletion analysis of cytochrome c oxidase from four regions of the brain in Alzheimer patients. The COI primer set amplifies an undeleted fragment of 1700 bp (a. lanes 1-4), COII, an 838 bp fragment (b. lanes 1 - 6) and COIII a 959 bp fragment (b. lanes 7 - 12). M, marker.

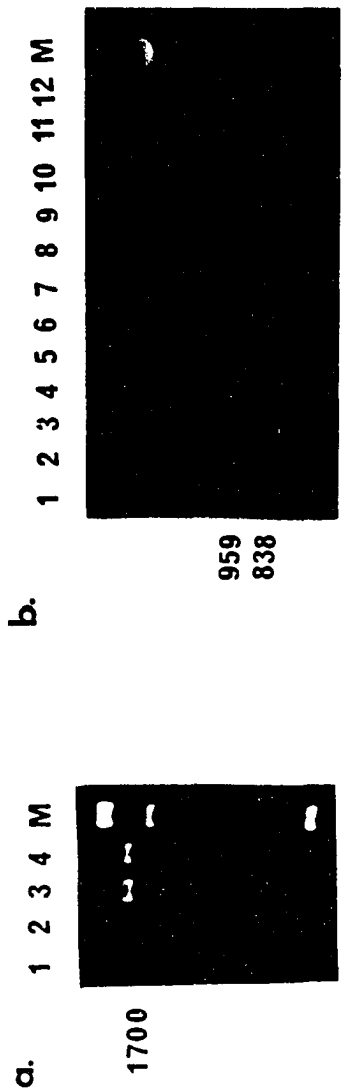

deletion was present, then a gel shift caused by a smaller, faster migrating PCR fragment would be evident, while an insertion would result in a band with retarded migration. Ten microliters of the PCR reaction were electrophoresed on a 1% agarose gel and visualized by ethidium bromide staining. No macrodeletions or insertions were detected by PCR using the COI_1 - COI_2 (Fig. 24A lanes 1 - 4), the $COII_1$ -$COII_{2i}$ (Fig. 24B lanes 1 - 6) or $COIII_1$ - $COIII_2$ (Fig. 24B lanes 7 - 12) primer sets.

2. Identification of Polymorphisms In COX I, II and III Using SSCP

Since by our analysis the mtDNA-encoded subunits COI, COII or COIII contained no large deletions or insertions that could account for abnormal cytochrome c oxidase activity, we screened Alzheimer brain tissue for point mutations using single strand conformation polymorphism (SSCP). SSCP can detect point mutations in single stranded DNA due to conformational changes induced by a single base change (Fig. 25). We screened a total of 24 different AD patients and a total of 16 control individuals showing no evidence of abnormal brain pathology. Information regarding sex and age of the patient samples is summarized in Table 8. In some cases, however, tissue was not available from all four brain regions. The COI, COII and COIII genes were PCR amplified from AD and control brain and restriction digested to yield optimal size fragments for SSCP (~350 bp see **Methods**). The COI gene (5904-7444) was amplified using two primer sets: COI_1 -H_2 and I_1 -COI_2, the COII gene (7586-8262) using primer sets: $COII_1$ - I_2 and J_1 -$COII_{2i}$ and COIII (9207-9990) using $COIII_1$ - $COIII_2$. Fragments

Figure 25

SCHEMATIC DIAGRAM OF SSCP ANALYSIS

Principle of single strand conformation polymorphism (SSCP) used for mutation detection. DNA region of interest is PCR amplified to yield double stranded DNA which is denatured then run on a polyacrylamide or vinyl-based gel. Single strands as they migrate through the gel take on unique conformations based on primary sequence. Single strands that are identical except for a point mutation would induce one band to migrate to an altered position in the gel.

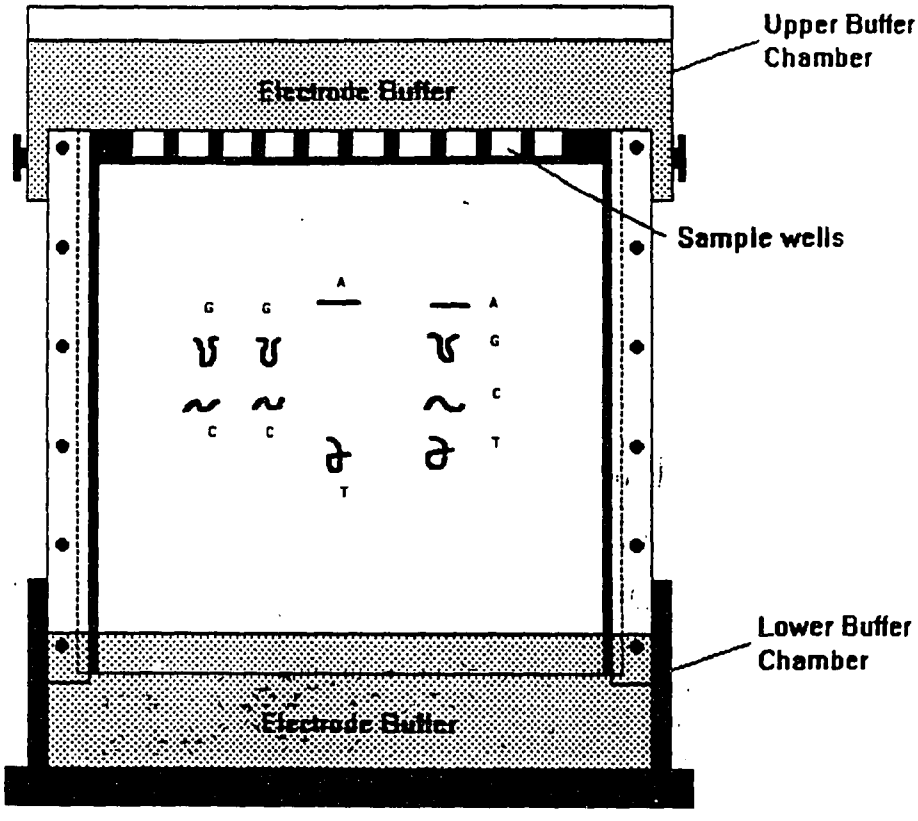

Figure 26

SSCP-GLYCEROL GEL OF THE LHON 11778 MUTATION

SSCP analysis of the $tRNA^{leu\ 11778}$ mtDNA mutation associated with Leber's Hereditary Optic Neuropathy (LHON). 250 ng of total genomic DNA isolated from cultured LHON lymphoblasts and 10 ng purified human placental mtDNA was PCR amplified with L_1-L_2 (np 11490-12194). Products were visualized by incorporating radiolabeled dCTP during the PCR. Following restriction digestion with Hinf I samples were loaded on hydrolink gels. Panel A (0% glycerol): lane 1; LHON undenatured, lane; 2 LHON denatured, lane 3; control denatured, lane 4; control undenatured. The 143 bp band carries the LHON mutation. Panel B (10% glycerol), 143 band was electroeluted, lane 1; LHON undenatured, lane 2; LHON denatured, lane 3; control undenatured, lane 4; control undenatured.

A)

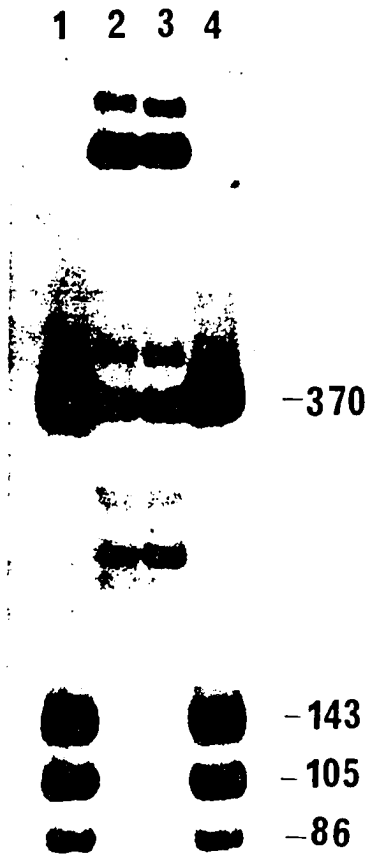

B)

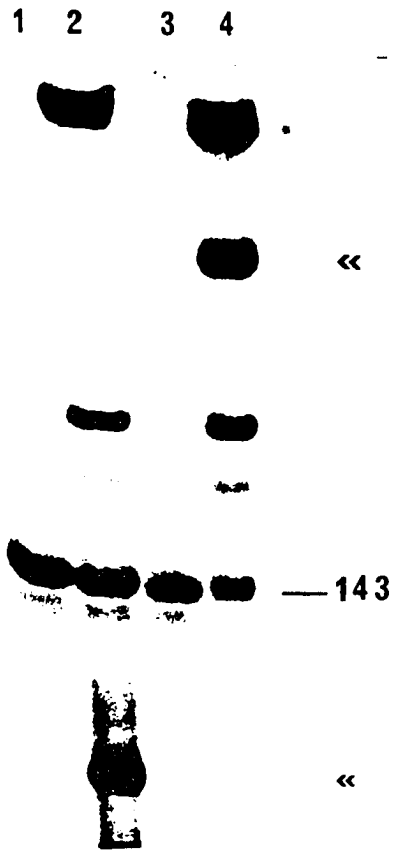

Table 8

AGE AND SEX DATA FOR BRAIN TISSUE USED IN COX I,II AND III SSCP MUTATION DETECTION

Patients:	n = 24
	sex: 12 ♂ 12 ♀
	age range: 60-92 yrs, mean 77
Controls:	n = 16
	sex: 14 ♂ 2 ♀
	age range: 21-72 yrs, mean 53

dATP during amplification. SSCP-PCR products were run on a 10% glycerol hydrolink gel; this percentage gel was determined to give a reproducible SSCP signature when tested on mtDNA from cultured cells containing the $tRNA^{leu}$ A->G^{11778} mutation associated with the mitochondrial myopathy Leber's Hereditary Optic Neuropathy (LHON) (45). The LHON region was amplified with primer set L_1-L_2 (11490-12194) which yields a 704 bp fragment. Control and LHON PCR products were then digested with Alu I which generates a 307, 143, 105 and 86 bp band. The 143 bp band which harbors the mutation was electroeluted then run under different SSCP conditions. Fig. 26 indicates that the LHON SSCP polymorphism was not detected in a 0% glycerol gel as seen in lanes 2 and 4 (A) versus lanes 2 and 4 (B). Thirty two polymorphisms were detected, 9 in COI (7 AD, 0 control), 6 in COII (3 AD, 3 control) and 17 in COIII (11 AD, 6 control). If one normalizes for the number of bases in each subunit and calculates the frequency of substitution based on the number of unique mutations, then COI is the least polymorphic subunit (5.2×10^{-3} changes/base; 8 nucleotide changes/1540 bp) while COIII is the most polymorphic (1.0×10^{-2} changes/base; 8 nucleotide changes/783 bp). As can be seen in Table 9A and B, dideoxy cycle sequencing confirmed the presence of point mutations in all but three cases, COIII AD# 1546, 1647, and 1977. Given the fact that some of the polymorphisms are the same nucleotide change although in different samples, 16 of the Complex IV mutations are new normal variants of the mitochondrial genome whereas 5 of the mutations have been previously identified as natural polymorphisms (118,120,121,122). There are a total of 17 transitions and 2 transversions. Three of the mutations are missense mutations that occur in COIII; the

Table 9A

MtDNA VARIANTS IDENTIFIED IN COX I, II AND III

Seqeunce variants identified in AD and control tissue by SSCP in Complex IV, subunits I, II and III. * previously reported variant, CA, cancer, BP, bronchial pneumonia, CHF, cardiac heart failure, MI, myocardial infarction. (+) indicates a distinct SSCP signature was detected.

Sample	Diagnosis	SSCP	Mutation	Position	Amino Acid
COI					
1977	AD	-	C->T	5915	asp
1816	AD	+	T->C	6137	phe
1974	AD	+	C->T	6371	ser
1977	AD	+	T->C	6524	thr
1977	AD	+	C->T	7028	ala*
3988	AD	-	C->T	7028	ala*
1816	AD	+	A->G	7245	thr
1640	BP	-	C->T	7254	asn
1640	BP	-	C->T	7274	gly
COII					
4308	AD	+	A->G	7768	met
3929	AD	+	A->G	7771	glu
4299	AD	+	G->A	7984	leu
1351	CA	+	A->G	7765	leu
1640	BP	+	A->G	7771	glu
1933	CHF	+	A->G	7975	pro
COIII					
1546	AD	+	-	-	-
1647	AD	+	-	-	-
1816	AD	+	G->T	9431	val
3929	AD	+	T->C	9540	leu*
3988	AD	+	G->C	9559	arg->pro*
1739	AD	+	T->C	9698	leu
1702	AD	+	C->T	9861	phe->leu
1816	AD	+	T->C	9698	leu
1573	AD	+	T->C	9899	his
3988	AD	+	T->C	9899	his
1977	AD	+	-	-	-
1401	MI	+	C->T	9431	val
1401	MI	+	G->A	9477	val->ile*
606	MI	+	T->C	9540	leu*
1640	BP	+	T->C	9540	leu*
606	MI	+	A->G	9545	gly
1640	BP	+	G->C	9559	arg->pro*

Table 9B

MtDNA VARIANTS IDENTIFIED IN INTERGENIC REGIONS OF COX I, II AND III

Case	Diagnosis	SSCP	Mutation	Position	Region
1977	AD	(+)	C->T	7476	$tRNA^{ser}$
1341	NC	(+)	9 bp del	start 8280	$COII/tRNA^{lys}$
3988	AD	ND	C->A	8282	$COII/tRNA^{lys}$
485	MS	(+)	T->C	10034	$tRNA^{gly}$

first mutation at bp 9477 changes valine to isoleucine (control). The Val->Ile change has previously been published by Marzuki et al. (118) and is considered to be a fairly common nonsynonymous substitution in mtDNA (123). The second amino acid change at bp 9559 changes argine to proline (AD). The G->C arg^{9559} transversion which was previously published by Wallace in an individual with LHON is present in a number of our brain samples (45). We detected this variant in 1 normal control, in 2 Alzheimer's brains and in placental mtDNA. The Arg^{9559} mutation is considered to be an ethnic variant representative of Caucasian populations. However, in a recent paper aimed at determining the last common ancestor of Europeans, Japanese and Africans (123) the authors noted that in their sequence analysis they did not find the 9559 mutation. Their conclusion was that the 9559 mutation did not represent a true ethnic polymorphism. However, as indicated above, we detected this transversion in a number of Caucasian individuals. The third missense mutation at bp 9861 is a new variant detected by SSCP in AD #1702 (Fig. 27A that alters a Phe -> Leu. The Phe at codon 219 is a moderately conserved residue, present in a humans, cow, whale and seal while Leu is found in rat, opossum and frog. (Fig. 27B). This variant was not observed in any of our control brain tissue nor has it previously been reported in a mitochondrial database consisting of over 60 references dating from 1983 - 1994 (124) nor in *"The report of the committee on human mitochondrial DNA"* accessed on the Internet (125). The mutation appears to be homoplasmic by sequencing.

For control # 1640 we detected two additional silent mutations in COI at bp 7256, C->T (Asn) and at bp 7274, C->T (Gly) that were detected prior to SSCP analysis for

Figure 27

CODON 219 PHE->LEU CHANGE IN COX III OF AN AD PATIENT

Identification of cytochrome c oxidase (COX) subunit III T->C point mutation at np 9861 in temporal cortex of an AD patient. (A) SSCP gel - region was amplified with $COIII_1$-$COIII_2$, digested with Sfa N1, Hha I and Hinc II. A unique SSCP signature is seen in the 236 bp band; lane C. Lanes A, B and D represent the normal pattern. (B) Mutation creates a phe->leu missense mutation in the carboxy terminus of COX III.

A) COX III SSCP

B) Conservation of Amino Acid 219 in COXIII

	TTC->CTC
human	ile-cys-***phe***-ile-arg-gln-leu
patient	ile-cys-***leu***-ile-arg-gln-leu
cow	val-cys-***phe***-phe-arg-gln-leu
seal	val-cys-***phe***-val-arg-gln-leu
whale	val-cys-***phe***-leu-arg-gln-val
frog	val-cys-***leu***-leu-arg-gln-ile

that region and are included in Table 9A. Additionally we detected four other mutations in tRNA's or small intergenic regions that separate COX I, II and III and thus are not included in Table 9A. A 9 bp deletion was found in the only short intergenic region of the genome between the COII and $tRNA^{lys}$ gene. The 9 bp deletion is considered to be an ethnic polymorphism present in Native Americans (126). The G- > A mutation at 7476 is moderately conserved (rat, human, frog) and has been reported in other samples (127,128) as well as in a patient with Rett Syndrome (129). The H_s transcript for this region does not code for a mature tRNA, however, the light strand transcript codes for $tRNA_{UCN}^{ser}$. The $tRNA^{gly}$ mutation occurs within the stem structure that connects the anticodon domain (124, Manfredi, Unpublished). All of these mutations are summarized in Table 9B.

Aberrant SSCP signatures were present in all brain regions of a particular sample and by SSCP appear to be homoplasmic mutations. As can be seen in Fig. 28A, a point mutation in AD #3988 leads to the same SSCP pattern in the parietal cortex and caudate of this patient (lanes 1 and 7). Lanes 2 - 6, and lane 8 are AD samples with the wild type SSCP signature, and lanes 10 and 11 are normal samples with the wild type pattern. This aberrant SSCP pattern was determined by dideoxy cycle sequencing (Fig. 28C) to be due to a T- > C transition at bp 9899 in subunit CO III that results in a silent mutation in histidine. Likewise, as seen in Fig. 28B, AD #1573 showed the exact same SSCP signature and similarly had the 9899 variant.

Figure 28

SSCP DETECTION OF THE 9899 VARIANT IN COX III

10% Hydrolink-MDE gel demonstrating single strand conformation polymorphisms in the COIII gene of Alzheimer's brain tissue. (A) The COIII gene was amplified with $COIII_1$-$COIII_2$ (9186-10,145) and digested to yield fragments of 236 bp, 194 bp, 185 bp, 157bp, 131 bp and 56 bp. Samples were denatured, loaded and electrophoresed for 17 to 20 hrs at 6W. A unique SSCP signature was detected in the 236 bp band in the parietal cortex (lane 1) and caudate (lane 7) of AD #3988. Lanes 2-6, 10, and 11 represent the wild type pattern. The sample in lane 9 did not amplify. (B) In the parietal cortex of AD# 1573 the same pattern was generated for the denatured 236 bp band. (C) Upon sequencing this shift was determined to be due to a silent T->C mutation at bp 9899.

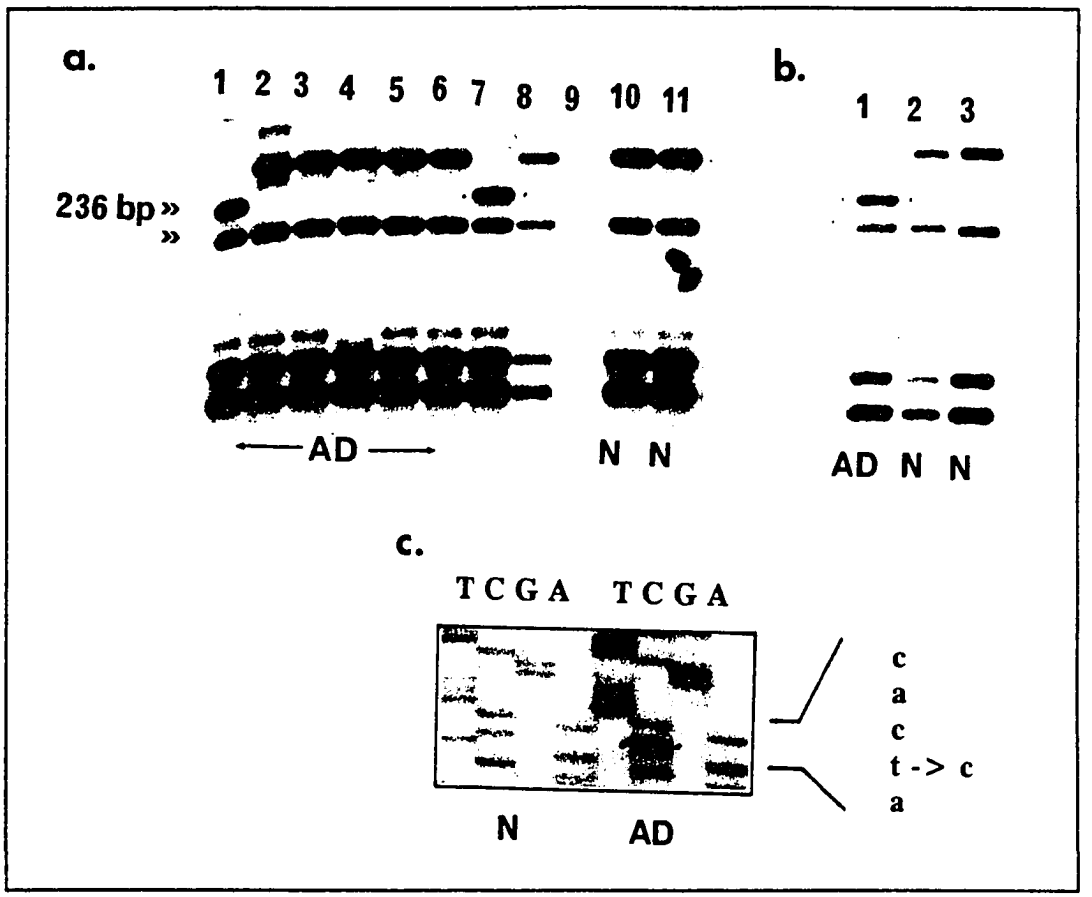

Additionally for one MS patient we detected what appeared to be an insertion in the COIII gene. Hinf I digestion of the $COIII_1$-$COIII_2$ PCR product yields a 562 bp and a 392 bp fragment. As can be seen in Fig. 29A, after Hinf 1 digestion the 567 bp double stranded DNA band for MS# 1401 had retarded migration on a non-denaturing poly- acrylamide gel compared to other Hinf I digested samples. The 567 bp band which spans np 9186-9753 was sequenced with read data obtained from np 9100-9800, yet, no insertions were detected that would lead to a slower moving band. Instead, the only change detected was a G -> A substitution (B) at np 9433 that converts Val->Ile. Since it was possible that due to band compression we were not detecting a small insertion we ran the digested products on a denaturing gel. If an insertion was truly present then fragment retardation would still be present on the denaturing gel. However upon electrophoresis in an 8 M urea gel the aberrant migratory pattern for the 567 bp fragment disappeared (C). Since this was a single stranded DNA gel to increase detection we performed silver staining since EtBr does not intercalate as well in single strands. This indicates that the reptated pattern observed initially was not actually due to an insertion rather it was due to a conformational shift in *double* stranded DNA. To further support this idea the entire COIII gene (9207-9990) for MS#1401 was sequenced (read data 9100-9994) but no insertions were detected. Since the only mutation detected in this region was the G->A substitution, we believe that the mutation is creating a (dA dT) tract, a dinucleotide motif which has previously been shown to create the phenomenon known as bent or curved DNA when it is repeated every 10 or 11 base pairs which would be in phase with the pitch of the double helix. The abnormal migration is reduced if the

Figure 29

ANOMALOUS MIGRATION OF DOUBLE STRANDED DNA

Anomalous migration of *double* stranded DNA due to a point mutation. (a) Agarose gel of COIII gene PCR amplified with $COIII_1$-$COIII_2$, digested with Hinf I which generates a 567 and 392 bp band. Slower moving upper band is seen in MS sample 1401, lane B. Lanes A, C and D normal digests. Lanes E and F; 1401 digest mixed with control digests. (b) Sequence analysis showing only mutation, a transition, detected in 567 bp band. (c) Hinf I digests were denatured and run on an 8M urea denaturing gel then silver stained to detect single and double strands. Lane A; 1401, lanes B and C; control. Upper band is undigested sample.

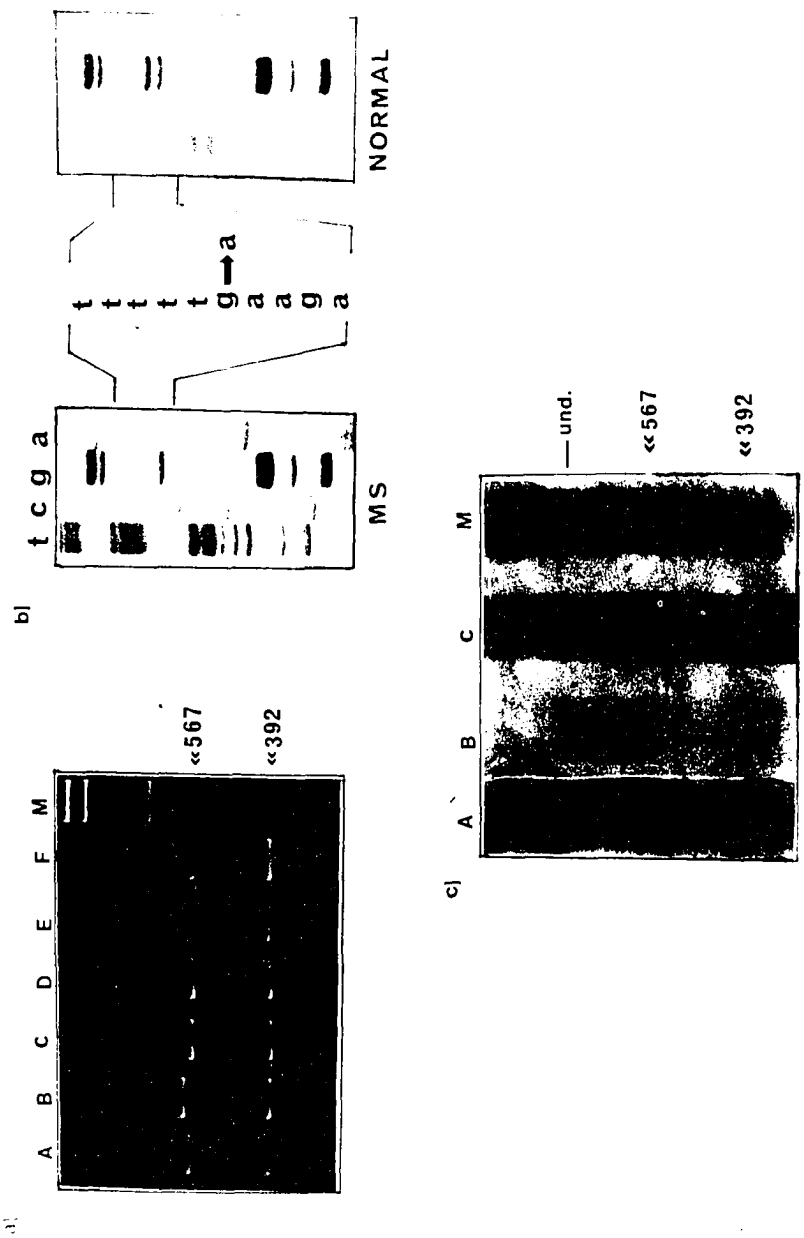

repeat motif occurs every 9 or 12 base pairs (156,157). The next repeat does not necessarily have to contain the same number of A's as the first. The G->A mutation creates a sequence that meets two requirements for bending; one is at least four adjacent A's and second, the degree of curvature increases if a C is on the 5' side and a T is on the 3' side of the A tract. For this mutated region a C is on one side although a T is not on the other. Additionally the stretch of base pairs containing the G->A mutation does not show a repeat of 9,10,11 Or 12 base pairs, thus, while the substitution creates an A tract that could lead to anomalous migration, it is lacking in other aspects of the model.

3. Evaluation of SSCP in Mutation Detection

While SSCP is widely used for mutation detection, there have been differing reports as to its efficacy. Earlier studies suggested that SSCP was 80% accurate in detecting known mutations (127) while other studies have determined the efficiency to be approximately 90% (128,129). One recent study reported that hydrolink MDE gels containing 10% glycerol are 68% efficient (130) at mutation detection. Thus, we wanted an estimate of how effective this technique was in our screening analysis. To determine whether point mutations existed that were not detected by SSCP we sequenced 99% of the COI and COII genes for three Alzheimer's patients and 99% of the COIII gene for two patients to determine if there were any additional mutations. If data was combined for the three patients then 100% of all three subunits were sequenced (Table 10). Alzheimer brain tissues that showed multiple mutations by SSCP were selected

Table 10

SSCP EFFICACY - SEQUENCING ANALYSIS

COI: 5904-7444

Primer	Position	3988	1816	1977
G_1	5717	ND = not done	ND	5780-6045
CO_1	5900	5930-6050	5940-6180	previous
H_1	6281	6150-6430 6331-6475	6331-6475	6150-6430 6175-6331 6331-6475 6361-6431
I_1	6471	6523-6720	6505-6709	6501-6761
4_1	6644	6686-6793	6669-6883	6681-6890
5_1	6818	6856-7005 6975-7117	6864-6937	6856-7067 6975-7117
6_1	7009	7051-7220	7051-7164	7051-7220
7_1	7186	7230-7482	7223-7460,70	7230-7482

COII: 7586-8262

Primer	Position	3988	1816	1977
7186_1	7186	7436-7664	ND	7436-7664
$COII_1$	7600	7652-7836	7664-7831	7641-7850
7800_1	7800	7830-8036 7849-8160	7834-8111	7830-8036
J_1	8188	8238-8324	8241-8370	8238-8375

COIII:9207-9990

Primer	Position	3988	1816	1977
K_1	9070	9116-9307	ND	see below
$COIII_1$	9186	9209-9370	ND	9215-9545
9342_1	9342	9441-9567	ND	see above
9523_1	9523	9586-9759	ND	9568-9800
9731_1	9731	9776-9887 9861-10091	ND	9764-10000

for dideoxy cycle sequencing analysis. We found no additional point mutations in COII or COIII. In COI we detected two additional silent mutations. One was a C->T mutation at bp 5915 in AD #1977 in PCR fragments that had not shown an altered SSCP pattern and a second silent mutation was detected at bp 7028 in AD #1977 and in AD #3988. AD #1977 did show a migrational shift using primer set I-COI (6471-7600). However, another mutation at bp 6524 was originally thought to cause the SSCP pattern. AD #3988 did not show a unique SSCP pattern using primer set I-COI. In some cases more than one base change was detected in a fragment having a conformational shift. Additionally, other investigators have noted that PCR-SSCP results in abnormal conformational patterns even when a base change is not present (134). We had three such cases where a SSCP signature did not result in a detectable point mutation, AD #1546, 1647 and 1977. These band shifts were not extremely noticeable on the SSCP gel and may reflect subtle changes in migratory differences for these lanes.

D. RHO ZERO STUDY

1. PC12(HGPRT-) Growth Characteristics in Ethidium Bromide

To determine whether an identified missense mtDNA mutations is indeed pathogenic in AD or, to determine whether mitochondrial DNA defects in general lead to OXPHOS defecits in AD could be addressed using a complementation study with a ρ^0 cell line. As described in the introduction these cells have lost all of their mtDNA but not their mitochondria; so with supplementation of certain metabolites, (pyruvate and uridine) they can generate ATP, albeit inefficiently, only through glycolysis. We sought to develop a ρ^0 cell that is of neuronal lineage that can be used in complemenation studies. AD cytoplasts can be fused with mt-DNA less cells to produce cybrid cells in which to study mtDNA mutational effects.

Ethidium bromide (EtBr) is known to be an inhibitor of mtDNA transcription and replication (102) and, thus, limits growth of cells cultured in the presence of the drug. The dye induces mtDNA loss by a mechanism that is not entirely understood. The selective pressure of the drug on mtDNA replication over nuclear DNA replication is believed to be due in part to the topology of mtDNA; mtDNA is a closed circular molecule, a structure which induces a high degree of superhelicity (102). With long term exposure to EtBr cells may become entirely mtDNA-less, a process we attempted with the rat neuronal cell line, PC12.

We used cells that were hypoxanthine-guanine phosphoribosyltransferase-deficient

(HGPRT$^-$). For the generation of ρ^0 cells, thymidine kinase deficient (TK$^-$) cells are usually used since a selection process in bromodeoxyuridine (BrdU) is eventually performed. Cells that are TK$^-$ can survive, since under normal cell growth cells do not need TK as the usual means for synthesizing dTTP is through dCDP. After cell fusion cells are transferred to media containing BrdU but not pyruvate or uridine. Pyruvate and uridine are often used to supplement respiratory deficient cells. Uridine is a necessary component in pyrimidine biosynthesis. Pyruvate is a key intermediate in a number of essential pathways. It can be transaminated to alanine, an essential amino acid used for a number of metabolic pathways. Pyruvate can also be carboxylated to oxaloacetate inside the mitochondria allowing glucose to be synthesized via glucose 6-phosphate. The ρ^0 cells die in the absence of these metabolites and the donor cells do not survive due to BrdU. The addition of BrdU will kill the TK$^+$ donor cells as BrdU is phosphorylated by TK and is then incorporated into DNA. BrdU has no effect on TK$^-$ cells. Thus, only fused cells will grow in this media. Since PC12 (TK$^-$) mutants were not available but (HGPRT$^-$) mutants were, we reasoned that the latter cell type could still be used if a selection was done in 6 thioguanine (6TG). HGPRT is used in the salvage pathway of purine biosynthesis and converts hypoxanthine to IMP and guanine to GMP. In the presence of HGPRT the ribose phosphate moiety of 5-phosphoribosyl 1-pyrophosphate (PRPP) will be transferred to 6TG thereby inhibiting cell growth.

Using previously described methods we exposed PC12 rat neuronal cells to low concentrations of EtBr in 12 well polylysine-treated plates. The parameters for EtBr sensitivity are however, species (cell) dependent. Nass et al. (102) reported that for

mouse L-cells and BHK hamster cells 5 ugs/ml of EtBr caused cell death in 8 to 10 days. Thus, to get a general range for PC12 sensitivity we did a titration in 0 to 20 ugs of EtBr. As can be seen in Fig. 30. up to 800 ngs/ml of the drug had no effect on cell viability as compared to the control in three days. A 25 % loss in viability was evident for the 2.0 ug/ml concentration. Since the 1000 ng range seemed detrimental to the cells we opted for the 100 ng range and initially cultured the cells in 100 and 200 ng/ml EtBr. Trounce et al. (136) reported that it took **13 weeks** for the osteosarcoma 143BTK- line to become mtDNA-less in **50 ngs/ml** EtBr. On the other hand, chick embryo fibroblasts (CEFs) exposed to **400 ng/ml** EtBr were almost ρ^0 by **week 3** (103). By day 7 since viability was similar for control and drug cultures, we increased the drug concentration to 500 and 1000 ngs, respectively. We hoped that a higher concentration, similar to the CEFs, would induce ρ^0 status sooner as long as viability was not compromised.

Cell growth was significantly reduced by day 18, approximately 4-10 fold over cells that contained no drug. This was true for the (+) EtBr cells without pyruvate and uridine (Fig. 31A) as well as with supplementation (Fig. 31B). The addition of pyruvate and uridine to cells that contained EtBr did not seem to have any positive effect on cell growth (Fig. 31B). This is not entirely unexpected since cells do not become dependent on these metabolites until they are almost mtDNA-less. By day 18 this may not be the case. The metabolites were included from the outset since they are not detrimental to the cells, and, we were unsure as to how long it would take the PC12 line to become mtDNA-less.

While cell growth was perturbed in the cells that contained EtBR, viability was

Figure 30

SENSITIVITY OF PC12(HGPRT$^-$) CELLS TO ETHIDIUM BROMIDE

Ethidium bromide toxicity of PC12 (HGPRT$^-$) rat cell line. Cells were grown in the drug for three days.

ETHIDIUM BROMIDE TITRATION FOR PC-12 (HGPRT$^-$) CELLS

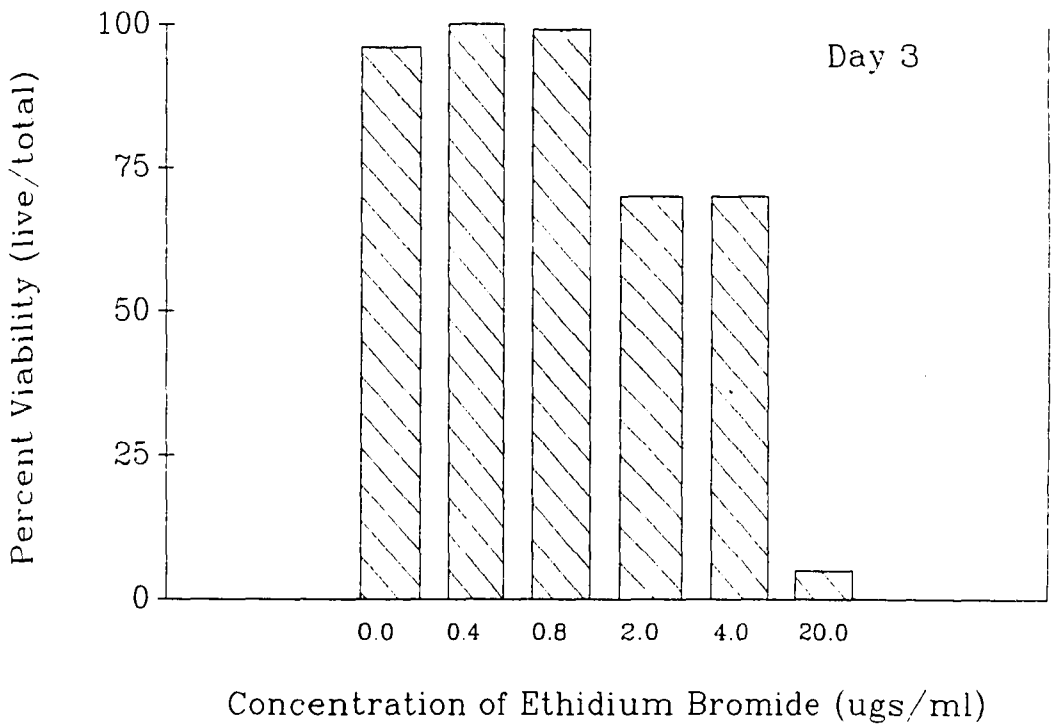

Figure 31

PC12 (HGPRT$^-$) GROWTH IN ETHIDIUM BROMIDE

Effect of different concentrations of ethidium bromide on PC-12 cell growth. Cell count was done in triplicate at 3 day intervals from 12 well plates (A) Cells grown in absence of pyruvate and uridine. (B) Cells cultured in presence of pyruvate and uridine.

A) PC-12 (HGPRT$^-$) CELL GROWTH w/o PYRUVATE and URIDINE

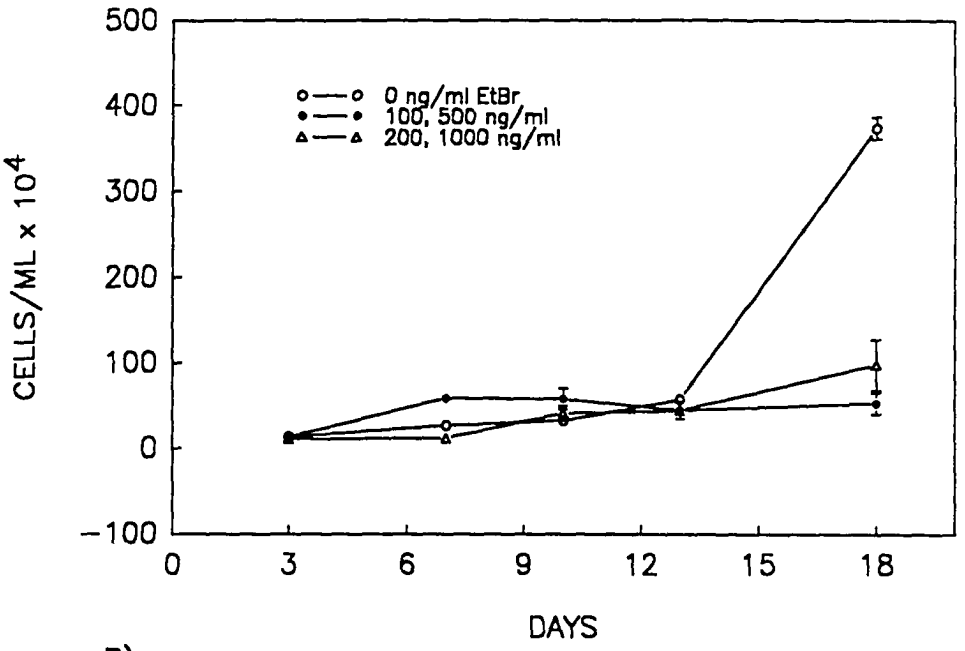

B) PC-12 (HGPRT$^-$) CELL GROWTH w PYRUVATE and URIDINE

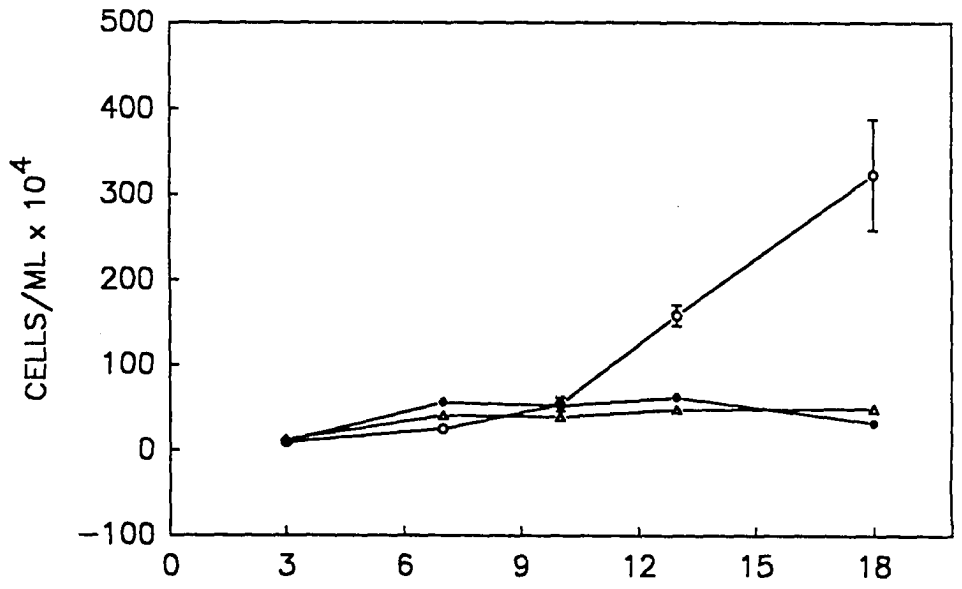

not affected for both high and low dye concentrations up to day 13. At this timepoint all of the cultures were between 94 and 100% viable (left half Fig. 32). By day 18 however cell viability was markedly reduced for the control and high drug concentration (right half Fig. 32). Viability was reduced for the control to 21% (-P-U), 31% (+P+U), since these cells had grown rapidly as evidenced by the growth profile in Fig 31 and had begun to die as a result of nutrient depletion. The 1000 ng/ml cell population declined to 8% (-P-U), 11% (+P, +U) viability by day 18. Over an extended period this concentration was most likely toxic. On the other hand the viability of the low drug group was still quite high, 80% for the -P-U population and 94% for the +P+U cells.

2. Assesment of Mitochondrial DNA Content

The PC12 cells were assessed for mtDNA content by Southern hybridization. After counting of cells at 3 day time points, total DNA was isolated using a proteinase K/SDS digestion. The small scale mtDNA isolation was not done since very few cells were collected from each well. The isolation represents DNA from live and dead cells. Two micrograms of total DNA was loaded per sample on a 0.8% agarose gel. Purified human placental mtDNA prepared by CsCl centrifugation was used as probe. Placental mtDNA is extremely homologous to rat mtDNA; thus, we envisioned no problems using placental mtDNA. We found that under low stringency hybridization conditions human mtDNA shares homology to the lambda DNA that was used as a marker. This was helpful since the marker did not have to be hybridized separately. Likewise, since human mtDNA

Figure 32

PC12 (HGPRT$^-$) VIABILITY

Viability of PC12 cells at day 13 and day 18 of ethidium bromide culture.

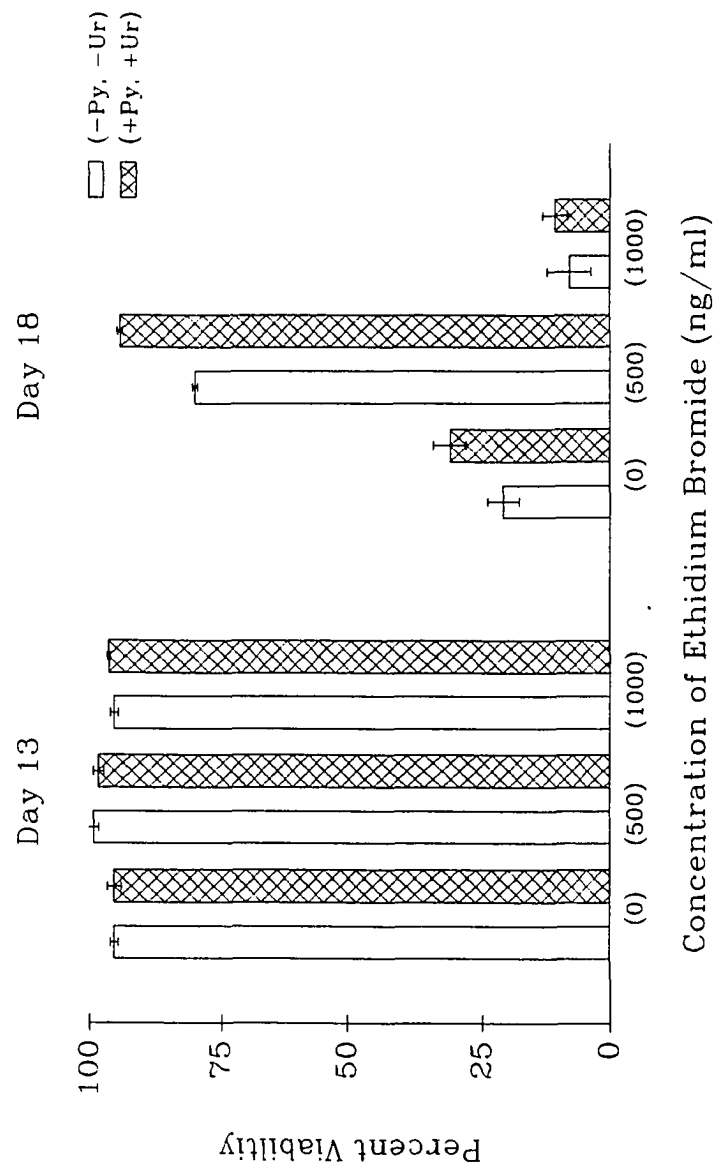

shared homology with lambda, it was possible that the probe would cross react with nuclear DNA. This could happen for rat or human mtDNA probes. However, nuclear DNA can be expected to be readily digested by the Bam H1; and thus, fragments around the same size as mtDNA would be unlikely and thus hybridization negligible. To test that the Bam H1 enzyme was working properly, a digest of pUC 19 DNA was included and digests containing a mixture of pUC19 with some of the PC12 DNA samples. Bam H1 linearizes pUC 19, and 300 ngs was digested to completion, as assessed on a 0.8% agarose gel. pUC 19 plus PC12 DNA samples were also digested to completion indicating that there was no inhibitory factors present in the PC12 DNA isolates (data not shown). We then looked at mtDNA content in the PC12 cells treated with EtBr.

Serial dilutions of purified human placental mtDNA were Bam H1 linearized and loaded on the same gel as the PC12 isolates to create a curve that could be used to equate optical density with weight. The standard curve was generated by densitometric scanning of lanes A to D seen in Fig 33. The weight of mtDNA loaded in each of these lanes ranged from 1 to 1000 pgs. As can be seen in the 1000 pg lane, nicked and catenates of mtDNA are present in this sample thus it would be erroneous to consider the entire 1000 pg load weight for the linearized band as yielding a particular OD. Instead, the relative percent of the linearized band was used to generate the standard curve. For example for the 1000 pg sample, 44% of the DNA was linearized thus .44 x 1000 pg = 440 pg. The 440 pg and its equivalent OD was used in the standard plot.

Analysis of mtDNA content would have been most helpful for day 18 however we performed calculations for day 13. The reason for this is that day 13 viability was

Figure 33

PLACENTAL MtDNA STANDARD CURVE

Standard curve used to estimate mtDNA content. (A). Serial dilutions of human placental mtDNA digested with Bam H1 - chemiluminescent Southern gel. Probe is human placental mtDNA. Bam H1 linearizes human mtDNA. Lane A, 1000pg; lane B, 100 pg; lane C, 10 pg; lane D, 1 pg. (B). Optical density plot of major species in lanes A to D.

A)

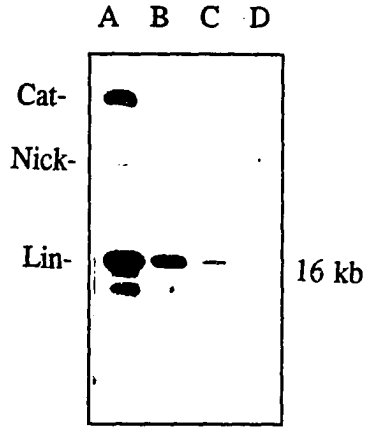

B)

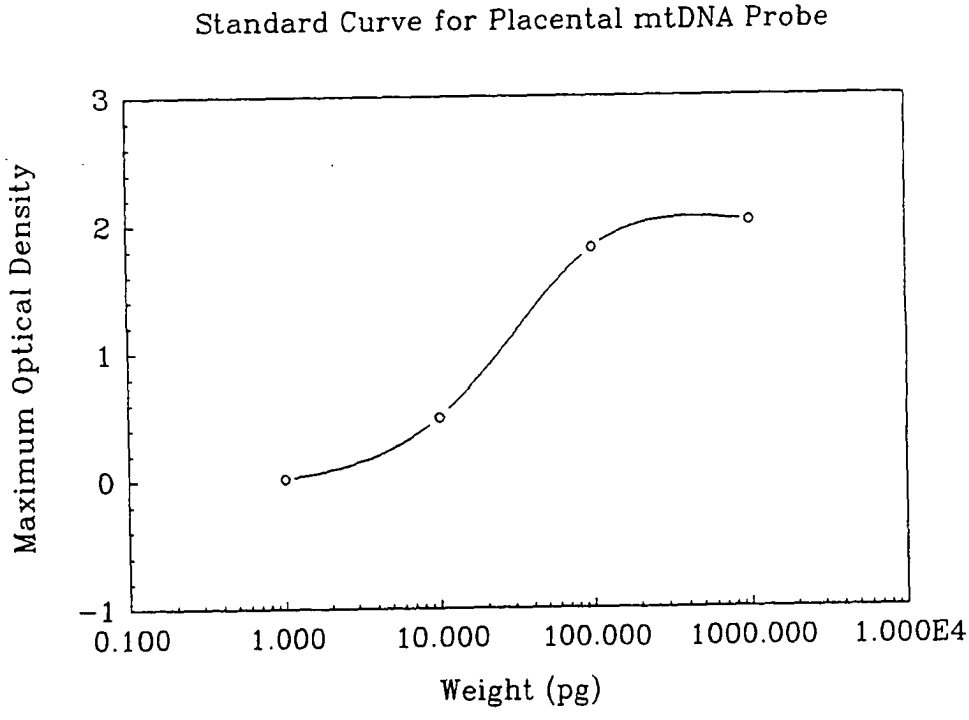

high for all experimental setups (see Fig. 32). By day 18 cell viability was low, thus, DNA isolations on this day would consist of live and dead cells. Dead cells would skew data since cell lysis and DNA degradation would begin to occur. The Southern blot shows that mtDNA is still present in cells grown in the presence of the drug as well as controls, as seen in Fig. 34 (A). Three species of bands are visible; the 5 and 11 kb bands produced by the Bam digest, and some linearized mtDNA at 16 kb. Optical densities for these bands were then used to determine the total weight of mtDNA present. To normalize based upon the number of live cells, this total of mtDNA weight was divided by cell number. As can be seen in Fig. 34 (B), while the lower drug concentration resulted in a slight reduction in mtDNA ($.8 \times 10^{-4}$ pgs/cell) as compared to the control (1.1×10^{-4}), the higher drug concentration seemed to have more mtDNA/cell (1.9×10^{-4}); thus, by day 13 it would appear that all of the cell lines have approximately the same amount of mtDNA. This is not entirely unexpected as some cell types can take up to 13 weeks to become mtDNA-less. These cells are currently being maintained in EtBr and will be reassessed at a later date for mtDNA content by Southern analysis.

Figure 34

SOUTHERN ANALYSIS OF PC12 MtDNA CONTENT DAY 13

(A) Southern chemiluminescent detection of mtDNA in PC12 cells treated wtih ethidium bromide. Total DNA was isolated, digested with Bam H1 and 2 μg run on a .8% agarose gel. Day 13 isolates is shown. Bam H1 generates an 11 kb and 5 kb band. Upper most band is linearized mtDNA cut at one Bam H1 site only. Probe was human mtDNA. Seen are Lane A, 1000 ngs/ml drug concentration; lane B, 500 ngs/ml; lane C, 0 ngs/ml. (B) Calculation of mtDNA content/live cell based on standard curve seen in Fig. 33(B) and cell growth curve in Fig. 31(B).

A)

B)

EtBr	5 kb	11 kb	16 kb	Weight	# Cells	mtDNA
0 ng	40 pg	100 pg	28 pg	168 pg	$158x10^4$ cells	$1.1x10^{-4}$ pg/cell
+	10	10	7	27	62	0.8×10^{-4}
++	32	40	20	92	48	1.9×10^{-4}

CHAPTER IV DISCUSSION AND CONCLUSIONS

DELETION INVESTIGATION

In an initial analysis, mtDNA isolated from rat brain was examined in order to determine if differences in postmortem duration induce non-disease specific degradation of mtDNA. We developed this experiment since there was some concern as to the different hours of postmortem delay present in our brain samples. Postmortem delay refers to the interval between time of death and subsequent time of autopsy. In our case this ranged from 5 to 27 hours for the samples obtained from the NNRSB and was not available for samples obtained from the Albert Einstein College of Medicine or paraffin embedded tissue. Within a few minutes of respiratory arrest a number of pathways become activated as the brain responds to oxygen deprivation. This is an important issue in the study of mtDNA mutations since one group found that the level of the KSS deletion was elevated 8 to 2200 fold in ischemic hearts compared to control hearts (91).

In this study rat brains were removed from the protective skull and placed at RT. In actuality, in the human environment the brain remains intact in the skull. Rats were sacrificed by decapitation which avoided any complications induced by phenylbarbituate inhalation. We found that even after having remained at RT for 30 hours there was no gross degradation of mtDNA as evidence by a lack of abnormal migratory bands detected

by Southern hybridization. In the heart study postmortem time was not the issue but changes were observed due to hypoxia. A comparison was made between a control group having mean age of 32 years and the ischemic group with an average age of 50 years (91). Numerous groups have documented an increase in the KSS deletion with age, so on this basis alone one would expect that the ischemic group would have an elevated percentage of this deletion. This study was later expanded, however, with age matched controls and in this case it was reported that a 7 to 220 fold induction in the KSS deletion was observed (137). There is, however, a significant difference in the hypoxic state present in the heart study versus the hypoxia that occurred immediately following decapitation in the rats: this difference is that is the heart study looked at cardiac ischemia caused by coronary artery stenois due to artherscleros is which is a long term phenomenon (years) whereas we are looking at a short term effect (hours). Hypoxia may induce mtDNA alterations in a chronic condition but have negligible effects otherwise. This is supported by studies which find no abnormal neuronal morphology if death occurs within several hours (3 to 6) after the initial hypoxic event. Necrosis only becomes apparent if an hypoxic event is followed by an extended survival period. Additionally, the heart study measured the KSS deletion using PCR whereas we used Southern analysis thus, there are differences in sensitivity. However, our purpose was to determine whether any macroscopic changes were occurring due to postmortem delay. One other group has looked at postmortem effects in a rat brain system using PCR and found no significant

changes. (C. Merril and S. Zullo, personnal communication) (138).

Since the differences in postmortem time did not seem to induce significant mtDNA degradation we launched into a study of deletions in AD and aged brain. AD is a primary differentiated dementia whereas PD is a neuromuscular disease that has dementia as a secondary manifestation. Both diseases lead to degeneration of neurons in the CNS while other types of nerve cells are unaffected. A definitive diagnosis for AD and PD is usually made at autopsy when characteristic lesions indicative of AD (plaques and tangles) or PD (Lewy bodies) are observed (4). Yet, AD and PD lesions are often found in association especially in the later stages of the diseases (139). The KSS deletion was initially reported to be elevated in the striatum of PD autopsy tissue compared to control subjects. This finding is now controversial (140). These results suggested that deletions in mtDNA may have a function in PD as well as in a similar neurological disorder such as AD. Thus, we undertook a study of deletions in AD. We developed a procedure for preparing mtDNA from as little as 50 mg of brain tissue, frozen or paraffin embedded. MtDNA was isolated from caudate, parietal cortex, hippocampus and temporal cortex. With this procedure mtDNA is readily visualized on agarose gels after restriction enzyme digestion without the need for extensive CsCl gradient ultracentrifugations. This isolation method would be very helpful in deletion analysis where low levels of a deletion are expected. Total DNA isolation often results in the need for multiple rounds of PCR up to 65 cycles for deletion analysis (Zullo personal communication). With such a high cycle number there is a greater risk of non-specific amplification. Another benefit of mtDNA enriched isolation is that after digestion

any residual nuclear DNA is often not present since Bam HI (6 base pair site) and Eco RI (6 base pair site) have multiple sites in chromosomal DNA. Southern analysis of these agarose gels did not reveal any 11 kb band (indicative of a 5 kb deletion in the 16 kb mt genome) in any of our brain mtDNA thus, we went to PCR-based methods to enhance detection.

A multiplex PCR program indicated that the deletion was indeed present in AD and aged brain (105) but it was not present in lymphoblast DNA from patients. This latter finding is not necessarily surprising since, if the deletion is harmful, these cells would produce fewer daughter cells and eventually the population would be depleted. This process would occur in rapidly dividing tissue such as blood. This initial PCR result, however, was a qualitative not quantitative finding. Two techniques were available for quantitative analysis, SD-PCR and Kinetic PCR. As we worked with these two methods we realized that both techniques were susceptible to a number of factors but more alarming was the different ratios of deleted mtDNA in the same sample detected by both methods. We compared these two widely used methods by determining the amount of the KSS deletion ($mtDNA^{\Delta 4977}$) in two regions of the brain from autopsy tissue of an individual with lung cancer. For both techniques mtDNA was linearized prior to amplification. When mtDNA was not linearized we found that there was greater inconsistency of amplification. This may be due to topological constraints induced by the circular mitochondrial molecule. Digestion with Bam H1 did not seem to inhibit amplification; this was most likely due to heat inactivation of the enzyme during the initial denaturation step of PCR. However, we did notice while using serial dilution PCR

that on some occasions the 250 ng dilution reaction using primer pair J1-KM did not amplify well whereas successive lower concentrations did. For the 250 ng reaction, 10 μl of a 25 ng/μl DNA digested sample was used. In these instances it appeared that the initial sample used for the Bam H1 digest was at a low concentration. For a low initial DNA concentration, a large volume of the enzyme and digestion buffer would be in the 250 ng reaction tube. Thus, it seems that in these cases $MgCl_2$ carry over from the restriction enzyme buffer may have been inhibiting amplification. Some primer sets are extremely sensitive to changes in magnesium concentration. This inhibition was not seen for kinetic PCR since only 25 ng of mtDNA was routinely used. Collection of data by serial dilution requires determining area by densitometry. We found Ficoll-containing dyes simplify scanning by eliminating the smiling effect generated during fast electrophoresis. Serial dilution PCR is a non-radioactive method whereas kinetic PCR uses labeled nucleotides at very low levels of radioactivity (7 kbq). Area determination for kinetic PCR by phosphorimaging is extremely fast and sensitive. There was, however, one caveat pertaining to this method; one must have a general idea of the deleted range expected in order to determine appropriate cycle time points, otherwise a plateau effect can be observed. For both methods it was necessary to test the efficiency of the primer pairs used to amplify deleted and normal mtDNA in order to ensure that there was not preferential amplification by one set of oligomers.

Measurement of the $mtDNA^{\Delta 4977}$ in the parietal cortex and caudate of the 59 year old subject by both methods revealed a greater ratio of deleted mtDNA in the caudate, consistent with a report stating that caudate, putamen and striatum have the greatest

amount of the common 5 kb deletion (141). Soong et al. (141) reported a ratio of 0.0021 in the caudate of a 57 yr old whereas we detected a ratio of 0.0141 in the caudate of our CA subject. Our measurement of the mtDNA$^{\Delta 4977}$ in parietal cortex was 0.0014. Corral-Debrinski et al. in an analysis of deleted mtDNA in the parietal cortex of aged patients reported a range of 0.063% (for a 67 yr old) to 1.2% (for a 77 yr old) as detected by serial dilution PCR (142). If we assume that a 59 yr old in their study would have had the same amount of deleted mtDNA as the 67 yr old (0.063%), then our 59 yr old CA patient had a level of deleted mtDNA (0.14%) that is slightly more than 2-fold higher than expected. This level is most probably an underestimation because a number of studies indicate that mtDNA deletions typically increase with age, thus the 59 yr old would actually be expected to have less than 0.063%. The seeming elevated levels of the mtDNA$^{\Delta 4977}$ in the caudate and parietal cortex in our sample are interesting, however, more CA samples and age matched controls need to be examined before any relationship between this cancer patient and defects in mtDNA can be established. We have used this CA patient solely as a source of material to provide a comparison of two PCR-based techniques commonly used in different laboratories to determine quantitative levels of mutant mtDNA.

Using kinetic PCR we arrive at an even greater ratio of the mtDNA$^{\Delta 4977}$ in the two regions examined. The range previously reported for the mtDNA$^{\Delta 4977}$ in striatum using kinetic PCR is 0.3% to 5.0%. Comparisons to caudate and parietal cortex is unavailable. We have found that, at least in our experience, kinetic PCR which uses a regression line to calculate the ratio of deleted to normal mtDNA is extremely sensitive to outliers which

can significantly skew the regression line and, thus, y-intercept points used to calculate the deleted product. However, serial dilution PCR which compares deleted to total mtDNA (normal plus mutant) using an optical density curve may be less susceptible to such deviations. We believe that serial dilution PCR was the most consistent. For example, the 12.5% deleted mtDNA determined by kinetic PCR should have been of sufficient amount to have been visible by Southern hybridization. However, we did not detect deleted mtDNA by Southern hybridization even after prolonged exposure of the film using chemiluminescent detection. Thus, the kinetic PCR method in our hands appears to overestimate the amount of deleted mtDNA.

We did not include a comparison to short cycle PCR (143) because this technique does not result in a specific percentage of deleted mtDNA that can be compared with the other methods.

While the analysis of mtDNA deletions in aging and neuromuscular diseases has been greatly accelerated by the use of PCR, this study is the first which indicates that PCR-based quantitative methods differ in their effectiveness in measuring mutant mtDNA and caution must be exercised in comparing values from different laboratories using different techniques.

We concluded that serial dilution PCR was more reliable at least in our experience and proceeded to use this method to investigate the KSS deletion in AD brain. We found a 12 fold average increase (0.0628% vs 0.0053%,) in $mtDNA^{\Delta 4977}$ in the temporal cortex as compared to age matched controls ($p = .116$ for a one-tailed t-test). If one includes two values from the Corral-Debrinski study (110) for the AD group that maintains the

same mean AD age as our group, then the fold difference is statistically significant for both a one-tailed t-test (p=.028) and a two tailed test (p=.057) (see Appendix D). Other AD values could not be included because they would increase the AD group mean age. Normal values from the Corral-Debrinski study could not be included since they were not reported for the temporal cortex.The actual values in AD brain ranged from .007% to .2230% while in controls these percentages went from 0.008% to 0.0141%. When we initiated this investigation no other reports on the KSS deletion in AD had been reported. Later, as interest in this area expanded sporadic reports surfaced. Corral-Debrinski et al. found a ratio of 0.00023 to 0.040 or a percentage of 0.023% to 4.0% in temporal cortex of 10 AD patients (111). The average value was 0.007848% or 0.78% which represents a 13 fold difference over the average AD value, 0.0628%, in our samples. This could be a reflection of the average ages used in both of these studies - our average age was 69 years whereas the Corral-Debrinski study had an average of 77 years, almost a decade difference. A ten year increase in age especially in the later decades often leads to a 20 fold increase in the KSS deletion (142). Our study, then, which finds a greater level of the KSS deletion in AD temporal cortex while consisting of a small sample size (n=5) is supported by at least one other study (n=10)(111).

In **normal** aged brain we found the temporal cortex to have an average percentage of 0.0053% of $mtDNA^{\Delta 4377}$ while another report found 0.028% There is no comparison available for temporal cortex at our average age (69); however, in the Corral-Debrinski study a 77 and 94 year old had levels that were 1.2% and 3.4% respectively. This would represent a 220 fold difference for a 68 yr old to a 77 yr old. Examination of the

diagnosis for the 77 yr old control indicated that this subject "showed mild to moderate atrophy of the frontal and temporal lobes with hippocampal shrinkage" thus it appears as if this does not represent pathologically normal brain tissue and could explain the 220-fold difference, in addition to age, between our control group and the 77 yr old value.

Other regions of the cortex have likewise been analyzed for the level of the KSS deletion. Blanchard et al. found there was no significant difference in the frontal cortex between AD (0.14%) and control subjects (0.12%) (112) while Corral-Debrinski et al found a 12-fold difference in this region before age 75 (111). After age 75 the AD patients actually had a 4-fold lower level of the deletion in the frontal cortex. The authors found this to be a general trend in all cortices - before age 75 the deletion levels increased but declined by age 80. Our study then correlates with the before age 75 results of Corral-Debrinski et al.

It has been hypothesized that mtDNA damage is the result of oxygen radical attack. Since free radical damage is believed to increase with advanced age, then in AD other factors, environmental or genetic, must be acting in concert to produce the elevated level of mtDNA damage seen in AD. On the other hand, it has been speculated that in the 80 yr old group the deletion levels (which start out higher than controls) have accumulated such that they begin to induce cell death in AD tissue. Most deletions that occur in the "hotspot" region leave the O_H and O_L intact, otherwise, these deletions would produce sterile genomes (146). Additionally, since the KSS deletion encompasses tRNAs, translation is often affected although not transcription. Thus, the deleted genomes are replicative competent and, could increase in *postmitotic* tissue, leading to

abnormal OXPHOS functioning. This is to differentiate from what may be happening in proliferative tissue. Since deletions are heteroplasmic, however, there are normal mtDNA available that could compensate for deleterious effects on translation. The amount of deletion necessary to induce OXPHOS damage is controversial (144,145) ranging from a few percent to 70%. It is our contention that the while the increase in mtDNA deletions potentially has adverse effects, it is not the primary event that initiates OXPHOS damage in AD brain rather, it may be a genetic defect in free radical scavenger systems. This is not to say, however, that therapeutic agents which target mtDNA damage would not be helpful in alleviating symptoms of the disease.

We also investigated the minor region of the genome in AD patients for the presence of deletions since this region of the genome in relation to neurological disease has not been well studied. Whereas the KSS deletion has been found in numerous tissues minor region deletions such as mtDNA$^{\Delta 3610}$ have only been found in select tissue such as skeletal muscle. Are there then tissue specific deletions in brain? We did not detect mtDNA$^{\Delta 3610}$ in any of our AD or control brain subjects. This suggests that some deletions are indeed tissue specific, implying different mechanisms for the genesis of deletions. The prevalent KSS deletion most likely originated during oogenesis or embryogenesis (146) whereas mtDNA$^{\Delta 3610}$ may have developed in adult somatic cells. While screening the minor region, we identified a fragment that we initially believed represented a new deleted mitochondrial genome. Characterization of this fragment indicated that it did indeed span a GCTAAG repeat but was actually an artifact of the PCR reaction, specifically due to mispriming of the right primer. Alternatively, a

process known as "jumping PCR" may have resulted in amplification of the deleted band. This rather rare event occurs when DNA is damaged in such a way that extension by the polymerase is terminated. In this scenario one primer (F_2 in this case) initially anneals to the correct sequence area but terminates prematurely (at the 3' end) within the repeat site. This aborted product at its 3' end then jumps and anneals to the second repeat sequence causing the generation of a deleted product (54). Either of these two scenarios could lead to our results however just simple mispriming is more likely considering the potential for complementarity with this primer. Although criteria for this primer were met by primer design programs, the observed mispriming denotes the necessity for homology searches when using "designing software".

POINT MUTATION ANALYSIS

After the deletion studies we turned our attention to the examination of point mutations in the mitochondrial genome. Individuals with the mitochondrial encephalomyopathies MERRF and MELAS often present with symptoms such as dementia, ataxia and seizures similar to AD. We screened for the MERRF 8344 $tRNA^{lys}$ mutation and the MELAS 3243 $tRNA^{leu(UUR)}$ mtDNA mutations and did not find any evidence of these alterations in any of our AD samples. However, these are not exclusive mutations associated with MERRF and MELAS. Seventy to eighty percent of the MERRF cases are due to the 8344 substitution while in a smaller percentage a

mutation in this same $tRNA^{lys}$ at np 8356 is found (146). Likewise, for MELAS 80% of the cases are due to the $tRNA^{leu(UUR)}$ 3243 mutation and another 10% are caused by a mutation in $tRNA^{leu(UUR)}$ at position 3271 (147). It may be that the low frequency mutations are present in AD mtDNA since there seems to be atypical clinical presentations associated with the rarer mutations. For instance, the 3243 MELAS mutation was also detected in individuals with progressive external ophthalmoplegia (PEO), a disease primarily considered to be caused by deletions (148). Alternatively, it is possible that other alterations in these tRNAs exist that are unique for AD.

We continued our investigation of point mutations in the mitochondrial genome of AD patients - in this instance screening for 2 recently reported AD-associated mutations: one in $tRNA^{gln}$ at np 4336 that is moderately conserved and the other mutation being in ND1 at np 3397 which alters a highly conserved methionine to valine (85). We did not detect the ND1 mutation in any of our samples but we did detect the $tRNA^{gln}$ variant in 4.2% (1/24) of our patient brain tissue and in 0% (0/16) of our control subjects. Shoffner et al. found this variant in 3.2% (2/62) AD patients 6.8% (5/73 of patients with AD + PD and 5.3% (2/38) of patients with PD for an overall of 5.2% (9/173) of patients examined. In the Shoffner et al. study all of the patients were Caucasian, thus they looked at the frequency of this variant in the normal Caucasian population since specific mtDNA polymorphisms are linked with ethnicity. In the control group this value was 0.7% (12/1691). The fact that this mutation is occurring with some frequency in controls could mean that this value represents individuals that have not yet manifested disease symptoms. This may be the case if the control group is significantly

younger than the AD group. (It is not necessary to age match the groups when studying point mutations since these do not accumulate in an age specific manner). Another theory is that an additional genetic factor, nuclear or mitochondrial, must be present to cause predisposition. We were able to obtain race data for a majority of our brain samples, especially the AD samples but not for all of the control samples. We detected the $tRNA^{gln4336}$ variant in the temporal cortex of AD #1802, which turned out to be a Caucasian subject. Our finding of this mutation in an AD subject supports Shoffner et al.'s initial findings, however we cannot exclude the possibility that detection of this mutation merely reflects an ethnic Caucasian variant. However, our percent of the affected AD group (4.2%) is very similar to the percent affected found by Shoffner et al.(3.2%). The relevance of this mutation remains to be determined by further studies. Since this region of the genome seemed to be a hotspot for AD associated mutations at least by RFLP analysis we analyzed this region further using SSCP. We detected four other mutations at np 3421, 3423, 3480 and 3843, all in ND1. The 3421 mutation is a new sequence polymorphism that by itself is a silent mutation but it occurs with 3423 in the same patient, AD #1702, and in combination changes a valine to isoleucine.

We continued to use SSCP analysis for mutation detection but focused on Complex IV, the cytochrome c oxidase gene, given the biochemical abnormalities described earlier in the introduction, including the depressed activity in platelets and in cerebral cortex and abnormal COX I, II and III mRNA levels.

SSCP was chosen for mutation detection first because it allows one to screen a large number of samples simultaneously (especially when the area to be analyzed covers

more than one exon) and second, because it lacks the use of hazardous chemicals that is often required with other mutation detection techniques such as heteroduplex analysis using osmium tetroxide (HOT). Additionally, SSCP does not require expensive equipment and the methodology is quite straight forward. However, the technique does have limitations, for example requiring the use of relatively small fragment sizes < 300 bp; we have found that PCR fragments between 200 to 250 base pairs showed the best resolution between polymorphic bands. Despite these limitations however, SSCP has been widely used in mutation detection since its debut in 1989. Since studies of the efficiency of SSCP have ranged from 90% to 60% (127,128,129,130) we decided to estimate how efficient the MDE-Hydrolink/glycerol gel was in our screening procedures. To obtain this information we sequenced 99% of the COI and COII from 3 AD patients (AD# 3988, 1977, 1816) and the COIII gene from 2 AD patients (AD# 3988 and #1977) that were previously analyzed by SSCP. For the COIII gene we found no additional mutations by sequencing, indicating a 100% efficiency for AD #3988 and #1977. Likewise for COII no sequence polymorphisms were detected that did not show single strand polymorphisms, indicating 100% efficiency. For the COI gene however, 3 additional mutations were detected, one in AD #3988 and 2 in AD #1977 but none in AD# 1816, thus, the percentage efficiency for each sample in COI was AD #1816, 100% (2/2 = 2 detected by SSCP out of 2 total mutations), 66% for AD# 1977 (2/3) and 0% for AD #3988 (0/1) giving a mean of 55% for COI. Our total estimation for the efficiency of the hydrolink-MDE/10% glycerol gels then, was approximately 80% for all three subunits, which represents the number of actual sequence variants/ the number of

positive SSCPs (8/10). Note our estimation of the efficiency of MDE-hydrolink/10% glycerol SSCP gels was determined in a different manner from previous studies. While other reports generated percentages by testing known polymorphisms we determined whether any unknown mutations escaped detection. Yet, our average efficiency is within ranges reported by other groups. Kim et al. report that SSCP efficiency on of mitochondrial sequences in the D-loop and in the $tRNA^{ile}$ gene was 75 to 80%. (149).

Calculation of the number of base changes in these three subunits indicates the order of increasing variability is COIII > COII > COI. Cytochrome c oxidase is the terminal complex of the electron transport chain resulting in the reduction of O_2 to H_20, oxidation of cytochrome c and transport of protons. COI, COII and COIII constitute the catalytic core of the Complex IV (150). COIII is thought to be involved in proton pumping while COII and COIII contain the heme and copper prosthetic groups. COII contains the high affinity binding site for cytochrome and recently COIII is believed to contain a low affinity site (151). Thus it may be that the order of variability in these three subunits reflects their individualized relevance in the overall functioning of the complex. COIII may be more polymorphic than the other subunits since it is not involved in substrate interaction whereas COI and COII maintain a more conserved structure since they interact with cytochrome c.

We used SSCP to analyze the mtDNA encoded COI, COII and COIII subunits of Complex IV since there have been an increasing number of studies that suggest a possible link between late onset Alzheimer's Disease and mtDNA mutations. Of the five complexes involved in OXPHOS only Complex IV appears to show reduced activity in

AD. The reason for the altered activity in Complex IV is unknown although a mtDNA involvement is supported by a study by Chandrasekaran et al. in which levels of COI and COIII mRNA in the temporal association cortex of AD brain were decreased [84]. The 12S rRNA, which is transcribed from a H_s promoter that is distinct from the COI, COII and COIII promoter, was not decreased in the AD subjects, suggesting, that transcriptional regulation may be responsible for the decreased cytochrome c oxidase activity. However, the major H_s transcript which codes for COI, COII and COIII transcribes a polycistronic message. This transcript codes for a number of other proteins involved in OXPHOS (cytochrome b, ATPase subunits 6 and 8, 7 subunits of NADH dehygrogenase) all of which form part of Complexes I, III and IV. Thus, if regulation is occurring at the level of transcription one would expect that other message levels would be decreased as well, thereby affecting all of the complexes of the electron transport chain complexes. Yet, there do not appear to be any deficiencies in Complex I, III or IV activity in AD brain which would be expected if a transcriptional block decreased mitochondrially encoded mRNA for Complex I, III or IV.

Alternatively, differences in mRNA stability may affect COI and COIII mRNA levels. A point mutation within the structural genes could affect COI, COII or COIII mRNA turnover. We identified three missense substitutions, arg^{9559}->pro, val^{9477}->ile and phe^{9861} ->leu. The first two mutations were previously reported as natural polymorphisms; val->ile is one common amino acid change in mtDNA while the transversion at 9559 is believed to be indicative of European sequences. We found this transversion in a number of our Caucasian samples even though one study reported that

the prevalence of the 9559 mutation in Europeans was perhaps due to a sequencing error (123). The third missense mutation at phe^{9861} was detected in an AD patient and represents a new variant since it has not been observed in any of our controls or in two mtDNA data bases which succinctly summarize missense and polymorphic mtDNA mutations (124,125). These missense mutations appear to by homoplasmic by sequencing and SSCP analysis yet there seem to be conflicting reports as to whether SSCP can detect heteroplasmy efficiently (152). RFLP analysis combined with autoradiography can be performed to determine heteroplasmy, however, this mutation does not fall within a restriction site and would necessitate the use of mismatch PCR to detect this variant. Although the phenylalanine at this position is conserved in a number of mammals the change to leucine would not appear to dramatically alter the hydrophobicity. However, the phe^{9861} mutation should not be excluded as a possible pathogenic variant until more AD and controls have been examined. The need to examine this phe -> leu mutation becomes more evident in view of the observation that a similar phe -> leu alteration brought about by a T->C transition at position 9957 of COIII has been found to be pathogenic in a progressive mitochondrial encephalomyopathy, hinting, that the aromatic ring may have some significance.

Our studies on the cytochrome c oxidase structural genes have not identified mutations that might be involved in the increased turnover of mRNA and/or produce an improperly translated protein. One possible explanation for this finding is that mutations that are not within the genes for COI, COII or COIII could be affecting mRNA levels in the following manner: human mitochondria are unique from their eukaryotic host in

that mitochondria contain a compact genome having no introns, rather, mtDNA is punctuated by a number of tRNAs. Such a genomic organization implies an extremely precise processing event. An enzyme having RNase P-like activity is postulated to play a role in producing mature transcripts (153), however the recognition signals along the polycistronic message are still unknown as well as whether processing is a sequential or simultaneous event. Flanking regions for COI, COII and COIII consist of tRNA's as well as a small intergenic region between COII and COIII. Thus, point mutations within tRNAs that border COI, COII and COIII could lead to improper splicing events and altered mRNA levels. In a preliminary investigation of the region that separates COI and COII (7445-7516), we detected a G->A mutation at bp 7476 in an AD patient that is moderately conserved (rat and Xenopus). The H_s transcript for this region does not code for a mature tRNA, however, the light strand transcript codes for $tRNA_{UCN}^{ser}$. Yet, processing within this region does occur for the H_s transcript and a point mutation here would not only alter the tRNA but could affect the mRNA processing events that lead to mature COI, COII and COIII mRNA. Thus, tRNA sequences between the CO subunits should be further investigated.

One aspect of AD research that investigators should not lose sight of is that whether heritable, sporadic, late or early onset all AD patients manifest similar neuropathology, that is, plaques and tangles. The different forms of the disease may originate at individual branches but at some point these paths must converge along a similar route that leads to neuronal degeneration. Could altered oxidative metabolism, produce the hallmark characteristics of AD? If the electron transport chain is defective

then ATP production driven by the proton motive force would be decreased. Parker et al describe two scenarios as a result of defective ATP production (154). Low ATP levels may induce certain metabolic processes among them, protein kinase activation which may in turn cause abnormal protein phosphorylation such as that seen in NFTs. Activation of bovine protein kinases has been shown to be induced by low ATP levels Furthermore, a deficient respiratory chain would lead to the accumulation of specific products or reactants. For instance, if Complex IV is perturbed then molecular oxygen concentrations may become elevated. The reaction of electrons with O_2 could produce oxygen radicals. Interestingly one study found that free radicals can induce cross-linking of tyrosly hydroxyl groups in the amyloid peptide potentially leading to aggregate formation (155). Thus, it is possible that free radicals and subsequent damage they induce in AD are either (a) due to increased production of oxygen radicals or (b) due to an inability to cope with normal production.

RHO ZERO STUDY

Our investigation of mtDNA in AD as well as other groups' have begun to detect variants of the mitochondrial genome present in some cases of AD. The $tRNA^{gln4336}$ that has been reported to be associated with 3.2% of AD cases was detected in 4.2% of our AD cases supporting this initial study. We detected a novel variant, $COIII^{9861}$, in approximately 4% of our AD cases that alters a phe-> leu at codon 219. The question

as to whether this and other identified mutations are indeed pathogenic in AD or, even to discern whether mitochondrial DNA defects in general lead to the OXPHOS problems seen in AD could be addressed using an alternate strategy; the use of a ρ^0 cell line would be most helpful in this regard. As described in the introduction these cells have lost all of their mtDNA but not their mitochondria so with supplementation of certain metabolites, (pyruvate and uridine) they can generate ATP, albeit inefficiently.

The $\rho^0$206 cell line (a derivative of the bromodeoxyuridine resistant 143B.TK$^-$ cell line) has been complemented with mtDNA from patients carrying the mitochondrial encephalomyopathy mtDNA mutations for MERRF and MELAS. While the $\rho^0$206 cell line provides one system for the study of AD associated mtDNA mutations, we believed that a ρ^0 investigation would be more beneficial if one used a cell type that was similar to the cell population affected in AD, i.e. a neuronal-like cell type. A neuronal mtDNA-less cell line can be used to transfer aberrant mtDNA carrying a specific mutation or it can be used to transfer mtDNA from a patient with no identified mutation. This latter study would at the very least give information on whether mtDNA plays any role in the disease. Thus, we embarked on a study aimed at developing a neuronal ρ^0 cell line through the use of ethidium bromide (EtBr). We chose the rat neuronal cell line PC12 since it has been well characterized by many groups, is used in numerous AD studies that examine amyloid deposition in AD, and lastly, because it has the excellent property of neuritic differentiation upon addition of NGF.

Similar to other drug studies, EtBr slowed cell growth of PC12 (HGPRT$^-$) cells although not cell viability at 100 and 200 ng/ml. By day 13 Southern analysis indicated mtDNA content was similar in all control and drug treated cells. After analyzing the effects of EtBr on cell growth, viability, and mtDNA content, one well from each experimental group was expanded into 10 cm petri dishes and the EtBr concentration was reduced back to 100 and 200 ng/ml since the higher drug concentrations were toxic upon extended exposure. These cells are currently being maintained in culture. For the future we plan to select clones of cells that are growing in discrete colonies on the petri dishes, an approach used by Trounce et al (136). Colonies represent cells that are either EtBr resistant or are surviving passage into the ρ^0 genotype. Petri dishes are ideal technically for colony seletion with adherent cells since dead cells detach from the plate and can be easily removed. MtDNA content from discrete populations grown in petri dishes at week 10 or 15 will probably provide a better assessment of ρ^0 status. The ρ^0 PC12 cell line can then be used in cybrid studies with AD mitochondria carrying the tRNA 4336 mutation as well as the COIII 9861 mutation. In addition it would prove very interesting to ascertain how these mtDNA-less cells respond to NGF. The ρ^0 PC12 would yield valuable information not only on the process of neurite outgrowth but on the involvement of mtDNA in AD, in the latter case either indicating mtDNA mutations are pivotal or opening the door to the study of nuclear encoded respiratory chain subunits.

LIST OF REFERENCES

1. Alzheimer's Disease and Related Disorders Association (ADRDA) fact sheet. National Headquarters, Chicago Illinois.

2. Adams R, Craig P and Parsons O. (1986). Neuropsychology of Dementia. Neurologic Clinics: Dementia 4,387-404.

3. Katzman R (1986). Differential diagnosis of dementing illness. Neurologic Clinics:Dementia 4,329-340.

4. Cummings JL (1990).Clinical diagnosis of Alzheimer's Disease J.L. Cummings and B.L. Miller (Eds.) In: Alzheimer's Disease: Treatment and Long Term Management New York, Marcel Dekker, Inc. pp 3-20.

5. Risse, S.C., Lampe, T.H., Bird, T.D., Nochlin, D., Mark-Sumi, S., Keenan, T., Cubberley, L., Peskind, E., and Raskind, M. (1990). Myoclonus, seizures and paratonia in Alzheimer's Disease. Alzheimer's Disease and Assoc. Disorders 4, 217-225.

6. Mayeux R, Stern Y and Spanton S (1985). Heterogeneity in dementia of the Alzheimer type:evidence of subgroups. Neurology 35, 453-461.

7. Holtzman DM and Mobley WC (1991). Molecular studies in Alzheimer's disease. TIBS 16, 140-144.

8. Perl DP and Pendlebury WW (1986). Neuropathology of Dementia. Neurologic Clinics:Dementia 4:2,355-368.

9. Murphy M. (1992). The molecular pathogenesis of Alzheimer's disease: clinical prospects. Lancet 340, 1512-1515.

10. Goate A, Chartier-Harlin MC, M Mullan, J Brown, F Crawford, L Fidani, L Guiffra, A Haynes, N Irving, L James, R Mant, P Newton, K Rooke, P Roques, C Talbot, R Williamson, M Rossor, M Owen, and J Hardy (1991). Segregation of a missense mutation in the amyloid precursor protein gene with familial Alzheimer's Disease. Nature 349,704-706.

11. Naruse S, Igarashi S, Kobayashi H et al. (1991). Missense mutation val->ile in exon 17 of amyloid precursor protein gene in Japanese familial Alzheimer's disease. Lancet 337,978-979.

12. Levy E, Carman MD, Fernandez Madrid IJ et al. (1990). Mutation of the Alzheimer's disease amyloid gene in hereditary cerebral hemorrhage, Dutch type. Science 248,1124-1126.

13. Saunders AM, Strittmatter WJ and Schmechel D (1993). Association of apolipoprotein E allele ϵ 4 with late onset familial and sporadic Alzheimer's Disease. Neurology 43,1467-1472.

14. Nalbantoglu J, Gilfix B, Bertrand P, Robitaille Y, Gauthier S, Rosenblatt D, Poirier J (1994). Predictive value of apolipoprotein E genotyping in Alzheimer's disease results of an autopsy series and an analysis of several combined studies. Ann Neurol 36, 889-895.

15. Hill JS, Pritchard, PH (1990). Improved phenotyping of apolipoprotein E: application to population frequency distribution. Clin Chem 36, 1871-1874.

16. Nee LE, Eldridge R, Sunderland T et al. (1987). Dementia of the Alzheimer type:clinical and family study of 22 twin pairs. Neurology 37, 359-363.

17. St.George-Hyslop PH, Myers RH, Haines JL et al. (1989). Familial Alzheimer's disease: progress and problems. Neurobiol Aging 10, 417-427.

18. Clark R, Goate A (1993). Molecular genetics of Alzheimer's disease. Arch Neurol 50, 1164-1172.

19. L. Heston and J. White (1991). Diseases that produce primary dementia. In: The Vanishing Mind: A Practical Guide to Alzheimer's Disease and Dementias New York, W.H. Freeman, pp 20.

20. Cohen D, Eisdorfer C and Leverenz J (1982). Alzheimer's disease and maternal age. J Am Geriat Soc 30,656-659.

21. Corkin S, Growdon JH and Rasmussen SL (1983). Parental age as a risk factor in Alzheimer's disease. Ann Neurol 13, 674-676.

22. Metter EJ, Riege WH, Benson DF, Kuhl DE and Phelps ME (1985). Patterns of regional cerebral glucose metabolism in Alzheimer's disease patients. Neurology and Neurobiology 18, 35-47.

23. Sokoloff L and Kety SS (1960). Regulation of cerebral circulation. Physiol Rev 40:4,38-44.

24. Brown GG, Levine SR, Gorell JM, Pettegrew JW, Gdowski JW, Bueri JA, Helpern JA and Welch KMA (1989). *In vivo* $_{31}$P NMR profiles of Alzheimer's disease and multiple subcortical multinfarct dementia. Neurology 39, 1423-1427.

25. Sims NR, Bowen DM, Neary D and Davison AN (1983). Metabolic process in Alzheimer's disease: Adenine nucleotide content and production of $^{14}CO_2$ from [U-^{14}C] glucose *in vitro* in human neocortex. J Neurochem 41, 1329-1334.

26. Gibson GE, Sheu K, Blass JP (1988). Reduced activities of thiamine dependent enzymes in the brains and peripheral tissues of patients with Alzheimer's Disease. Arch Neurology 45, 836-840.

27. Sorbi S, Bird ED, and Blass JP (1983). Decreased pyruvate dehydrogenase complex activity in Huntington's and Alzheimer's brain. Ann Neurology 13, 72-78.

28. Sims NR, Finnegan, JM and Blass JP (1987). Altered metabolic properties of cultured skin fibroblasts in Alzheimer's disease. Ann Neurol 21,451-457.

29. Blass JP and Gibson, GE (1991). The role of oxidative abnormalities in the pathophysiology of Alzheimer's disease. Rev Neurol 147:6-7,513-525.

30. Mariani C, Bresolin N, Moggio M, Ferrante C, Ciafaloni E, Sertorelli S, Ciccone A, Scarlato G (1991). Muscle biopsy in Alzheimer's disease: morphological and biochemical findings. Clin Neuropathol 10, 171-176.

31. Peterson C and Goldman JE (1986). Alterations in calcium content and biochemical processes in cultured skin fibroblasts from aged and Alzheimer donors. Proc Natl Acad Sci, USA 83,2758-2762.

32. Khansari N, Whitten HD, Chun YK, and Fudenberg HH (1985). Immunological dysfunction in Alzheimer's disease. J Neuroimmuno 7, 279-285.

33. Blass JP, Baker AC, Ko L and Black RS (1990). Induction of Alzheimer antigens by an uncoupler of oxidative phosphorylation. Arch Neurol 47, 864-869.

34. Baker AC, Ko L and Blass JP. (1988). Systemic manifestations of Alzheimers disease.Age 11, 60-65.

35. Saraiva AA, Borges MM, Madeira MD, Tavares, MA and Paula-Barbosa MM (1985). Mitochondrial abnormalities in cortical dendrites from patients with Alzheimer's disease. J Submicrosc Cytol 17, 459-464.

36. Terry RD and Wisniewski HM (1972). Ultrastructure of senile dementia and of experimental analogs. In: Aging and the Brain C.M. Gaitz (ed.) Plenum Press New York, pp 89-116.

37. Wallace DC (1994). Mitochondrial DNA sequence variation in human evolution and disease. Proc Natl Acad Sci USA 91, 8739-8746.

38. Gray MW (1989). Origin and evolution of mtDNA. Annu Rev Cell Biol 5, 25-50.

39. Birky CW, Acton A, Dietrich R and Carver M. Mitochondrial transmission genetics:replication, recombination and segregation of mitochondrial DNA and its inheritance in crosses. In: Mitochondrial Genes, G. Attardi, P. Borst and P.P. Slonimski (Eds.) Cold Spring Harbor Press, Cold Spring Harbor, New York, pp 333-348.

40. Wallace D, Lott M, Lezza A, Seibel P, Voljavec A and Shoffner J (1990). Mitochondrial DNA mutations associated with neuromuscular diseases: analysis and diagnosis using the polymerase chain reaction. Pediatric Res 28, 525-552.

41. Wallace DC (1989). Mitochondrial DNA mutations and neuromuscular disease. Trends Genet 5,9-13.

42. Veltri K, Espiritu M, Singh G (1990). Distinct genomic copy number in mitochondria of different mammalian organs. J of Cellular Physiology 143, 160-164.

43. Gibson GE and Peterson CP (1981). Aging decreases oxidative metabolism and the release and synthesis of acetylcholine. J Neurochem 37,978-984.

44. Luft R (1994). The development of mitochondrial medicine. Proc Natl Acad Sci USA 91 8731-8738.

45. Wallace DC, Singh G, Lott MT, Hodge JA, Schurr TG, Lezza AM, Elsas LJ and Nikoskelainen EK (1988). Mitochondrial DNA mutation associated with Lebers Hereditary Optic Neuropathy. Science 242, 1427-1430.

46. Holt IJ, Harding AE, Petty RKH and Morgan-Hughes, JA. (1990). A new mitochondrial disease associated with mitochondrial DNA heteroplasmy. Am J Hum Gen 46, 428-433.

47. Shoffner JM, Wallace DC (1990). Oxidation phosphorylation diseases. Disorders of two genomes. Adv Hum Genet 19, 267-330.

48. Shoffner J, Lott MJ, Lezza AMS, Seibel P, Ballinger SW and Wallace DC (1990). Myoclonic epilepsy and ragged red fiber disease (MERRF) is associated with a mitochondrial tRNA Lys mutation. Cell 61, 931-937.

49. Goto Y, Nonaka I, and Horai S (1990). A mutation in the tRNA Leu(UUR) gene is associated with the MELAS subgroup of mitochondrial encephalomyopathies. Nature 348, 651-653.

50. Yoneda M, Chomyn A, Martinuzzi A, Hurko O and Attardi G (1992). Marked replicative advantage of human mtDNA carrying a point mutation that causes the MELAS encephalomyopathy. Proc Natl Acad Sci USA 89, 11164-11168.

51. Chomyn A, Meola G, Bresolin N, Lai S, Scarlato G, and Attardi G (1991). In vitro genetic transfer of protein synthesis and respiration defects to mitochondrial DNA-less cells with myopathy-patient mitochondria. Mol and Cell Biol 11(4), 2236-2244.

52. Yoneda, M., Miyatake, T., Attardi, G. (1994). Complementation of mutant and wild-type human mitochondrial DNAs coexisting since the mutation event and lack of complementation of DNAs introduced separately into a cell within distinct organelle. Mol and Cell Biol 14(4), 2699-2712.

53. Grunwald, F., Zierz, S., Brioch, K., Schumacher, S., Bockish, A., and Biersack, H. (1990). HMPAO-SPECT imaging resembling Alzheimer-type dementia in mitochondrial encephalopathy with lactic acidosis and stroke-like episodes (MELAS). J Nucl Med 31, 1740-1742.

54. Cortopassi, G., Arnheim, N. (1990). Detection of mitochondrial DNA deletion in tissues of older humans. Nucl Acid Res 18, 6927-6933.

55. Cortopassi GA, Shibata D, Soong NW and Arnheim, N (1992). A pattern of accumulation of a somatic deletion of mitochondrial DNA in aging human tissues. Proc Natl Acad Sci USA 89, 7370-7374.

56. Yen, T., Pang, C., Hsieh, R. et al. (1992). Age-dependent 6kb deletion in human liver mitochondrial DNA. Biochem Intern 26, 457-468.

57. Yen, C., Su, J., King, K., and Wei, Y. (1991). Ageing-associated 5kb deletion in human liver mitochondrial DNA. Biochem Biophys Res Commun 178, 124-131.

58. Katayama, M., Tanaka, M., Yamamoto, H. et al. (1991). Deleted mitochondrial DNA in the skeletal muscle of aged individuals. Biochem Intern 25, 47-56.

59. Hattori, K., Tanaka, M., Sugiyama, S. et al. (1991). Age-dependent increase in deleted mitochondrial DNA in the human heart: possible contributory factor to presbycardia. Amer Heart Journal 6, 1735-1742.

60. Ballinger SW et al.(1992) Maternally transmitted diabetes and deafness associated with a 10.4 kb mitochondrial DNA deletion. Nature Genet 1, 11-15.

61. Gold M, Rapin I, and Shanske S. Mitochondrial inheritance of acquired deafness. Annals NY Acad Sci 301-302.

62. Zeviani M, Morares CT, DiMauro S, et al. (1988). Deletions of mitochondrial DNA in Kearns-Sayer Syndrome. Neurology 38, 1339-46.

63. Moraes CT, DiMauro S, Zeviani M, et al. (1989). Mitochondrial DNA deletions in progressive external ophthalmoplegia and Kearns-Sayre Syndrome. New Engl J Med 320, 1293-1299.

64. Madsen,C., Ghivizzani, S.and Hauswirth, W. (1993). *In vivo* and *in vitro* evidence for slipped mispairing in mammalian mitochondria. Proc Natl Acad Sci 90, 7671-7675.

65. Domena JD, Mosbaugh DW (1985). Purification of nuclear uracil-DNA glycosylase from rat liver:identification of two distinct subcellular forms. Biochemistry 24,7320-7328.

66. Tomkinson AE, Bonk RT, Linn S (1988). Mitochondrial endonuclease activitities specific for apurinic/apyrimidinic sites in DNA from mouse cells. J Biol Chem 263, 12532-12537.

67. Bolden A, Noy G, Weissbach A (1977). A DNA polymerase of mitochondria is a gamma polymerase. J Biol Chem 252, 3351-3356.

68. Levin CJ, Zimmerman SB (1976). A DNA ligase from mitochondria of rat liver. Biochem Biophys Res Commun 69, 514-520.

69. Lindahl, T.(1993). Instability and decay of the primary structure of DNA. Nature 362, 709-714.

70. Kunkel TA, Loeb L. (1981). Fidelity of mammalian DNA-polymerases. Science 213, 765-767.

71. Tritschler HJ and Medori R. (1993). Mitochondrial DNA as a source of human disorders. Neurology 43, 280-288.

72. Holmes GE, Berstein C, Bernstein H. (1992). Oxidative and other DNA damages as the basis of aging: a review. Mutat Res 275, 305-315.

73. Cutler RG. (1975). Evolution of human longevity and genetic complexity of governing aging rate. Proc Natl Acad Science

74. Miquel, J. (1992). An update on the mitochondrial-DNA mutation hypothesis of cell aging. Mutat Res 275, 209-216.

75. Hruszkewycz AM (1992). Lipid peroxidation and mitochondrial DNA degeneration. Mutat Res 275 243-248.

76. Hayakawa M, Torii K, Sugiyama S, Tanaka M, Ozawa T. (1991). Age-associated accumulation of 8-hydroxydeoxyguanosine in mitochondrial DNA of human diaphragm. Biochem and Biophys Res Commun 179(2), 1023-1029.

77. Meococci P, MacGarvey U and Beal MF (1994). Oxidative damage to mitochondrial DNA is increased in Alzheimer's Disease. Ann Neurol 36,747-751.

78. Harman D (1972). The biologic clock: the mitochondria? J Am Geriatr Soc 20,145-147.

79. Clayton DA (1982). Replication of animal mitochondrial DNA. Cell 28, 693-705.

80. Parker WD, Filley CM and Parks KK. (1990b). Cytochrome oxidase deficiency in Alzheimer's Disease. Neurology 40, 1302-1303.

81. Parker Jr W, Mahr N, Filley C, Parks J, Hughes D, Young D and Cullum C. (1994). Reduced platelet cytochrome *c* oxidase activity in Alzheimer's disease. Neurology 44, 1086-1090.

82. Kish SJ, Bergeron C, Rajput A, Slobodan D, Mastrogiacomo F, Chang L, Wilson J, DiStefano and Nobrega J. (1992). Brain cytochrome oxidase in Alzheimer's Disease. J of Neurochem 59,776-779.

83. Parker Jr. W, Parks J, Filley C, Kleinschmidt-DeMasters BK (1994). Electron transport chain defects in Alzheimer's disease brain. Neurology 44, 1090-1096.

84. Chandrasekaran K, Giordano T, Brady D, Stoll J, Martin L, and Rapoport S. (1994). Impairment of mitochondrial cytochrome oxidase gene expression in Alzheimer's Disease. Mol Brain Res 24,336-340.

85. Shoffner JM, Brown MD, Torroni A, et al. (1993). Mitochondrial DNA variants observed in Alzheimer Disease and Parkinson Disease patients. Genomics 17,171-184.

86. Swierczynski J, Scislowski O and Aleksandrowicz Z. (1976). High activity of alpha glycerophosphate oxidation by human placental mitochondria. Biochem Biophys Acta 429,46-54.

87. Drouin J (1980). Cloning of human mitochondrial DNA in Escheria coli. J Mol Biol 140,15-34.

88. Southern EM (1975). Detection of specific sequences among DNA fragments separated by gel electrophoresis. J Mol Biol 98,503-517.

89. Anderson S, Bankier AT, Barrell BG, deBruijn M, Coulson AR, Drouin J, Eperon I, Nierlich D, Roe B, Sanger A, Schreier P, Smith A, Staden R and Young IG (1981). Sequence and organization of the human mitochondrial genome. Nature 290, 457-465.

90. Chamberlain JS, Gibbs RA, Ranier JE and Caskey CT (1990). Multiplex PCR for the diagnosis of Duchenne Muscular Dystrophy. In:PCR Protocols: A Guide to Methods and Applications, MA Innis, DH Gelfand, JJ Sninsky and TJ White (Eds.) Academic Press, New York, pp 272-281.

91. Corral-Debrinski M, Stepien G, Shoffner JM, MT Lott Kanter K and Wallace DC (1991). Hypoxemia is associated with mtDNA damage and gene induction: Implications for cardiac arrest. JAMA 266, 1812-1816.

92. Ozawa T, Tanaka M, Ikebe S, Ohno K, Kondo T and Mizuno Y. (1990). Quantitative determination of deleted mitochondrial DNA relative to normal DNA in parkinsonian striatum by a kinetic PCR. Biochem Biophys Res Commun 172, 483-489.

93. Sanger F, Nicklen S and Coulson AR (1977). DNA sequencing with chain terminating inhibitors. Proc Natl Acad Sci USA 74,5463-5467.

94. Seibel P, DeGoul F, Romero N, Marsac C and Kadenbach B. (1990). Identification of point mutations by mispairing PCR as exemplified in MERRF disease. Biochem Biophys Res Commun 173:2, 561-565.

95. Hayashi, K. (1991). PCR-SSCP: A simple and sensitive method for detection of mutations in genomic DNA. PCR Methods and Applications 35, 34-38.

96. Orita M, Iwahana H, Kanazawa H, Hayashi K, and Sekiya T. (1989). Detection of polymorphisms of human DNA by gel electrophoresis as single strand conformation polymorphisms. Proc Natl Acad Sci USA 86,2766-2770.

97. Caetano-Anolles G and Gresshoff PM. (1994). Staining nucleic acids with silver an alternative to radioisotopic and fluorescent labeling. Promega Notes 45, 13 18.

98. Yavin E and Yavin Z. (1974). Attachment and culture of dissociated cells from rat embryo cerebral hemispheres on polylysine-coated surface. J Cell Biol 62 540-546.

99. Greene LA, Aletta JM, Rukenstein A and Green SH. (1987). PC12 Pheochromocytoma cells: culture, nerve growth factor treatment, and experimental exploitation. Methods in Enzymol 147, 207-216.

100. King M and Attardi G (1989). Human cells lacking mtDNA: Repopulation with exogenous mitochondria by complementation. Science 246, 500-503.

101. King M, Godman G, King D (1972). Respiratory enzymes and mitochondrial morphology of HeLa and L cells treated with chloramphenicol and ethidium bromide. J Cell Biol 53, 127-142.

102. Nass MMK (1972). Differential effects of ethidium bromide on mitochondrial and nuclear DNA synthesis in vivo in cultured mammalian cells. Exptl Cell Res 72, 211-222.

103. Desjardins P, Frost E and Morais R (1985). Ethidium bromide-induced loss of mitochondrial DNA from primary chicken embryo fibroblasts. Mol Cell Biol 5:5, 1163-1169.

104. Wiseman A and Attardi G (1978). Reversible ten-fold reduction in mitochondrial DNA content of human cells treated with ethidium bromide. Molec gen Genet 167, 51-63.

105. Hamblet NS and Castora FJ (1992). Detection and quantitation of deleted mitochondrial DNA in brain tissue of Alzheimer's patients. Cold Spring Harbor Laboratory:Molecular Biology of Aging. *Abstract.*

106. Wei, Y (1992). Mitochondrial DNA alterations as ageing-associated molecular events. Mutation Res 275, 145-155.

107. Schapira AHV and Cooper JM (1992). Mitochondrial function in neurodegeneration and ageing. Mutation Res 275, 133-143.

108. Hamblet NS and Castora FJ (1995). Mitochondrial DNA deletion analysis: a comparison of PCR quantitative methods. Biochem Biophys Res Commun 207,839-847.

109. Munro BH, Visintainer MA and Page EB (1986). T-tests: Measuring the difference between group means. In: Statistical Methods in Health Care Research, J.B. Lippincott Company,Philadelphia, 155-173.

110. Wei, Y (1992). Mitochondrial DNA alterations as ageing-associated molecular events. Mutation Res 275, 145-155.

111. Corral-Debrinski M, Horton T, Lott M, Shoffner J, McKee A, Beal M, Graham B, Wallace D. (1994). Marked changes in mitochondrial DNA deletion levels in Alzheimer brains. Genomics, 23, 471-476.

112. Blanchard BJ, Park T, Fripp WJ, Lerman LS and Ingram VM (1993). Neuroreport 4, 799-802.

113. Sheu KR, Chen X, Schon EA (1994). Are there deletions of mitochondrial DNA in Alzheimer's Disease? Neurology 44:2. A390. *Abstract*

114. Lin, FH, Lin R, Wisniewski HM, Hwang YW, Grunde-Iqbal, I, Healy-Louie G and Iqbal K (1992). Detection of point mutations in codon 331 of mitochondrial NADH dehydrogenase subunit 2 in Alzheimer's brain. Biochem Biophys Res Commun 182, 238-246.

115. Petruzzella V, Chen X and Schon E (1992). Is a point mutation in the mitochondrial ND2 gene associated with Alzheimer's disease? Biochem Biophys Res Commun 186, 491-97.

116. Howell N, McCullough D, Kubacka I, Halvorson S and Mackey D. (1992). The sequence of human mtDNA: the question of errors versus polymorphisms. Amer J Hum Genet 50, 1333-1337.

117. Ozawa T, Tanaka M, Ino H, Ohno K, Sano T, Wada Y, Yoneda M, Tanno Y Miyatake T, Itoyama S, Ikebe S, Hattori N, and Mizuno Y. (1991). Distinct clustering of point mutations in mitochondrial DNA among patients with mitochondrial encephalomyopathies and with Parkinson's disease. Biochem Biophys Res Commun 176, 938-946.

118. Marzuki S, Noer AS, Lertrit P, Thyagarajan D, Kapsa R, Utthanaphol P, and Byrne E (1991). Normal variants of human mitochondrial DNA and translation products:the building of a reference data base. Hum Genet 88:139-145.

119. Massuci, *Unpublished.* Reference database supplied by FM Santorelli and EA Schon, Department of Neurology, Columbia University, NY, NY.

120. Ozawa T, Tanaka M, Ino H, Sano, T, et al. (1991). Distinct Clustering of Point Mutations among Patients with Mitochondrial Encephalomyopathies and Parkinson's Disease. Biochem Biophys Res Commun 176,938-946.

121. Yoneda, M, Tanno Y, Horai S. et al. (1990). A Common Mitochondrial DNA Mutation in the $tRNA^{lys}$ of Patients with Myoclonus Epilepsy Associated with Ragged Red Fibers. Biochem Int 21,789-796.

122. Monnat RJ, Loeb LA. (1985). Nucleotide sequence preservation of human mitochondrial DNA. Proc Natl Acad Sci USA 82, 2895-2899.

123. Horai S, Hayasaka K, Kondo R et al. (1995). Recent African origin of modern humans revealed by complete sequences of hominoid mitochondrial DNAs. Proc Natl Acad Sci USA 92, 532-536.

124. Santorelli FM and Schon EA (1995). *Personal Communication.*

125. Wallace DC, Lott MT, Brown MD, Huoponen K and Torroni A. (1994). Report of the committee on human mitochondrial DNA. Http://infinity.gen.emory.edu

126. Torroni A, Neel JV, Barrantes R, Schurr TG, and Wallace DC. (1994). A mitochondrial DNA "clock" for the Amerinds and its implications for timing their entry into North America. Proc Natl Acad Sci USA 91, 1158-1162.

127. Houshmand M, Larsson NG, Holme E, Oldfors A, Tulinius MH and Andersen, O. (1994). Automatic sequencing of mitochondrial tRNA genes in patients with mitochondrial encephalomyopathy. Bichem Biophys Acta 1226, 49-55.

128. Brown MD, Voljavec AS, Lott MT, MacDonald I, Wallace DC. (1992). Leber's hereditary optic neuropathy; a model for mitochondrial neurodegenerative diseases. FASEB J 6,2791-2799.

129. Burgess CE, Lewis D, Naidu S and Castora FJ (1995). Search for a genetic marker for Retts Syndrome: single strand conformation polymorphism of mitochondrial tRNA genes. *Submitted.*

130. Sarkar G, Yoon H and Sommer S (1992). Dideoxy finger-printing(ddF): A rapid and efficient screen for the presence of mutations. Genomics 13,441-443.

131. Moyret C, Theillet C, Puig PL, Moles JP, Thomas G, Hamelin R (1994). Relative efficiency of denaturing gradient gel electrophoresis and single strand conformation polymorphism in the detection of mutations in exons 5 to 8 of the p53 gene. Oncogene 9,739-43.

132. Hayashi K, and Yandell DW (1993). How sensitive is PCR-SSCP? Hum Mutat 2, 338-46.

133. Vidal-Puig A and Moller DE (1994). Comparative sensitivity of alternative single strand conformation polymorphism (SSCP) Methods. Biotechniques 17: 490-496.

134. Rosen DR, Siddique T, Patterson D, Figlewicz DA, Sapp P, Henati A et al. (1993). Mutations in Cu/Zn superoxide dismutase gene are associated with familial amyotrophic lateral sclerosis. Nature 362:59.

135. Manfredi, G., Bonnila, E., Schon, E.A., S. DiMauro, S. and Moraes, C.T. (1994). A Mitochondrial DNA Missense Mutation in the Cytochrome C Oxidase Subunit III Gene Associated with a Progressive Encephalopathy. Miami Short Reports 4,17.

136. Trounce I, Neill S, and Wallace DC (1994). Cytoplasmic transfer of the mtDNA nt8933 T->G (ATP6) point mutation associated with Leigh syndrome into mtDNA-less cells demonstrates cosegregation with a decrease in state III respiration and ADP/O ratio. Proc Natl Acad Sci USA 91, 8334-8338.

137. Corral-Debrinski M, Shoffner JM, Lott MT, and Wallace DC. (1992). Association of mtDNA damage with aging and coronary artherosclerotic heart disease. Mutation Res 275, 169-179.

138. Zullo S and Merril S. (1995). *Personal communication*

140. Ikebe S Tanaka M, Ohno K, Sato W, Hattori K, Kondo T, Mizuno Y and Ozawa T. (1990). Increse of deleted mitochondrial DNA in the striatum in Parkinson's Disease and senescence. Biochem Biophys Res Commun 170, 1044-1048.

141. Soong NW, Hinton DR, Cortopassi G and Arnhiem N. (1992). Mosaicism for a specific somatic mtDNA mutation in adult human brain. Nature Genet 2, 318-323.

142. Corral-Debrinski M, Hortin T, Lott MT, Shoffner JM, Beal MF and Wallace DC. (1992). Mitochondrial DNA deletions in human brain: regional variability and increase with advanced age. Nature Genet 2, 324-329.

143. Cortopassi G, Shibata D, Soong NW and Arnheim N. (1992). A pattern of accumulation of a somatic deletion in mtDNA in aging human tissue. Proc Natl Acad Sci USA 89,7370-7374.

144. Corbisier P and Remacle J. (1990). Involvement of mitochondria in cell degeneration. Eur J of Cell Biol 51,173-182.

145. Hayashi J, Ohta S, Kikuchi A, Takemitsu M, Goto Y and Nonaka I (1991). Introduction of diseae related mitochondrial DNA deletions in Hela cells lacking mitochondrial DNA results in mitochondrial dysfuntion. Proc Natl Acad Sci USA 88,10614-10618.

146. Schon EA (1994). MtDNA and the genetics of mitochondrial disease. In: Mitochondrial Disorders in Neurology (AHV Schapira and S. DiMauro, eds) Oxford, England, Butterworth-Heinemann Ltd. pp 31-48.

147. Goto Y, Nonaka I and Horai S. (1991). A new mtDNA mutation associated with mitochondrial encephalomyopathy, lactic acidosis and stroke like episodes (MELAS). Biochem Biophys Acta 1097, 238-240.

148. Moraes CT, Ciacci F, Silvestri G, Shanske S, Sciacco M, Hirano M, Bonilla E and DiMauro S. (1993). Atypical clinical presentations associated with the MELAS mutation at position 3243 of human mitochondrial DNA. Neuromuscul Disord 3 43-50.

149. Kim LY, Brown MD and Wallace DC (1995). Single strand conformation polymorphism for the detection of point mutations in the mitochondrial DNA. Anal Biochem 224, 608-611.

150. Capaldi, R.A. (1990). Structure and function of cytochrome c oxidase. Ann Rev Biochem 59, 569-96.

151. Cooper JM and Clark JB (1994). The structural organization of the mitochondrial genome. In: Mitochondrial Disorders in Neurology (AHV Schapira and S. DiMauro, eds) Oxford, England, Butterworth-Heinemann Ltd. pp 1-30.

152. Thomas AW, Morgan R, Sweeney M, Rees A and Alcolado J (1995). The detection of mitochondrial DNA mutations using single strand conformation polymorphism (SSCP) analysis and heteroduplex analysis. Hum Genet 94(6), 621-623.

153. Nardelli M, Tommasi S, D'erchia A, Tanzariello F, Tullo A, Primavera A, DeLena M, Sbisa E, and Saccone C (1994). Detection of novel transcripts in the human mitochondrial DNA region coding for ATPase8-ATPase6 subunits. FEBS Letters 344;10-14

154. Parker Jr W, Parks J (1995). Cytochrome *c* oxidase in Alzheimer's disease brain: Purification and characterization.Neurology, 45, 482-486.

155. Dyrks T, Dyrks E, Hartman T, Masters C and Beyreuther K (1992). Amyloidgenicity of βA4 and βA4-bearing amyloid protein precursor fragments by metal catalyzed oxidation. J Biol Chem 267, 18210-18217.

156. Crothers D, Haran T, Nardeau J (1990). Intrinsically bent DNA. J Biol Chem 265, 7093-7096.

157. Trifonov EN (1985). Curved DNA. Crit Rev in Biochem 19,89-106.

APPENDIX A

List of Postmortem Brain Tissue
Supplied by W.W. Tourtellotte, M.D., Ph.D.
Director
National Neurological Research Specimen Bank

SHIPMENT REPORT

Natasha S. Hamblet

HSB#	AGE SEX	DIAGNOSIS	SEC	STRUCTURE	AUTOLYSIS TIME (HRS.)	AMOUNT (GMS)
1546	75/M	Alzheimer's	10	caudate	8.0	0.9
			10	temporal cortex		0.9
			14	hippocampus		0.4
			14	parietal cortex		0.8
1556	81/M	Alzheimer's	9	caudate	7.5	0.6
			6	temporal cortex		0.5
			11	parietal cortex		0.4
1573	79/M	Alzheimer's	16	caudate	7.0	0.7
			16	temporal cortex		1.1
			7	parietal cortex		0.7
1607	80/F	Alzheimer's	4	caudate	5.5	0.3
			6	temporal cortex		0.5
			10	parietal cortex		0.9
1630	86/F	Alzheimer's	5	caudate	7.0	0.8
			5	temporal cortex		0.5
			10	parietal cortex		0.5
1702	76/F	Alzheimer's	4	caudate	5.5	1.0
			11	parietal cortex		0.5
1674	84/F	Alzheimer's	3	caudate	6.0	0.6
			11	parietal cortex		0.9
1647	76/M	Alzheimer's	8	caudate	5.0	0.5
			8	temporal cortex		0.5
			8	hippocampus		0.5
			12	parietal cortex		0.3
1739	78/M	Alzheimer's	7	caudate	8.0	0.5
			7	temporal cortex		0.6
			10	hippocampus		0.8
			12	parietal cortex		0.4
1765	77/M	Alzheimer's	9	caudate	5.5	0.7
			9	temporal cortex		0.6
			13	parietal cortex		0.6
1770	75/M	Alzheimer's	8	caudate	8.5	0.4
			8	temporal cortex		0.5
			15	parietal cortex		0.8
1802	65/F	Alzheimer's	5	caudate	6.5	1.2
			5	temporal cortex		0.4
			10	parietal cortex		0.8
1807	75/M	Alzheimer's	5	caudate	5.5	0.7
			5	temporal cortex		0.5
			12	parietal cortex		0.7
316	89/F	Alzheimer's	7	caudate	7.5	0.9
			7	temporal cortex		0.5
			11	hippocampus		0.3

SHIPMENT REPORT

Natasha S. Hamblet

HSB#	AGE SEX	DIAGNOSIS	SEC	STRUCTURE	AUTOLYSIS TIME (HRS)	AMOUNT (GMS)
			17	parietal cortex		1.0
1974	85/F	Alzheimer's	8	caudate	7	0.7
			8	temporal cortex		0.8
			15	parietal cortex		1.0
1977	81/F	Alzheimer's	6	caudate	5	0.6
			7	temporal cortex		0.4
			13	hippocampus		0.6
			15	parietal cortex		1.0
1327	52/M	Control	16	parietal cortex	19	1.8
1341	48/M	Control	13	parietal cortex	9	1.2
1347	66/M	Control	15	parietal cortex	9	0.7
1350	59/M	Control	11	parietal cortex	7	0.8
1351	59/M	Control	6	caudate	9	0.3
			6	temporal cortex		0.4
			11	parietal cortex		0.4
1355	58/M	Control	5	caudate	9.5	0.3
			5	temporal cortex		0.7
1401	59/M	Control	12	hippocampus	23	0.5
			17	parietal cortex		1.0
1406	40/M	Control	9	caudate	18	0.5
			9	temporal cortex		0.3
			16	parietal cortex		0.6
1413	67/M	Control	4	temporal cortex	22	0.6
			15	parietal cortex		0.5
1415	59/M	Control	8	caudate	11	0.8
			15	parietal cortex		0.8
1441	64/M	Control	16	parietal cortex	10	0.7
1539	68/M	Control	9	temporal cortex	16.5	0.3
			12	parietal cortex		1.1
1569	61/M	Control	8	temporal cortex	9	0.3
			19	parietal cortex		0.9
1640	66/M	Control	5	caudate	15.5	0.7
			15	parietal cortex		0.6
1818	59/M	Control	6	temporal cortex	15	0.8
			14	parietal cortex		0.5
1846	73/M	Control	8	caudate	26.5	1.2
			8	temporal cortex		0.9
			11	parietal cortex		1.2
1903	70/M	Control	8	caudate	13	0.9
			8	temporal cortex		1.0
			15	parietal cortex		1.2
1933	38/M	Control	8	caudate	15	0.2

SHIPMENT REPORT

Natasha S. Hamblet

HSB#	AGE SEX	DIAGNOSIS	SEC	STRUCTURE	AUTOLYSIS TIME (HRS.)	AMOUNT (GMS)
			8	hippocampus		0.5
			15	parietal cortex		0.5

HSB#	AGE SEX	DIAGNOSIS	SEC	STRUCTURE	AUTOLYSIS TIME (HRS.)	AMOUNT (GMS)
694	68/F	Alzheimer's	8&9	caudate	7.5	0.4
			8	temporal cortex		0.6
			14	parietal cortex		1.2
			15	parietal cortex		0.9
576	72/M	Alzheimer's	6	caudate	7.0	1.5
			8	temporal cortex		0.9
			12	hippocampus		0.4
			16	parietal cortex		0.3
1476	77/F	Alzheimer's	7	caudate	6.2	0.6
			7	temporal cortex		0.4
			16	parietal cortex		1.1
1513	81/F	Alzheimer's	7	caudate	7.5	0.2
			7	temporal cortex		0.4
			11	parietal cortex		0.6
1537	64/F	Alzheimer's	8	caudate	5.5	1.5
			8	temporal cortex		0.8
			16	parietal cortex		0.7

APPENDIX B

Autopsy Samples Received: Dr. Peter Davies
Albert Einstein College of Medicine

CASE	AGE(yrs)	NEUROPATHOLOGY DIAGNOSIS
3822	67	AD:sparing limbic system and brain stem, amyloid angiopathy, cerebellar plaques
3929	90	AD: plaques-only type,atherosclerotic and hypertensive vascular disease
3988	85	AD: plaques only type, hypertensive vascular disease, lacunar infarcts (mixed dementia)
4073	92	AD: atherosclerotic vascular disease, hypertensive vascular disease, lacunar infarcts
4299	64	AD:artherosclerotic vascular disease, leukoencephalopathy,amyloid angiopathy
4308	76	AD: amyloid angiopathy, leukoencephalopathy, cerebellar plaques, microinfarcts
4390	65	AD: hyperacute anoxic-ischemic changes, cerebral cortical dysplasia
4395	60	AD: amyloid angiopathy, cerebellar plaques
4460	80	AD: amyloid angiopathy, cerebellar and basal ganglia plaques, Lewy bodies compatible with PD
4027	75	Control:hypertensive vascular disease, lacunar state diffuse Lewy bodies
4284	41	normal

APPENDIX C

Lymphocyte Cell Lines
Alzheimer's Disease Research Centers National Cell Repository

Cell Line #	Age(yrs)	Description
200	71	Married In
938	85	Married In
890	70	Married In
767	89	Married In
915	67	Married In
291	71	Biopsy Confirmed AD
38	85	Probable AD
36	70	Probable AD
135	89	Probable AD
617	67	Possible AD
347	60	Offspring Of Affected
105	41	Offspring Of Affected
835	58	Offspring Of Affected
628	43	Offspring of Affected
863	50	Offspring of Affected
429	27	Normal
1079	32	Normal

APPENDIX D

Table 4 QUANTITATION OF mtDNA^{4977} IN THE TEMPORAL CORTEX

GROUP 1 ALZHEIMER'S				GROUP 2 CONTROL		
CASE #	AGE	% DELETED		CASE #	AGE	% DELETED
1537	64	.0070		1569	61	.0079
1802	65	.2230		1413	67	.0014
694	68	.0141		1539	68	.0013
576	72	.0560		1903	70	.0141
1807	75	.0138		1846	73	.0016
A.2*	63	.3000				
A.4*	72	.3600				
Mean Age: 68.4 yrs Mean % mtDNA^{4977}: .1391% s^2 = .023				Mean Age: 68 yrs Mean % mtDNA^{4977}: .0053% s^2 = .00003		

* Corral-Debrinski et al. 1994.

AUTOBIOGRAPHICAL STATEMENT

Personal Data

Date of Birth: April 9, 1965
Georgetown, British Guiana (Guyana)

Education

State University of New York at Stony Brook, Stony Brook, New York, September, 1983 to August, 1987. Bachelor of Science in Biochemistry and French Literature.

Eastern Virginia Medical School/Old Dominion University, Norfolk, Virginia, Department of Biochemistry, September, 1990 to present. Doctoral Candidate in Molecular/Cell Biology.

Special Educational Programs

1987: Université de Rennes, Bretagne, France, French Grammar and Composition.

1980-1983: Uniondale High School Advanced Placement (AP) Program in Biology, English and French, Uniondale, New York.

1981-1983: Adelphi University/Uniondale High School Advanced Science Program, Chemistry and Physics.

Appointments

1992-1995: NIH National Research Service Award Predoctoral Fellow, Department of Biochemistry, Eastern Virginia Medical School, Norfolk,VA.

1991-1992: Graduate Research Assistant, Department of Biochemistry, Eastern Virginia Medical School.

1990-1991: Graduate Teaching Assistant, Department of Biology, Old Dominion University, Norfolk, VA.

1988-1989: Research Assistant, Department of Molecular Virology, St.Luke's/ Roosevelt Hospital Center and Columbia University College of Physicians & Surgeons, New York, NY.

1986-1987: Undergraduate Research Assistant, Medical Physics Laboratory, University Hospital, State University of New York at Stony Brook.

1985-1987: Undergraduate Student Technician, Department of Radiation Oncology, University Hospital, State University of New York at Stony Brook.

1985: Biology Tutor, College of Arts and Sciences, State University of New York at Stony Brook

Academic Honors

1995: Outstanding Graduate Research Award, Sigma Xi, Scientific Research Society, Virginia Tidewater Chapter
1983-1987: New York State Regents Scholarship
1983-1987: Phi Sigma Iota, Foreign Language Honor Society
1983: Kiwanis Scholarship
1980-1983: National Honor Society
1977-1980: National Junior Honor Society
1975-1976: St. Roses Ursaline Convent Entrance Exam Scholarship

Bibliography

N.S. Hamblet and F.J. Castora, (1995). "Identifcation of Sequence Variants Mitochondrial DNA Encoded Cytochrome C Oxidase Subunits in Alzheimer's Disease Using Single Strand Conformation Polymorphism", Submitted.

N. S. Hamblet and F.J. Castora, (1995). "Mitochondrial DNA Deletion Analysis: A Comparison of PCR Quantitative Methods", Biochem. Biophys. Res. Commun., 207, 839-847.

N.S. Hamblet and F.J. Castora, (1994). SSCP and Deletion Analysis of mtDNA from Four Regions of the Brain in Elderly and Alzheimer's Patients", Miami Short Reports, Molecular Biology & Human Disease, Vol 4 - Supplement, W29p.

N.S. Hamblet and F.J. Castora, (1993). "Analysis of Cytochrome Oxidase Gene Coding Region in Mitochondrial DNA of Alzheimer's Patients", FASEB J. 7, A1085.

N.S. Hamblet and F.J. Castora, (1992). "Alzheimer's Disease and Associated Mitochondrial DNA Lesions". FASEB J. 6, A516.

D.J. Volsky, G.Li, N. Hamblet, B. Volsky, R.S.Decker, M.G. Pellegrino and M.J. Potash, (1992). "Evaluation of Multiple Parameters of HIV-1 Replication Cycle in Testing of AIDS drugs *in vitro*", Antiviral Research, 17, 335-347.

Unpublished Abstracts

N.S. Hamblet and F.J. Castora, (1992). "Detection and Quantitation of Deleted mtDNA in Brain Tissue of Alzheimer's Patients", Cold Spring Harbor Laboratory: Molecular Biology of Aging, Cold Spring Harbor, New York.

D.J. Volsky, N. Hamblet, B. Volsky, M.G. Pellegrino, S. Decker, and G.Li, (1990). A New Approach for Testing the Effects of AIDS Drugs on HIV-1 Expression and Replication *in vitro*. Sixth International Conference on AIDS, San Francisco, California.

D.J. Volsky, N. Hamblet, B. Volsky, M.G. Pellegrino, and G. Li, (1990). A Need for Multi-parameter Virological Testing in Screening Potential AIDS Drugs *in vitro*. International Society for Antiviral Research, Third International Conference on Antiviral Research, Brussels, Belgium.

D.J. Volsky, M.Pellegrino, N. Singh Hamblet, G.Li, K.Logan, J. Aswell and S. Decker. (1989). "Quantitative Analysis of HIV-1 Expression Using Magnetic Particle RNA-RNA Hybridization Assay", American Society of Microbiology Annual Meeting, New Orleans, Louisiana.

Oral Presentations

"Mitochondrial Dna Mutations in Alzheimer's Disease", Columbia University, Department of Neurology, February, 1995.